ABSTRACT

A SINGLE-CHAIN GMCSF-MOG TOLEROGENIC VACCINE EXPANDS MOG-SPECIFIC $CD25^{+}$ $FOXP3^{+}$ REGULATORY T CELLS THROUGH LOW-EFFICIENCY ANTIGEN RECOGNITION EVENTS TO INHIBIT EXPERIMENTAL AUTOIMMUNE ENCEPHALOMYELITIS

by

Cody Deumont Moorman

December 2019

Director of Dissertation: Mark D. Mannie Ph.D.

Department of Microbiology and Immunology

at East Carolina University Brody School of Medicine

Previous studies showed that tolerogenic vaccines comprised of single-chain GMCSF-neuroantigen (NAg) fusion proteins inhibited experimental autoimmune encephalomyelitis (EAE) in rodents. The studies detailed here provide evidence that GMCSF-NAg vaccines elicited tolerance through the expansion of preexisting NAg-specific regulatory T cells (Tregs) via low-efficiency antigen recognition that was below the CD40/CD40L activation threshold. GMCSF-NAg-induced tolerance was dependent upon vaccine-induced Tregs, because treatment of mice

with a Treg-depleting mAb reversed vaccine-induced tolerance. Vaccine-induced T cell responses were investigated using T cell receptor (TCR) transgenic OTII-FIG mice which recognize $OVA^{323-337}$ as a high-efficiency antigen, and 2D2-FIG mice which recognize MOG^{35-55} as a low-efficiency antigen and NFM^{13-37} as a high-efficiency antigen. Subcutaneous vaccination of 2D2-FIG mice with the low-efficiency GMCSF-MOG vaccine elicited a major Treg population that appeared within 3 days, was sustained over several weeks, expressed canonical Treg markers, and was present systemically in the blood, spleen, and lymph nodes. The GMCSF-MOG vaccine required covalent linkage because a vaccine that contained GM-CSF and MOG^{35-55} as separate molecules did not elicit Treg responses. GMCSF-MOG vaccination elicited Tregs when introduced either subcutaneously or intravenously as well as in the proinflammatory adjuvants CFA and alum. The GMCSF-MOG-induced Tregs were immunosuppressive and prevented the proliferation of MOG^{35-55}-specific T cells. The GMCSF-MOG vaccine not only elicited Tregs but also induced a desensitized MOG^{35-55}-specific (2D2) T cell repertoire because the vaccine decreased the number of 2D2 $CD3^+$ T cells, reduced the overall expression of the 2D2 TCR, and increased the $CD4^-$ T cell compartment.

The ability of GMCSF-NAg vaccines to induce Tregs was dependent upon the efficiency of T cell antigen recognition, because treatment of OTII-FIG and 2D2-FIG mice with the high-efficiency GMCSF-OVA and GMCSF-NFM vaccines respectively, did not elicit Treg responses. The high-efficiency GMCSF-NFM vaccine induced a vigorous T conventional cell (Tcon) memory response and activated the CD40L/CD40 co-stimulatory pathway. In contrast, the low-efficiency GMCSF-MOG vaccine elicited Tregs and lacked sufficient TCR signal strength to activate CD40L/CD40 pathway. Activation of the CD40L/CD40 pathway using an agonistic anti-CD40 mAb precluded Treg expansion with the low-efficiency GMCSF-MOG vaccine in

2D2-FIG mice. Therefore, the strength of the TCR stimulus and the downstream activation or exclusion of the CD40L/CD40 costimulatory pathway was the switch that controlled Tcon versus Treg responses respectively. Remarkably, the low-efficiency GMCSF-MOG vaccine retained Treg expansive activity when co-administered with the high-efficiency GMCSF-NFM vaccine in 2D2-FIG mice.

The GMCSF-MOG vaccine appeared to predominantly drive Treg expansion rather than Treg induction because the emergence of Tregs was delayed in 2D2-FIG-*Rag*$^{-/-}$ mice which have reduced frequencies of pre-existing Tregs as compared to 2D2-FIG mice. Pre-existing Tregs were also required for tolerance because GMCSF-MOG was encephalitogenic in 2D2-FIG-*Rag1*$^{-/-}$ mice but not in 2D2-FIG mice. Likewise, GMCSF-MOG was an effective prophylactic in Treg-sufficient C57BL/6 mice and prevented active EAE. Overall, these studies provide evidence that GM-CSF is an effective tolerogenic adjuvant when combined with low-efficiency peptides that fall below the CD40L/CD40 triggering threshold. Thus, a subthreshold CD40L/CD40 response delimits a critical parameter needed for antigen-specific tolerance and expansion of pre-existing Treg populations.

A SINGLE-CHAIN GMCSF-MOG TOLEROGENIC VACCINE EXPANDS MOG-SPECIFIC $CD25^+$ $FOXP3^+$ REGULATORY T CELLS THROUGH LOW-EFFICIENCY ANTIGEN RECOGNITION EVENTS TO INHIBIT EXPERIMENTAL AUTOIMMUNE ENCEPHALOMYELITIS

A Dissertation

Presented To the Faculty of the Department of Microbiology and Immunology

Brody School of Medicine at East Carolina University

In Partial Fulfillment of the Requirements for the Degree of

Doctor of Philosophy in Microbiology and Immunology

by

Cody Deumont Moorman

December 2019

© Cody Deumont Moorman, 2019

A SINGLE-CHAIN GMCSF-MOG TOLEROGENIC VACCINE EXPANDS MOG-SPECIFIC $CD25^{+}$ $FOXP3^{+}$ REGULATORY T CELLS THROUGH LOW-EFFICIENCY ANTIGEN RECOGNITION EVENTS TO INHIBIT EXPERIMENTAL AUTOIMMUNE ENCEPHALOMYELITIS

By

Cody Deumont Moorman

APPROVED BY:

DIRECTOR OF DISSERTATION: _____
Mark D. Mannie, Ph.D.

COMMITTEE MEMBER: _____
Isabelle M. Lemasson, Ph.D.

COMMITTEE MEMBER: _____
R. Martin Roop II, Ph.D.

COMMITTEE MEMBER: _____
Rachel L. Roper, Ph.D.

COMMITTEE MEMBER: _____
Mary Jane Thomassen, Ph.D.

CHAIR OF THE DEPARTMENT OF MICROBIOLOGY AND IMMUNOLOGY: _____
Everett C. Pesci, Ph.D.

DEAN OF THE GRADUATE SCHOOL: _____
Paul J. Gemperline, Ph.D.

ACKNOWLEDGEMENTS

I would like to attest my upmost appreciation and gratitude to the individuals whose knowledge, kindness, and patience made this dissertation a reality. I would like to recognize the Graduate Program Committee for accepting me into the Department of Microbiology and Immunology in 2014. This opportunity was presented to me at a defining time in my life where I was deciding between a career in science research, which I loved, or pursuing a career in quality control in the pharmaceutical industry. I can confirm that becoming a research scientist has enhanced my life by allowing me to embrace my inquisitive, curious, and creative nature. Thank you for identifying my potential and presenting me with this opportunity and the financial support to make it possible.

I would like to recognize my advisory committee members Drs. Isabelle Lemasson, Marty Roop, Mary Jane Thomassen, and Rachel Roper. I appreciate your time, advice, patience, and instruction which has been instrumental for both my education and professional development. Thank you all for your guidance and encouragement over the past 5 ½ years. My utmost gratitude goes to my mentor Dr. Mannie. I am grateful for his time, patience, advice, expertise, leadership and efforts. He has fueled my love for immunology as a science by demonstrating how incredibly complex yet, somehow, still simple the immune system is. The immense impact Dr. Mannie's has had on my development as a person and scientist is more that I can ever give him credit for here. Thank you, Dr. Mannie.

I would like to thank my parents Mark and Denise Moorman and my brother Joshua for their love and support. Thank you for encouraging my interest in biology. I would like to thank my grandparents Elizabeth and Robert Joyce for their love, kindness, and support. I would like to

thank my friends Alex Bastian, Alex May, Alice Carson, Amanda Sanchez, Alyssa Sparacio, Chelsea Schnepf, Kathryn Macallister, Laura Hamilton, Max Evans, Monica Speed, Rachel Hughes, Ra-un Campbell, Stephanie Bernedo, and Taylor Holste for their love and support. Thank you for caring about me, visiting me in a less-than-exciting city, taking my frequent calls, traveling with me, and opening up your homes when I needed to escape.

TABLE OF CONTENTS

LIST OF TABLES

LIST OF FIGURES

LIST OF ABBREVIATIONS

2D2	MOG35-55 and NFM13-37-specific T cell clone
ADCC	antibody-dependent cellular cytotoxicity
APC	antigen presenting cell(s)
APL	altered peptide ligand(s)
BBB	blood-brain barrier
BCR	B cell receptor(s)
Breg	regulatory B cell(s)
CD	cluster of differentiation
CD25	IL-2 receptor alpha chain
CFA	complete Freund's adjuvant
CHO-S	chinese hamster ovary cells
CIS	clinically isolated syndrome
CMV	Cytomegalovirus
CNS	central nervous system
CPM	counts per minute
CTLA-4	cytotoxic T lymphocyte antigen-4
DC	dendritic cell(s)
DMT	disease modifying therapy(s)
DNA	deoxyribonucleic acid
EAE	experimental autoimmune encephalomyelitis
EBV	Epstein-Barr virus

FACS	fluorescence activated cell sorting
FBS	fetal bovine serum
Fc	fragment crystallizable region
FDA	Food and Drug Administration
FIG	FOXP3-IRES-GFP, FOXP3 reporter
FOXP3	forkhead box P3
GFP	green fluorescent protein
GM-CSF	granulocyte-macrophage colony stimulating factor
GMCSF-MBP	GM-CSF fused to the MBP39-87
GMCSF-MOG	GM-CSF fused to the MOG35-55 peptide
GMCSF-NAg	GM-CSF fused to a neuroantigen
GMCSF-OVA	GM-CSF fused to the OVA323-339 peptide
GMCSF-PLP	GM-CSF fused to the PLP139-151 peptide
HBSS	Hank’s balanced salt solution
HEK	human embryonic kidney cells
HLA	human leukocyte antigen
HSCT	hematopoietic stem cell transfer
IDO	indoleamine 2,3-dioxygenase
IL	interleukin
IFN-β	interferon-beta
IFN-γ	interferon-gamma
Ifngr1	interferon gamma receptor 1 gene
i.p.	intraperitoneal

IPEX	immunodysregulation polyndocrinopathy enteropathy X-linked syndrome
iTreg	induced regulatory T cell
IV	intravenous
JCV	John Cunningham virus
LAG-3	lymphocyte-activation gene-3
LAP	latency associated peptide
mAb	monoclonal antibody
MACS	magnetic-activated cell sorting
MBP	myelin basic protein
M-CSF	macrophage-colony stimulating factor
MFI	mean fluorescent intensity
MHC	major histocompatibility complex
MHCI	major histocompatibility complex class I
MHCII	major histocompatibility complex class II
MOG	myelin oligodendrocyte glycoprotein
MS	multiple sclerosis
NAg	neuroantigen
NFM	medium neurofilament
nmole	nanomole(s)
NO	nitric oxide
NOD	non-obese diabetic
OTII	OVA323-339-specific T cell clone

OVA	ovalbumin
PBMC	peripheral blood mononuclear cells
PDL-1/2	programmed death-ligand-1/2
PD-1	programmed cell death-1
PLP	proteolipid protein
PML	progressive multifocal leukoencephalopathy
PPMS	primary progressive multiple sclerosis
pTreg	peripheral regulatory T cell
Ptx	pertussis toxin
RA	retinoic acid
Rag1	recombination activating gene 1
RBC	red blood cell(s)
rDC	regulatory dendritic cell(s)
RNA	ribonucleic acid
RRMS	relapsing-remitting multiple sclerosis
SC	subcutaneous
SD	standard deviation
SDS-PAGE	sodium dodecyl sulfate-polyacrylamide gel electrophoresis
SEM	standard error of the mean
SPMS	secondary progressive multiple sclerosis
Tcon	T conventional cell
TCR	T cell receptor
TGF-β	transforming growth factor-beta

TH1	T helper 1
TH2	T helper 2
TH17	T helper 17
TSDR	Treg-specific demethylated region
Treg	regulatory T cell
tTreg	thymic regulatory T cell
Tresp	T responder cell
Tr1	type 1 regulatory T cell
Vα3.2	alpha chain of the 2D2 TCR clone
Vβ11	beta chain of the 2D2 TCR

CHAPTER 1

INTRODUCTION

1.1 Immune tolerance a brief overview

Immune tolerance is a state in which the immune system is unresponsive to a set of antigens. Maintaining immune tolerance to self-antigens is required for immune homeostasis and the prevention of autoimmune disease. On the other hand, the ability to effectively respond to foreign antigens is crucial for an effective immune defense. T and B cells are required for antigen-specific adaptive immune responses (1). Antigen specificity is determined by the T cell receptor (TCR) or B cell receptor (BCR) which are generated from random gene rearrangement. The random rearrangement of TCR and BCR generates a myriad of unique receptors that are capable of recognizing a multitude of antigens which can respond to any number of potentially harmful pathogens. Consequently, TCR and BCR are also generated that can recognized self-antigens and lead to the loss of self-tolerance. Therefore, the immune system must purge or suppress these autoreactive lymphocytes in order to maintain self-tolerance (2).

Central tolerance is a mechanism by which autoreactive T and B cells are purged from the lymphocyte repertoire. During T cell development in the thymus, newly rearranged TCR are tested against self-peptides in major histocompatibility complexes class I and II (MHCI and MHCII). T cells are first tested in the thymus cortex by specialized cortical thymic epithelial cells which express a unique proteasome that generates a diverse set of self-peptides/MHC. The T cell repertoire is further refined in the thymus medulla by specialized medulla thymic epithelial cells which express Aire, a transcription factor that drives the expression of non-thymic genes, generating a comprehensive set of self-peptides/MHC. In the thymus, T cells with TCR that

strongly recognize self-antigen/MHC are negatively selected and undergo apoptosis. T cells with TCR that do not interact with MHC molecules die from neglect due to a lack of survival signals. T cells with TCR that weakly recognize self-antigen/MHC are positively selected and compose the peripheral T cell repertoire. Finally, T cells with TCR that recognize self-antigen/MHC with an intermediate-affinity differentiate into regulatory T cells (Tregs) (3). Likewise, autoreactive B cells are purged during development in the bone marrow based on self-reactivity. B cells that receive strong BCR signals from self-proteins are negatively selected and undergo apoptosis, while weakly reactive B cells are positively selected and compose the peripheral B cell repertoire (4). The proper selection of the T and B cell repertoire is a fundamental mechanism for preventing the development of autoimmunity (5, 6).

Negative thymic selection, however, is incomplete and autoreactive T cells are found in the peripheral T cell repertoire (7). Peripheral tolerance is maintained by regulatory mechanisms that ensure peripheral autoreactive T cells are inactivated, deleted, or suppressed. One mechanism which maintains peripheral tolerance is the induction of apoptosis or anergy in autoreactive T cells. High-affinity antigen-recognition events during homeostatic conditions in the absence of costimulatory molecules induces T cell anergy and apoptosis effectively eliminating autoreactive T cells (8). However this mechanism proves ineffective in inflammatory environments when costimulatory molecules are expressed. Under such circumstances, peripheral tolerance is maintained by Tregs which exert dominant antigen-specific immune suppression in order to prevent the activation of self-reactive T cells (9). Tregs are essential for the prevention of autoimmunity. For example, humans and mice that lack Tregs as a result of nonsense mutation in FOXP3, the Treg lineage transcription factor, develop a fatal autoimmune disease known as immunodysregulation polyendocrinopathy enteropathy X-linked and Scurfy

respectively (10, 11). Furthermore, experimental depletion of Tregs can exacerbate or induce autoimmune disease in animals (12).

There are two main subsets of Tregs. Thymically-derived Tregs (tTregs) which differentiate in the thymus and peripherally-induced Tregs (pTregs) that are generated from naive T cells in the periphery. Naïve T cells can differentiate into pTregs during inefficient antigen recognition or during antigen stimulation in the presence of Treg lineage-skewing molecules such as TGF-β, IL-2, and retinoic acid (RA) (13). Anatomical compartments such as the mucosa, gut, lungs, skin, and liver favor pTreg induction in order to maintain tolerance to harmless extended self-antigens such as food, allergens, and the commensal microbiota (14-17). However, pTregs are notoriously plastic and can lose their immunosuppressive phenotype in inflammatory environments (18). Both tTregs and pTregs are maintained by pools of self-antigen/MHCII and low levels of IL-2 which directly support FOXP3 expression and Treg effector function (19). The expression of high levels of CD25 (IL-2 receptor α-chain), Neuropilin 1, and Helios have been shown to stabilize the Treg phenotype (20-23).

Tregs are activated by their cognate self-antigen and exert many effector functions in order to suppress local inflammation and autoimmune responses. Tregs suppress autoreactive immune responses through the production of anti-inflammatory cytokines such as IL-10, TGF-β, and IL-35 together with suppressive molecules such as indoleamine 2,3-dioxygenase (IDO) and galectin-1. These molecules reduce antigen presenting cell (APC) activation, reduce costimulatory molecule expression, induce effector T cell apoptosis or anergy, and can recruit naïve T cells into the Treg lineage. Tregs also produce cytotoxic molecules including granzymes and perforin that induce apoptosis of T conventional cells (Tcon) and APC. Tregs also express CTLA-4 and LAG3 which directly block costimulatory molecules (e.g., CD80 or CD86) and

MHCII molecules respectively to block T cell activation. Additionally, Tregs can sequester the T cell growth factor IL-2, deplete local glucose, and breakdown extracellular ATP which serves to reduce effector T cell proliferation (21, 23, 24). Other regulatory cell subsets such as Type 1 regulatory T cells (Tr1), regulatory B cells (Bregs), and regulatory dendritic cells (rDC) also participate in the maintenance of peripheral tolerance (25-27).

Tolerance to one antigen can be spread to another distant antigen via a mechanism of infectious tolerance. Tregs mediate infectious tolerance through the formation of a suppressive microenvironment. Tregs that recognize their cognate antigen/MHCII on APC are activated, inducing effector functions which reduce APC activation and suppress nearby T cells (28). Therefore, if antigens A and B are presented on the same APC, a Treg specific for antigen A can suppress T cells that recognize antigen B at the surface of the APC. During this process the antigen A-specific Treg can not only suppress the antigen B-specific T cells but can also induce the antigen B-specific T cell to become a pTreg through the production of TGF-β (29). The newly generated antigen B-specific pTreg can subsequently suppress antigen B-specific immune responses and further spread tolerance to yet other antigens. Therefore, immune responses against numerous self-antigens presented on a single APC can be suppressed by a limited number of Tregs which recognize only a few of the total self-antigens presented (28).

These regulatory mechanisms are critical for maintaining immune homeostasis and resolving ongoing inflammation. However, Tregs and Tcons must be in balance. If Tregs dominate immune responses, they can exert broad immunosuppression and prevent clearance of pathogens and aid the development of cancers. Conversely, if Tcons dominate the immune responses, autoimmune diseases can arise (19). Just as tolerance can be spread so can immunogenic responses via a mechanism of epitope spreading. Antigen-specific T cell responses

can be diversified during inflammation, whereby the primary immune response provides sufficient momentum to drive the activation of T cells that recognize unrelated epitopes at the site of inflammation. Epitope spreading is beneficial during the clearance of pathogens, but can serve to exacerbate autoimmune disease (30).

Self-tolerance is a robust system that prevents autoimmunity and allows an effective adaptive immune responses to pathogens. However, immune tolerance fails in an estimated 50 million Americans who suffer from autoimmune disease. Developing therapies which reinforce regulatory mechanisms and reestablish the balance between Treg and effector T cells could provide therapeutic relief and potentially cure autoimmunity (31).

1.2 Multiple Sclerosis a brief overview

Multiple Sclerosis (MS) is a debilitating autoimmune disease of the central nervous system (CNS) and is the leading cause of non-traumatic disability in young adults. MS is a complex disease driven by both genetic and environmental factors that result in immunological insult to myelin and the formation of inflammatory lesions in the white and grey matter of the brain (32). MS is a heterogeneous disease that results in a variety of symptoms, the most common being weakness, fatigue, pain, depression, and visual impairments while less common yet more severe symptoms including varying levels of paralysis. The diverse clinical manifestations correlate with timing and location of the inflammatory lesion within the brain (33).

There are currently an estimated 913,000 individuals afflicted by MS in the United States alone and MS prevalence is increasing worldwide due to enhanced screening and evolving environmental triggers (34, 35). MS exerts profound socioeconomic impacts on patients and their

family affecting career, education, family planning, and relationship decisions while also imposing a heavy financial burden due to the enormous cost of disease management (36, 37). MS is typically diagnosed between the ages of 20-40 and is 2 to 3 times more prevalent in women than men (33).

The first clinical sign of MS is the development of clinically isolated syndrome (CIS) which is a self-limiting neurological episode resulting from CNS inflammation and demyelination. CIS is not diagnostic but predictive of MS since 60-85% of patients with CIS are eventually diagnosed with MS. The diagnosis of MS is made following a second neurological episode that is temporally and spatially separate from the inflammatory lesions involved in CIS (38). There are 3 clinically distinct forms of MS. Relapsing remitting MS (RRMS) is the most common form of MS and is characterized by periods of disease relapses in which CNS inflammation and symptoms are exacerbated followed by periods of remission in which patients partially recover. Over time, relapses cause increasing CNS damage which alters MS pathogenesis from an inflammation-driven disease into a neurodegenerative disease known as secondary progressive MS (SPMS). It is estimated that 90% of patients with RRMS will transition into SPMS within 25 years of their initial RRMS diagnosis (39). The third type of MS is primary progressive MS (PPMS) which is relatively rare and accounts for about 15% of total MS cases. SPMS and PPMS are characterized by steadily increasing neurodegeneration and CNS atrophy resulting in steadily increasing disability without periods of relapse (40). The pathogenesis of PPMS and SPMS are poorly understood, however it appears to be somewhat independent of inflammation since immunosuppressive drugs have little effect on managing these forms of MS (41).

MS is a complex disease that arises from the combination of environmental and genetic risk factors. The genetic component of MS can be realized when studying MS aggregation within autoimmune susceptible families. It was determined that the risk of developing MS was increased 115 fold for a monozygotic twin, 10-15 fold for sibling or parent, and 5 fold for a second-degree relative of an individual with MS, while there was no increased risk among non-related spouses and adopted children (42, 43). Furthermore, MS is more common in individuals of European descent and relatively rare in individuals of African, Asian, and Native American descent again suggesting a genetic component to the disease (44, 45). Genome-wide association studies have been able to identify individual alleles and single nucleotide variants that are involved in the development of MS (46). The strongest genetic association with the development of MS is linked to a span of 160 genes on chromosome 6p21.3 which are directly involved in immune function and include the MHC genes. To date, the MHCII allele HLA-DRB1*15:01 has the strongest individual risk association with MS and has a detectable gene dose effect and increases the odds of developing MS by about 3 fold. Interestingly, certain MHC class I alleles are protective and negatively associated with the development of MS (47). Overall, 110 non-MHC risk variants have been identified and include the genes for IL-7 receptor alpha, IL-2 receptor alpha, and myelin oligodendrocyte glycoprotein (MOG) (48-50). There are over 200 identified risk variants that are linked to the development of MS. The individual effects of a single gene variant is relatively small. However, when combined, these genetic factors account for about 30% of the total risk of developing MS (46, 51).

The environmental factors that drive MS can be divided into two groups. First are environmental factors that cause broad immune dysregulation and second are environmental stimuli that trigger myelin-reactive lymphocyte activation (52). Environmental factors such as

sun-exposure, obesity, and smoking are linked to immune dysregulation and the development of MS (53). Geographical studies revealed that MS prevalence surges with increasing latitude. These observations indicated that decreased sun exposure at high latitudes led to decreased levels of vitamin D which favored immune dysregulation. Studies have shown that reduced levels of vitamin D lead to decreased levels of anti-inflammatory mediators such as Tregs and the cytokines IL-10 and TGF-β. Reduced vitamin D also leads to the increased production of pro-inflammatory mediators such as T helper type 1 and 17 cells (TH1 and TH17) and the cytokines IFN-γ, TNF-α, IL-6, IL-12, and IL-17 which skew the immune response towards inflammation (54). Obesity is another factor that causes extensive immune dysregulation. Obesity induces a state of chronic low-grade inflammation that favors pathogenic TH1 and TH17 cells and decreases the frequency of anti-inflammatory Tregs and Bregs (55, 56). Individuals with a body mass index that exceeded 27 kg/m^2 at 20 years of age had a 2 fold increased risk of developing MS as compared to normal weight controls (57). Smoking also increases the risk of developing MS by 1.5 fold and exacerbates existing MS by increasing the rate of RRMS transitioning into SPMS (58). Additional environmental factors such as an aberrant microbiome, reduced vitamin A, and increased chemical exposure can cause immune dysregulation and favor the development of MS (59-61).

The second group of environmental stimuli consist of viral and microbial agents which trigger the activation of autoreactive lymphocytes through molecular mimicry or bystander activation to unleash MS. Molecular mimicry is when pathogens and their host have proteins that share homologous amino acid sequences (62). It has been suggested that molecular mimicry is driven by evolutionary pressure that instigates pathogens to adopt host-like proteins to act as camouflage in order to prevent immune recognition (63). Consequently, immune responses

directed toward these pathogens inadvertently activate self-reactive lymphocytes that recognize both pathogen and self-antigens to cause autoimmunity (62). Bystander activation is another mechanism that can unleash self-reactive lymphocytes. Pathogen-specific immune responses causes the activation of APC which upregulate costimulatory molecules and produce pro-inflammatory cytokines that favor the activation of self-reactive T cells. For example, an immune response to a CNS tropic virus will cause CNS inflammation, cell damage, and release of inflammatory mediators which in turn overcome local regulatory mechanisms allowing the activation of self-reactive effector T cells in the CNS to drive autoimmunity. Additionally, virus may play a direct role in immune mediated CNS inflammation in which chronic CNS infection of myelin, neurons, microglia, B cell or astrocytes elicits a viral-specific immune response causing CNS inflammatory lesions (64).

The putative agents that might drive these processes and MS include Epstein-Barr virus (EBV), Human herpes virus 6, Varicella-zoster virus, Human endogenous retroviruses, Cytomegalovirus (CMV), *Clostridium perfringens*, and *Chlamydophila pneumoniae* (65-67). However, it is unclear which pathogens or how many pathogens are directly linked to the development of MS. EBV is a favored putative cause of MS. For example, almost 100% of patients with MS are seropositive for EBV antibodies indicating a prior infection, and MS is extremely rare in EBV negative patients. Additionally, patients that present with delayed EBV resulting in mononucleosis have a 2.3-fold increase in risk of developing MS. Studies have also shown that EBV has protein peptides that expand and activate cross-reactive T cells that recognize myelin basic protein (MBP), a dominate component of myelin, through molecular mimicry. Additionally, persistent EBV infection can assist in the maintenance, differentiation, and activation of autoreactive B cells. Studies also suggest that EBV infection increases blood

brain barrier (BBB) permeability allowing leukocyte infiltration (68). While there is mounting evidence for the involvement of EBV in MS, there is no causal link, and evidence suggests that other viral and microbial agents can also drive the development of MS (67).

MS is widely considered to be a $CD4^+$ T cell-driven disease. It is hypothesized that autoreactive $CD4^+$ T cells are activated and expanded in the periphery by molecular memory and/or bystander activation and subsequently cross the BBB. Once in the CNS T cells are reactivated by local APC presenting myelin antigens (69). Reactivation of these myelin-reactive T cells subsequently drives effector functions resulting in the recruitment of $CD8^+$ T cells, B cells, macrophages, and monocytes driving the formation of demyelinating lesions (70). Studies using experimental autoimmune encephalomyelitis (EAE), the animal model of MS, have shown that both TH1 and TH17 $CD4^+$ T cells have pathogenic roles in MS. For example, adoptive transfer of myelin-reactive TH1 or TH17 T cells are sufficient to drive experimental EAE. Additionally, blockade of the TH17 effector molecules IL-17 and IL-23 ameliorate EAE. Both TH17 and TH1 cells are found in MS lesions and are increased in the peripheral blood mononuclear cells pool (PBMC) during the development of MS and during relapses (52, 69, 71). Furthermore, skewing T cells away from TH1 and TH17 lineages and toward a TH2 phenotype has shown therapeutic benefit in EAE and MS. (72, 73)

$CD8^+$ T cells are also found in MS lesions at increased frequencies compared to $CD4^+$ T cells. However, the role of $CD8^+$ T cells is unclear. Evidence suggests that $CD8^+$ T cells participate in both pathogenic and regulatory mechanisms in MS. For example, $CD8^+$ T cells have been shown to damage oligodendrocytes and neurons, and the abundance of $CD8^+$ T cells directly correlates with axonal damage. Additionally, $CD8^+$ T cells express a unique set of TCR suggesting they participate in an antigen-specific immune response (74). However, $CD8^+$ T cells

also have regulatory properties since CD8 knockout mice exhibit increased EAE severity, and adoptive transfer of myelin-specific $CD8^+$ T cells can ameliorate EAE (75). Furthermore, certain MHCI genes which directly stimulate $CD8^+$ T cells are associated with protection from the development of MS (51).

B cells are also thought to play a role in disease pathogenesis because clonally expanded B cells and oligoclonal immunoglobulins are present in the CNS of MS patients. Increased levels of B cell activity and oligoclonal bands are correlated with disease progression. Furthermore, patients with advanced MS develop ectopic tertiary lymphoid structures within the CNS that support plasma cells and B cell persistence (76). Myelin-specific antibodies have been identified in MS patients and have been shown to participate in demyelination in conjunction with complement activation. Interestingly, the clinical success of a B-cell depleting antibody in the treatment of MS has illuminated a previously unappreciated role for B cells that is independent of antibody production since the therapy spares plasma cells. Evidence suggests B cells act as important APC that support pathogenic TH1 and TH17 T cells leading to increased disease severity (77). Conversely, B cells including Bregs have been implicated in regulatory roles through the production of anti-inflammatory cytokines IL-35 and IL-10 (25, 78).

Myeloid cells such as resident microglia and infiltrating macrophages, monocytes, and DC are found in MS lesions and outnumber lymphocytic cells. Myeloid cells are suggested to have both pro and anti-inflammatory functions in MS. Myeloid cells are important APC that can activate disease-driving T cells through the expression of costimulatory molecules and pro-inflammatory cytokines. Additionally, myeloid cells can produce cytotoxic molecules that induce cell damage (79). For example, monocytes can drive CNS inflammation by increasing BBB permeability via the production of metalloproteases and make pro-inflammatory cytokines like

IL-6 and IL-12 (80, 81). Monocyte infiltration is directly correlated with patient relapses and the level of MS severity. Additionally, macrophages and microglia can produce reactive oxygen species, nitric oxide, and bind myelin-specific antibody via Fc receptors resulting in antibody-dependent cellular cytotoxicity (ADCC) of oligodendrocytes and neurons, exacerbating disease (82, 83). However, myeloid cells can also suppress CNS inflammation by removing CNS debris and by producing anti-inflammatory cytokines. For example, M2 macrophages, which have an anti-inflammatory profile, make regulatory cytokines such as IL-10, TGF-β, and IL-4 that can resolve neuro-inflammation (84) .

Regulatory subsets such as Tregs, Tr1, and Bregs are dysregulated in MS. Studies have reported that Treg numbers, suppressive capacity, and migratory abilities are reduced in MS patients as compared to healthy controls (52, 85). For example, Tregs from MS patients are less efficient at controlling effector T cell proliferation and express less FOXP3 (86, 87). Although, significant differences in total Treg numbers are not observed, MS patients have reduced numbers of $CD39^+$ Tregs and recent thymic emigrant Tregs as compared to healthy controls. These Treg subsets are associated with enhanced suppressive capabilities and their reduction represents a Treg deficiency in MS patients (88, 89). Finally, there is evidence that chemokine receptors are dysregulated on Tregs which prevent Treg migration into the CNS (90). Bregs and Tr1 cells are also impaired in MS and have reduced suppressive capabilities as a result of reduced IL-10 production (91, 92) .

1.3 EAE the animal model of MS

EAE is an inducible inflammatory disease of the CNS that has many clinical, immunological, and histological similarities to MS. Interestingly, the first known examples of induced CNS autoimmunity were complications following smallpox, measles, and rabies

vaccinations in humans. It was subsequently determined that the vaccine-induced encephalitis was not due to the viral agents but a result of contaminating rabbit CNS tissues which stimulated CNS-directed autoimmunity. Following these observations many different models of EAE have been developed in small rodents and non-human primates to model CNS inflammation and MS (93).

EAE, like MS, is a $CD4^+$ T cell driven disease. Myelin-reactive T cells infiltrate the CNS and are activated by their cognate antigen on local APC eliciting effector functions and the recruitment of B cells, macrophages and monocytes. The activation of this immune cascade drives the formation of inflammatory lesions which form focal plaques that are histologically similar to the lesions seen in MS (94, 95). The spatial and temporal locations of the lesions induce distinct clinical symptoms such as paralysis, spasms, vision impairment, vertigo, and torticollis (head tilt) which mimic some of the symptoms seen in MS (96). Like MS, EAE is also subject to regulatory mechanisms that involve Tregs, Tr1, and Bregs (97).

EAE can have varying disease courses depending on the animal species and strain used. Classical EAE is driven by inflammatory lesions in the spinal cord, optic nerve, and meninges that presents as an ascending motor paralysis which originates in the tail and progresses with severity to the forelimbs. Conversely, atypical EAE is driven by the formation of parenchymal lesions in the brain with or without spinal cord involvement and presents with varying symptoms including rigid unilateral paralysis, torticollis, and vertigo. Different subsets of MS patients exhibit unique lesion loads in the brain and spinal cord. A majority of MS patients develop lesions in the brain with or without spinal cord involvement which can be best modeled with atypical EAE. Conversely, a subset of patients present primarily with spinal cord lesions and can be best modeled with classical EAE (98). Classical EAE presents as a uniform disease and

therefore has increased statistical power. However, atypical EAE exhibits an assorted range of symptoms which makes data interpretation more difficult but better simulates the diverse clinical presentations of MS (96). The distinct clinical courses of EAE are also of interest because they can be used to model the different clinical presentations of MS. For example monophasic, relapsing remitting, and chronic EAE can model CIS, RRMS, and PPMS respectively (99).

There are two main procedures used to induce EAE. The first, active EAE, is induced with CNS tissue or myelin antigens such as MBP, proteolipid protein (PLP), and myelin oligodendrocyte protein (MOG) emulsified in complete Freud's adjuvant (CFA). Disease typically develops within 9-12 days and results in a variety of clinical presentations depending on the animal model used. For example, a monophasic self-limiting form of EAE can be induced with MBP^{69-87}/CFA in Lewis rats, while a chronic from of EAE can be induced with MOG^{35-55}/CFA in C57BL/6 mice. Additionally, a relapsing remitting form of EAE can be generated by immunizing SJL mice with $PLP^{139-151}$ /CFA. It was determined that SJL mice experienced relapses which were associated with the involvement of new myelin-peptide targets due to epitope spreading (100). Active EAE induction in SJL mice and C57BL/6 mice typically results in classical EAE, however neutralization of IFN-γ can induce atypical EAE in these strains (101, 102). Evidence suggest that IFN-γ inhibits brain inflammation while favoring spinal cord inflammation causing the distinct clinical symptoms (93).

The second method of inducing EAE is known as passive EAE and which is induced by the adoptive transfer of encephalitogenic myelin-reactive $CD4^+$ T cells. Myelin-reactive T cells can be generated by active immunization of animals or collected from myelin-reactive TCR transgenic mice. Myelin reactive T cells can be skewed *in vitro* using recombinant cytokines to generate TH1 or TH17 cells which can induce classical or atypical EAE respectively (71, 95).

Passive EAE allows researchers to study the effector phase of EAE because the induction phase is bypassed in this model (93).

Other animal models of MS include Theiler's murine encephalomyelitis virus (TMEV) and cuprizone intoxication-induced demyelination and CNS inflammation. TMEV is a small single stranded RNA virus in the Picornaviridae family which causes persistent viral infection of macrophages, microglia, and astrocytes causing $CD4^+$ T cell, macrophage and B cell infiltration into the brain and CNS inflammation. After a period of 45-55 days a $PLP^{139-151}$specific response can be detected. Over time the myelin-specific response can be spread via epitope spreading to additional myelin antigens. TMEV can induce a chronic-progressive demyelination leading to spastic hind limb paralysis in SJL and C57BL/6 mice. TMEV-induced demyelination is an important model because it mimics the possible viral etiology of MS (103). Cuprizone is a neurotoxic copper chelating agent which can be used to induce oligodendrocyte degeneration and death resulting in extensive demyelination and in the activation of numerous inflammatory pathways. The extent of demyelination is controlled by duration, dose, and frequency of cuprizone administration. Cuprizone-induced demyelination is mainly used to develop therapies designed to counteract demyelination and stimulate remyelination (104).

While EAE simulates clinical, immunological, and histological features of MS there are substantial differences which must be considered. A major disparity between EAE and MS is the use of an immunization step to induce EAE, while MS occurs spontaneously. Very few models of spontaneous EAE exist and most rely on the use of myelin-specific TCR transgenic mice in order favor disease development. Additionally, there are many genetic and phenotypic differences between the immune systems of rodents and humans. While differences exist, EAE

has been a powerful tool for deriving therapeutics, and understanding pathogenic and regulatory mechanisms which control MS (95).

1.4 Current therapeutics for the management of MS

There currently is no cure for MS. However, there are 16 FDA approved disease modifying therapies (DMT) that are used to manage MS. First-line therapies are immunomodulatory and have modest efficacy, however these therapies often cannot restrain disease development over time. When first-line therapies fail, more aggressive approaches are needed. These second-line therapies employ broad-spectrum immunosuppression to alleviate patient symptoms (32). At present all 16 available DMT are approved for the treatment of RRMS while only three are approved for the treatment of SPMS. Moreover, only one DMT, ocrelizumab, has been approved for the treatment of PPMS (105). Management of severe MS relapses which cause increased disability can be treated with a 3-5 day high-dose IV corticosteroids. However, corticosteroids are immunosuppressive and can cause osteoporosis, weight gain, and cataracts and long term use is inadvisable (106). Individual symptoms arising from CNS damage such as bladder dysfunction, fatigue, depression, dizziness, tremors, sexual dysfunction, and spasticity are managed with a wide variety of available medications that are not MS-specific (32).

The first-line therapies for MS include IFN-β (Avonex, Plegridy, Rebif, Betaseron and Extavia) and glatiramer acetate (Copaxone and Glatopa). IFN-β was the first FDA approved drug for the treatment of MS. IFN-β is a cytokine that is produced by a wide variety of cells that mediates anti-viral immunity by controlling the transcription of >1000 genes (107). IFN-β has a range of immunomodulatory and anti-proliferative properties that have proven beneficial for the treatment of MS. Frequent injection of IFN-β decreases CNS lesions, disease burden, and

reduces patient relapses. Evidence suggests IFN-β treatment decreases inflammatory cytokines, increases anti-inflammatory agents, prevents T cell activation, limits lymphocyte trafficking, and induces Tregs to mediate the beneficial effects seen in treatment of MS (108, 109). While IFN-β therapy is generally well-tolerated, common side effects include flu-like symptoms, headache, and injection site reactions. For unknown reasons, up to 30% of MS patients do not respond to IFN-β treatment. Furthermore, long term treatment can lead to the development of neutralizing antibodies against IFN-β which, in turn, limits therapeutic activity and impairs viral immunity (110, 111).

In addition to IFN-β, glatiramer acetate is a common first-line therapy for the treatment of MS. Glatiramer acetate is a peptide polymer comprised of repeating units of the amino acids, glutamic acid, lysine, alanine, and tyrosine that was designed to mimic MBP a putative immune target in MS pathology. Originally designed to induce EAE, glatiramer acetate had unexpected therapeutic activity and protected mice from the development of CNS inflammation. Evidence suggests an important immunomodulatory property of glatiramer acetate is the skewing of T cell phenotype from a pathogenic TH1 and TH17 to an anti-inflammatory TH2 phenotype, which is protective in MS (112).

The progressive nature of MS often renders the first-line immunomodulatory drugs ineffective and requires more aggressive immunosuppressive second-line therapies to manage patients' symptoms. Since MS is a T cell-mediated disease, therapies which effectively shut down the adaptive immune response have proven to be efficacious. Several mechanisms are utilized to impair the adaptive immune response including T and B cell depletion, immunocyte migration blockade, neutralization of effector molecules, and inhibition of T and B cell clonal expansion (113). The advent of monoclonal antibodies (mAb) has made it possible to target and

neutralize effector molecules and deplete immune cell subsets via ADCC and complement-dependent cytotoxicity and have changed the landscape of MS therapeutics (114).

The mAb natalizumab (Tysabri) and small molecules fingolimod (Gilenya) and siponimod (Mayzent) are therapeutics which block T cell migration in order to achieve immunosuppression and treat MS (113, 115). Natalizumab was the first FDA approved mAb for treatment for MS and is specific for the adhesion molecule alpha-4 integrin. Blockade of alpha-4-integrin prevents the migration of activated immunocytes across the BBB into the CNS. Fingolimod and siponimod are partial agonists of the sphingosine 1-phosphate receptors which are required for lymphocyte egress from the lymph nodes. Fingolimod and siponimod induces the internalization and degradation of sphingosine 1-phosphate receptors leading to lymphocyte sequestration within the secondary lymphoid tissues (113). Prevention of immunocyte migration into the CNS reduces patient relapses and neuro-inflammation, however, the lack of CNS immunosurveillance can result in the reactivation of John Cunningham virus (JCV) leading to fatal CNS inflammation known as progressive multifocal leukoencephalopathy (PML). JCV is highly prevalent, affecting 50% of the population but it is typically benign and controlled by the immune system. However the risk of JCV reactivation increases with the duration of therapeutic immunosuppression and approximately 4.3 out of 1,000 patients treated with natalizumab eventually develop fatal PML (116).

Leukocyte depletion strategies have also been effective in managing MS. The mAb alemtuzumab (Lemtrada) is specific for CD52 and depletes T and B cells while the mAb ocrelizumab (Ocrevus) is specific for CD20 and depletes B cells. A third mAb, daclizumab (Zinbryta), which depletes $CD25^+$ T cells was previously available but was removed from the market by the manufacturer over safety concerns (117). Lymphocyte depletion essentially resets

the adaptive immune system to achieve therapeutic success. However, the temporary depletion of lymphocytes leaves patients highly vulnerable to infections (118). Alemtuzumab is also associated with the frequent occurrence of secondary autoimmunity which usually affects the thyroid (119). T cell-depletion can also be achieved with the small molecule dimethyl fumarate (Tecfidera). Evidence suggest that dimethyl fumarate is immunomodulatory and has beneficial outcomes due to the induction of lymphopenia and the activation of anti-oxidant pathways. Dimethyl fumarate has adverse side effects and, like natalizumab and fingolimod, is linked to the development of PML (120).

Preventing immune cell proliferation is another therapeutic strategy used in the treatment of MS. Cytotoxic agents are used to prevent immune cell proliferation and have shown varying levels of success. Mitoxantrone (Novantrone) is a chemotherapeutic agent which causes DNA crosslinking, DNA breaks, RNA damage, and inhibits topoisomerase which is required for DNA damage repair. Teriflunomide (Aubagio) is a selective inhibitor of dihydroorotate dehydrogenase which prevents de novo pyrimidine synthesis, thereby preventing DNA replication, while cladribine (Mavenclad) is a purine analog which inhibits DNA polymerase leading to cell cycle arrest. These extensive genetic disruptions induce apoptosis and prevent the proliferation of rapidly dividing cells such as the activated leukocytes participating in the pathogenesis of MS. However the high levels of cytotoxicity lead to a slew of side effects, some of which are life-threatening. Mitoxantrone has been known to lead to cardiotoxicity, therapy-related acute leukemia, and liver damage and has a lifetime cumulative dose limit of 140 mg per square meter of body surface area which reduces clinical use. Teriflunomide and cladribine are also associated with adverse side effects including hair loss, liver damage, and increased rates of infections (113).

There are several non-FDA approved therapies which have clinical relevance. Hematopoietic stem cell transplant (HSCT) has been conducted in severe cases of MS that are refractory to standard therapeutic intervention. Patient-derived hematopoietic stem cells can be harvested, expanded and reinfused into patients whose immune systems have been wiped out using chemotherapy. Following the HSCT patients' immune systems can be reconstituted and can function semi-normally "curing" MS. However due to the pre-existing neurological degeneration and the genetic and environmental causes of MS up to 30% of patients relapse (121). In addition to HSCT, plasma exchange or plasmapheresis is another non-FDA approved therapy that is associated with clinical benefit. Evidence suggests that plasmapheresis is beneficial in MS by removing myelin-reactive antibodies from circulation (122).

The clinical efficacy of a DMT directly correlates with the level of immunosuppression achieved and consequently with the level of adverse risk (123). Increased levels of immunosuppression leave patients susceptible to opportunistic infections and/or the development of cancers (124, 125). The risks and benefits of MS therapies are not fully understood yet due to the frequent release of new therapies and the lack of long term data. Evidence suggests that early diagnosis and therapeutic intervention can delay the short term (2-3 years) progression of MS. However, when analyzing long term outcomes (>3 years), DMT generally have little effect on the overall progression of MS (126). As MS progresses, the disease transitions from a manageable inflammatory disease into a less controllable neurodegenerative disease. PPMS and SPMS are primarily driven by neurodegeneration and are difficult to treat which is reflected by the relative lack of available therapies (127). Furthermore DMT exert a huge financial burden on patients and the healthcare system coming in at a yearly cost of 60,000 USD per patient (128).

Treatment options for MS have changed drastically over the last decade with the approval of 10 new DMT. Current DMT offer therapeutic relief for some patients with MS. However, DMT are far from ideal and have life-threatening side effects, come at an enormous cost, and do not alter the long-term trajectory of MS. The main problem with current MS therapies is the lack of disease-specific activity. DMT are immunomodulatory or immunosuppressive and impair overall immune function. Ideal therapies would only target the disease driving leukocytes while leaving the rest of the immune system intact. The development of targeted therapies are needed for the safe and effective treatment of MS (129).

1.5 Tolerogenic vaccines in development for the treatment of MS

Tolerogenic vaccines are a diverse class of antigen-specific therapies that are designed to restore self-tolerance without the induction of general immunosuppression making them highly attractive approaches for the treatment of MS. Tolerogenic vaccines intended for the treatment of MS will need to restore myelin-specific immune tolerance while preserving the integrity of the general adaptive immune response. The induction of myelin–specific tolerance should be an effective and potentially curative therapy for MS and have minimal side effects (130).

Because MS is a T cell-driven disease, tolerogenic vaccine strategies focus on attenuating the aberrant myelin-reactive $CD4^+$ T cell response. There are a number of ways to attenuate the pathogenic T cell repertoire which include the induction of anergy or apoptosis in effector T cells, skewing T helper cells away from pathogenic TH1 or TH17 subsets, and/ or enhancing immunoregulatory subsets such as Tregs (129). Numerous tolerogenic vaccines strategies have been devised that can be divided into 3 distinct groups based on the composition of the vaccine. The first group is peptide-based vaccines which are composed of myelin proteins with or without tolerogenic adjuvants, the second group includes DNA-based vaccines comprised of genetic or

viral vectors, and the third group is cell-based vaccines that utilize transfer of leukocytes to induce myelin-specific tolerance (131).

Tolerogenic vaccines are currently experimental as they are either preclinical or in early clinical trials. A major concern regarding tolerogenic vaccines is the potential to inadvertently sensitize instead of tolerize the antigen-specific immune response and therefore exacerbate disease. These fears were realized during a clinical trial that tested the efficacy of altered peptide ligands (APL) of MBP as a therapeutic for RRMS. APL were peptides that had amino acid substitutes that altered TCR-antigen recognition. The thought was that APL would lead to effector T cell anergy and apoptosis. However, when translated into human clinical trials the results were disastrous and resulted in a 62% increase in active lesions (131, 132). The clinical trial was halted and the field of tolerogenic vaccines was tainted. Thorough preclinical and clinical testing is required in order to determine the most effective strategies to induce myelin-specific tolerance. Rodent models of EAE have proven to be an effective experimental tool for deriving MS therapies. EAE is a relevant model for studying myelin-specific tolerance since EAE and MS share many of the same pathogenic and regulatory mechanisms. Murine models of EAE were used during the development of 9 of the current FDA approved DMT and have been crucial in determining the mechanisms by which DMT modulate MS (97).

A major challenge currently thwarting the development of tolerogenic vaccines is that the antigens driving MS are unknown. The myelin-specific T cell repertoire is complex and many CNS antigens have been suggested to play a role in disease development (133). There is a substantial body of evidence suggesting epitopes of MBP, MOG, and PLP are involved in the MS autoimmune response. For example patients with MS have increased levels of autoreactive antibodies and activated autoreactive T cells against MBP, MOG and PLP as compared to

healthy controls (134, 135). However there seems to be little consistency across patients regarding which epitopes drive disease. This is likely explained by the fact that each patient can display different myelin epitopes based on their MHC haplotypes. Therefore the myelin antigens that drive disease most likely vary drastically patient to patient. Additionally, the antigenic targets in MS might change over time as the disease progresses via epitope spreading. For example, MS might be initiated against an epitope of MOG, however as CNS damage progresses, other distinct epitopes of MOG and additional myelin proteins might be targeted therefore spreading the immune responses. Designing antigen-specific vaccines to an unknown and moving target is difficult (133, 136). It may be possible to overcome this hurdle by reinforcing immunological tolerance to a number of CNS proteins through the induction of myelin-specific Tregs which can resolve inflammation to unrelated CNS antigens through a mechanism of infectious tolerance (28, 137).

A common strategy among tolerogenic vaccines is to target myelin antigens to APC subsets that favor tolerogenic responses. DC are a diverse group of professional APC that direct both immunogenic or tolerogenic T cell responses. Numerous studies have described unique subsets of regulatory DC (rDC) that are able to drive tolerance through the induction of T cell anergy, apoptosis, or by expanding Tregs. Regulatory DC are phenotypically diverse, however they have common immunoregulatory features. First, rDC typically express low amounts of costimulatory molecules CD80, CD86, and CD40 as well as reduced levels of MHC molecules which results in inefficient T cell activation that can lead to effector T cell anergy and induction of Tregs. Second, rDC produce anti-inflammatory cytokines such as TGF-β and IL-10 which drive Treg differentiation and inhibit conventional T cells. Third, rDC express high levels of inhibitory molecules such as PDL-1/2, CTLA-4, FasL, and TRAIL which can induce T cell

apoptosis and anergy through direct contact with T cells. Finally, rDC produce inhibitory products such as RA, IDO and soluble CD25 that block T con expansion (27, 138, 139). Numerous other professional APC subsets have been described that favor tolerogenic responses. Directing myelin antigens to tolerogenic APC such as rDC can lead to the induction of tolerance and may be beneficial in the treatment of MS.

The most successful induction of antigen-specific tolerance in humans has been with peptide-based therapies used to treat allergic disease. Subcutaneous, oral, and transdermal administration of allergens has proven effective in treating allergic disease (140). Allergen vaccination essentially loads antigens into the skin, oral, and gut mucosa which favor tolerogenic responses. These anatomical compartments favor tolerance in order to maintain homeostasis to harmless environmental and microbial agents (141). The skin, oral, and gut mucosa express increased levels of anti-inflammatory molecules such as IL-10, TGF-β, RA, IDO, and prostaglandin E2 and have specialized APC subsets such as $CD103^+$ DC and Langerhans cells that favor immune tolerance and Treg responses (142-144). Evidence suggests that allergen-based vaccination expands allergen-specific Tregs which, in turn, attenuate the pathogenic antigen-specific $CD4^+$ T cell response to control allergic disease (145). The successful management of allergic disease has led to the exploration of peptide-based therapies for the treatment of MS.

Peptide-based vaccines have been tested in EAE and MS with varying success. The mechanisms through which these vaccines induced tolerance was determined to be dependent on the peptide dose. High-dose peptide therapy induced tolerance through the induction of T cell anergy and apoptosis, while low-dose peptide therapies induced immunodominant regulatory responses that included the expansion of Treg populations. The induction of immunodominant

regulatory responses are likely favorable to the induction of T cell anergy and/or apoptosis when devising therapeutic vaccines (144, 146, 147). Dominant regulatory responses are controlled by Tregs, TR1, and Bregs which are long lived cells that provide protection over years and can drive infectious tolerance providing protection against a number of CNS antigens. Conversely, T cell anergy can be overcome with strong antigenic stimulation and a bolus of IL-2 (148). Additionally, the induction of apoptosis does not eliminate all of the antigen-specific T cells and new thymically derived myelin-reactive T cells can be recruited and drive disease progression (149). Therefore high-dose peptide therapies would have to be administered regularly to maintain myelin-specific T cell depletion or inactivity and would likely only be effective against T cells with the same specificity as the peptide administered (150, 151).

Another variable that has proven difficult to solve is the best route of administration for peptide-based tolerogenic vaccines. Many factors such as the level of invasiveness and efficacy need to be taken in to account. The relative ease of administering myelin peptide via oral, intranasal, or transdermal sites provides ideal vaccine routes. Oral administration of MBP^{68-88} to Lewis rats, full length MBP to B10.PL mice, and $PLP^{139-151}$ to SJL mice prevented the development of EAE (146). Unfortunately, oral administration of myelin peptides have been unsuccessful thus far in human clinical trials. A phase-III clinical trial tested the efficacy of orally administrated bovine MBP + PLP and found no significant differences between the treatment and placebo groups (152). Alternatively, myelin antigens have been delivered to the mucosa through nasal administration. Intranasal administration of $PLP^{139-191}$, MBP^{1-11}, and MBP^{89-101} was found to induce tolerance in multiple murine models of EAE. However, the efficacy of intranasal peptide vaccines has not been tested in human clinical trials (146).

Transdermal administration of myelin peptides has shown promise in both preclinical EAE and in a human clinical trial. Transdermal administration of MBP^{1-11} and $PLP^{139-151}$ to B10.PL and SJL mice respectively protected mice from developing EAE and was dependent on regulatory $CD4^+$ $CD25^-$ T cells. A small clinical trial was conducted to test the safety and efficacy of transdermal administration of MOG, MBP and PLP in patients with RRMS. The clinical trial had positive outcomes and resulted in a reduction in annual relapses and in CNS inflammation. These results show therapeutic promise for transdermal application and needs to be replicated in a larger scale phase III clinical trial (146).

The administration of peptides via intramuscular, subcutaneous, intraperitoneal, intravenous, intrathymic, and pulmonary instillation are more invasive but have shown preclinical efficacy (146, 153-156) . These routes of peptide delivery have shown various levels of therapeutic benefit, however, the exact route that results in the most robust induction of tolerance is unclear. The differences in therapeutic efficacy between antigen delivery routes can be highlighted by a study that compared the delivery routes of $PLP^{139-151}$ and ICAM-1 in hyaluronic acid on the clinical outcomes in EAE. The ranked order of disease prevention as measured by the percent of disease free animals on day 25 was as follows: pulmonary instillation > intraperitoneal > intramuscular > intravenous > subcutaneous. Pulmonary delivery had the most robust activity and prevented EAE in 100% of the challenged mice while only 35% were protected by subcutaneous administration (156). This study emphasizes that the route of peptide delivery can have profound effects on tolerance induction. Studies are needed that compare dose, administration route, and vaccine frequency in order to determine the best strategies to drive antigen-specific tolerance. Several clinical trials have been carried out to investigate subcutaneous, intramuscular and intravenous peptide vaccines and have been shown to be safe,

and some have shown clinical efficacy reducing the rate of relapse and disease progression as measured by MRI (131). However, these therapies lacked robust efficacy and therefore need improvement (136).

Efforts to improve peptide-based therapies have been devised and include targeting myelin antigens to tolerogenic APC and the use of tolerogenic adjuvants. The immune response to myelin peptides can be directly modulated by the use of tolerogenic adjuvants which are a diverse group of molecules that skew the immune responses toward tolerogenic outcomes (157). Myelin peptides and tolerogenic adjuvants can be co-delivered in nanoparticles, microparticles, and liposomes for enhanced activity. Co-administration of myelin peptides with tolerogenic adjuvants including vitamin D, IL-10, TGF-β, GM-CSF, retinoic acid, rapamycin, and aryl hydrocarbon receptor ligands, have been shown to ameliorate EAE (158-160). For example, intra-lymph node injection of MOG^{35-55} and rapamycin, which is immunosuppressive, encapsulated in degradable poly (lactide-co-glycolide) microparticles was found to increase the number of Tregs and ameliorate EAE. The vaccine proved to be antigen-specific as the same microparticles that lacked MOG^{35-55} failed to ameliorate EAE (161). Another strategy to enhance naked peptide vaccines includes targeting antigens to specific APC that have regulatory functions. Targeting can be accomplished by tethering myelin antigens to antibodies, cytokines, and the Fc portion of immunoglobulin, which in turn bind their respective surface target and induce receptor mediated endocytosis leading to enhanced antigen presentation on the target APC (162-165). An effective example of antigen targeting was with the DEC-205 mAb which targeted tethered myelin antigens to $DEC205^+$ DC, an APC subset shown to favor the Treg lineage. Enhanced antigen presentation of myelin peptides on these $DEC205^+$ APC led to the

induction of Tregs and prevented EAE (166). These efforts have led to a wide variety of vaccine strategies that show promising preclinical efficacy.

A second group of tolerogenic vaccines are DNA-based vaccines. The goal of DNA-based vaccines is to introduce myelin genes into cell subsets that can presented the translated myelin peptides in MHCII molecules to induce tolerance. Early studies showed that intradermal injection of plasmid DNA encoding MBP could be internalized by local skin resident APC which in turn stimulated MBP-specific TH2 T cell responses and prevented the development of EAE (167, 168). DNA-vaccines have since been enhanced through the incorporation of genes encoding tolerogenic cytokines and by controlling the cell subsets that express the DNA-vaccine cargo by utilizing cell specific promoters. For example co-administration of a DNA vaccine that encoded MOG^{35-55} under the DC specific promoter Fascin1 and a DNA vaccine that encoded the cytokines IL-10 and TGF-β significantly suppressed EAE as it caused MOG to be expressed in a tolerogenic environment. However when MOG^{35-55} expression was controlled by the ubiquitously active CMV promoter no differences were observed in the EAE disease course (169). Therefore, including immunosuppressive cytokines and controlling the cell subset that expresses the DNA vector can shift vaccine outcomes.

Another DNA-based vaccine strategy is the use of viral vectors to deliver myelin genes. For example, Adeno-associated virus was utilized to deliver a gene construct which encoded full-length MOG under the control of a hepatocyte-specific promoter as the liver is a major site of peripheral tolerance induction. The vector was efficiently incorporated into the genome and MOG was expressed in hepatocytes resulting in the expansion of MOG^{35-55}-specific Tregs and the prevention of EAE (170). A major concern is that DNA vaccines might integrate into the genome and cause DNA mutations that increase the risk of developing malignancies.

Furthermore, autoimmune responses may be redirected to tissues which ectopically express myelin antigens. To date, two clinical trials have been reported which utilized a DNA-based vaccine which encoded full length MBP under the CMV promoter to treat patients with RRMS and SPMS. Both clinical trials determined the DNA vaccine was safe, however no statistical differences in annual relapse rates were found (131).

Cell-based tolerogenic vaccines utilize the transfer of autologous T cells, B cells, and APC to drive immune tolerance (75, 131, 138, 171). The possibility of using autologous T cells as a therapy was first realized in a study that showed immunizing Lewis rats with irradiated MBP-specific T cells could prevent MBP-driven EAE. Upon transfer, the MBP-specific T cells elicited anti-idiotypic responses against the MBP-specific TCR, and anti-ergotypic responses against activation markers such as CD25 which led to the clearance of activated MBP-specific T cells and attenuated disease. Autologous T cell vaccination has since been tested in 11 small early stage clinical trials and was shown to be safe. However, the results from these clinical trials vary greatly with some studies reporting a reduction in relapse rates and disease progression while others reported no differences (172).

Efforts in cell-based therapies have since focused on the transfer of autologous Tregs. Adoptive transfer of both antigen-specific and poly-clonal Tregs has been shown to ameliorate EAE. However, adoptive transfer of polyclonal Tregs can lead to general immunosuppression and are less effective at preventing EAE as compared to myelin-specific Tregs (173, 174). There are two major hurdles preventing clinical translation of Treg-based immunotherapies. First, Tregs are relatively plastic and can lose their immunosuppressive phenotype and convert into pathogenic T cells and exacerbate disease (175). Second, generating large numbers of pure Tregs has proven difficult due to the hyporesponsive nature of Tregs in vitro (176). Overcoming these

barriers will allow clinical translation of Treg therapies. Adoptive transfer of Bregs, myelin-specific $CD8^+$ T cells and rDC have also shown therapeutic benefit in models of EAE. However these therapies have not been tested in human clinical trials (75, 91, 138).

Cell-based and peptide-based vaccine platforms can be combined as an effective means of inducing myelin-specific tolerance. Most strategies focus on adoptive transfer of ex vivo-expanded rDC. loaded with myelin peptides. Regulatory DC can be derived ex vivo by incubating DC with immunomodulatory molecules such as dexamethasone, rapamycin, vitamin D, TGF-β, IL-10, and GM-CSF (27). These rDC can be loaded with myelin antigens and reinfused into mice to ameliorate EAE (138). Additional strategies have used myelin-coated apoptotic leukocytes for the treatment of EAE and MS. Apoptotic cells have been shown to trigger regulatory mechanisms that can lead to tolerance (177, 178). For example infusion of myelin-coupled apoptotic splenocytes resulted in antigen uptake by macrophages which in turn presented the myelin antigens, produced IL-10, expressed PD-L1, and expanded Tregs to ameliorate EAE. It was determined that Tregs were disposable for tolerance induction but were required for long-term maintenance of tolerance (179). These results suggested that both apoptotic/anergic responses established tolerance while Tregs maintained tolerance long term. A phase I clinical trial was completed using apoptotic autologous T cells coupled with myelin derived peptides. This study showed that the treatment was safe, feasible, and moderately effective at controlling disease progression (180). Additionally, there are three clinical trials underway that are investigating the safety and efficacy of myelin-loaded tolerogenic DC for the treatment of MS (131). The outcomes of these trials will determine the future promise of this vaccine platform for the treatment of MS.

Successful tolerogenic vaccines must be effective in the inflammatory environment found in MS patients. Many of the current preclinical vaccine strategies rely on steady-state homeostatic environments to drive tolerance and prevent induction of disease. As such, these strategies serve only as a pretreatment before the onset of EAE. While these strategies might prevent the initial development of MS, they will likely be ineffective at treating established disease with ongoing inflammation. Tolerogenic vaccines designed to treat active disease should be tested in the contexts of inflammatory environments as a therapeutic treatment after the onset of EAE (130). There are many promising tolerogenic vaccine platforms currently in development. However, none of the tolerogenic vaccines tested in MS have had robust clinical efficacy and none have received FDA approval (136). Therefore, efforts should be directed to developing vaccine platforms that induce robust tolerance and are efficacious in inflammatory environments. Strategies that expand Tregs are ideal because Tregs employ long-lived dominant regulatory mechanisms (181). Additionally, Tregs can establish tolerance to distant myelin antigens through mechanisms of infectious tolerance (28).

1.6 Cytokine-neuroantigen fusion proteins as tolerogenic vaccines

Cytokine-neuroantigen (NAg) fusion proteins are a class of preclinical tolerogenic vaccines designed to induce myelin-specific tolerance as a therapy for MS. The idea behind the vaccine platform was that cytokines could be used to target MHCII restricted myelin antigens to specific APC subsets that express those cytokine receptors. The vaccine was designed so that the cytokine would not only target NAg but would also concurrently provide immunomodulatory signals that favored the induction of $CD4^+$ T cell tolerance (130, 164, 182). The vaccine platform was based on the knowledge that both APC subset and local cytokine milieu influence T cell lineage decisions. Our lab hypothesized that individual APC subsets could be targeted based on

the differential expression of specific cytokine receptors. For example NAg fused to IL-4 would theoretically target the tethered NAg to B cells which express elevated levels of the IL-4 receptor. Our lab selected the immunomodulatory cytokines IFN-β, GM-CSF, M-CSF, IL-16, IL-2, and IL-4 and fused them with or without linker to immunodominant MHCII restricted neuroantigens that were encephalitogenic in rodent models of EAE. The vaccines were then tested for their ability to target NAg to specific APC subsets and modulate the immune response to protect rodents from EAE (130, 164, 182-190) .

The fusion proteins consisted of species-specific cytokines as the N terminal domain and dominant myelin peptides as the C- terminal domain (182). In one cytokine fusion protein (NAg-IL16), the NAg made up the N terminal domain while the cytokine was the C-terminal domain in order to persevere the optimal activity of IL-16 (183). The cytokine fusion proteins had the full activity of the free cytokine as measured via bioassays. The cytokines GM-CSF, M-CSF, IL-2, and IL-4 were chosen to target NAg to myeloid APC, macrophages, T cells, and B cells respectively. As designed, these vaccines showed an exquisite ability to load the tethered antigen into the target APC niche. GM-CSF, IL-2, and IL-4 fused to MBP^{73-87} were >1000 fold more potent than MBP^{73-87} alone at inducing the proliferation of MBP-specific $CD4^+$ T cells using DC, blastogenic rat T cells, and B cells respectively (182, 184, 185). Additionally, M-CSF fused to MBP^{73-87} resulted in 100 fold increase in antigen potency measured by antigen-specific T cell proliferation when cultured with myeloid APC. Covalent linkage of the cytokine domain to NAg was required for antigen targeting. These results were consistent with a model in which the cytokine targeted the tethered NAg to the cytokine receptor resulting in receptor-mediated endocytosis and enhanced NAg presentation on MHCII molecules. These studies showed that antigen targeting was dependent on the cytokine receptor since antigen targeting was blocked by

the additional free cytokine. For example, the antigen potency of GMCSF-NAg was blocked by free GM-CSF but not by M-CSF. Conversely, the antigen potency of MCSF-NAg was blocked by free M-CSF but not GM-CSF (185). The enhanced antigen potency was due to antigen stimulation of MBP-specific T cells and not due to mitogenic activity of the cytokines because T cell proliferation was blocked by a MHCII-specific mAb (164).

Cytokine fusion partners were not only selected based on their ability to target APC subsets but also on their immunomodulatory properties. The cytokines IL-2 and IL-16 were selected because of their ability to directly regulate $CD4^+$ T cell responses (164). For example, IL-2 was selected since it is a critical T cell growth factor and has been shown to stabilize Tregs through the induction and maintenance of FOXP3 expression (191). The cytokines GM-CSF and G-CSF were selected based on their ability to induce rDC which in turn expand Tregs (192, 193). Additionally, IFN-β was selected as a fusion partner because of its immunomodulatory properties that have proven beneficial in the treatment of MS (108).

Initial studies testing the tolerogenic activity of cytokine fusion proteins were performed in the Lewis rat model of EAE which can be induced using MBP^{73-87} in CFA. The vaccines were comprised of native rat cytokines fused to the encephalitogenic peptide MBP^{73-87}. The vaccines were tested as a pretreatment before the induction of EAE and as a therapeutic after the onset of EAE. The pretreatment regimen was utilized to determine if cytokine fusion proteins elicit tolerogenic memory responses which could prevent encephalitogenic challenge after the clearance of the physical vaccine. Conversely, the therapeutic treatment regimen was used to determine the vaccines' efficacies. The vaccines inhibited EAE as both a prophylactic and therapeutic in the ranked order as follows: GMCSF-NAg, IFNβ-NAg> NAg-IL16 > IL2-NAg> MCSF-NAg> IL4-NAg, and NAg alone. The vaccines IL4-NAg and NAg did not significantly

inhibit EAE as either a pretreatment or therapeutic intervention. In most cases, covalent linkage of the cytokine and NAg domain was required for the inhibition of EAE since vaccination with an equimolar mix of cytokine and NAg as separate molecules did not prevent EAE (164). However, a vaccine comprised of IFN-β + MBP^{73-87} as individual molecules had significant tolerogenic activity that was similar to the fusion protein IFNβ-MBP and protected rats from EAE when administered as a prophylactic and therapeutic vaccine (188). NAg-IL16, IL2-NAg, and MCSF-NAg had significant tolerogenic activity and restrained EAE (184, 185). However, GMCSF-NAg and IFNβ-NAg were the most efficacious and the focus of proceeding research efforts. Studies were moved into murine models of EAE to investigate the mechanisms of action of GMCSF-NAg and IFNβ-NAg.

1.7 IFN-β as an adjuvant for NAg-specific tolerance

Fusion proteins were constructed that consisted of murine IFN-β as the N-terminus domain covalently linked to either MOG^{35-55} or $PLP^{139-151}$ as the C-terminus domain. IFNβ-PLP was an effective prophylactic and prevented $PLP^{139-151}$ -induced EAE in SJL mice. Additionally, INFβ-MOG was effective prophylactic and therapeutic that prevented and ameliorated MOG^{35-55}-induced EAE in C57BL/6 mice. Contrary to the results obtained in Lewis rats, covalent linkage of IFN-β and NAg was required for tolerogenic activity in mice (164, 189). Since covalent linkage was required in murine models of EAE, our lab tested the concept that cytokine and NAg could be tethered through non-covalent hydrostatic bonds facilitated by alum adjuvant. The use of alum adjuvant to link vaccine components would be advantageous because different NAg could be easily swapped in the vaccine formulation whereas covalent linkage required new genetic constructs for each fusion protein.

Alum proved to be an effective binding agent which facilitated tolerance. A vaccine comprised of IFN-β + MOG^{35-55} in alum was an effective tolerogen when administered as prophylactic and as a therapeutic in MOG^{35-55}-induced EAE in C57BL/6 mice. Because the vaccine had prophylactic activity, the finding suggested that the vaccine elicited tolerogenic memory that was potentially mediated through the induction of Tregs. Treatment of mice with PC61 a Treg-depleting anti-CD25 mAb abrogated vaccine-induced tolerance and restored susceptibility to EAE. It was determined that IFN-β treatment during antigen stimulation drove Treg induction *in vitro.* IFN-β-mediated Treg induction was dependent on TGF-β since the addition of a mAb against TGF- β prevented IFN-β-induced Tregs. IFN-β-induced Tregs were immunosuppressive and prevented EAE following adoptive transfer into C57BL/6 mice. Furthermore, IFN-β + MOG^{35-55} in alum induced Tregs *in vivo* in transgenic mice that had a TCR specific for MOG^{35-55} (189). These results showed that IFN-β is an effective tolerogenic adjuvant in peptide-based vaccines that engenders Treg responses to induce antigen-specific tolerance that prevented EAE in rodents (188, 189).

1.8 GM-CSF as an adjuvant for neuroantigen-specific tolerance

Fusion proteins were also constructed that consisted of murine GM-CSF as the N-terminus domain, covalently linked to encephalitogenic peptides MOG^{35-55} or $PLP^{139-151}$ as the C-terminus domain. The GM-CSF domain from GMCSF-NAg proteins retained full biological activity. Both GM-CSF and GMCSF-NAg induced the proliferation of bone marrow cells starting in the 1-10 pM range. The GM-CSF domain of murine GMCSF-MOG targeted MOG for ~1000 fold enhanced antigen potency measured by MOG^{35-55} -specific T cell proliferation when cultured with splenic APC compared to MOG^{35-55} alone (190).

GMCSF-NAg vaccines were tolerogenic in murine models of EAE as well. GMCSF-MOG was a robust tolerogen that prevented MOG^{35-55}-induced EAE in C57BL/6 mice when administered as a prophylactic vaccine. For example, 75% of mice pretreated with GMCSF-MOG were protected from the development of EAE whereas none of mice treated with GM-CSF + MOG^{35-55} or saline were protected from severe paralytic EAE. Covalent linkage of the fusion protein domains was required for tolerogenic activity, since vaccination with an equal molar mix of GM-CSF and MOG^{35-55} did not protect mice from EAE. GMCSF-MOG also induced tolerogenic memory because GMCSF-MOG prevented EAE even when administered a week prior to EAE induction (190). GMCSF-MOG also had profound therapeutic efficacy and reversed established disease. After the onset of MOG^{35-55} -induced EAE, C57BL/6 mice treated with GMCSF-MOG recovered and had mild disease associated with limited tail paralysis, while mice treated with control vaccines MOG and saline showed no recovery and maintained severe disease associated with hind limb paralysis (187). GM-CSF not only engendered tolerance when fused to MOG^{35-55} but also when combined with the encephalitogenic $PLP^{139-151}$ peptide. Prophylactic and therapeutic treatment with GMCSF-PLP inhibited $PLP^{139-151}$ -induced EAE in SJL mice (187, 190). Tolerance was antigen-specific since GMCSF-PLP inhibited $PLP^{139-151}$ induced EAE but not MOG^{35-55} induced EAE (187).

Significantly, GMCSF-NAg vaccines were tolerogenic in inflammatory environments. Vaccines of GMCSF-MOG and GMCSF-PLP protected mice from EAE when administered adjacent to or when directly included in the encephalitogenic emulsion. For example, 50% of mice that received GMCSF-MOG mixed directly in the MOG^{35-55} and CFA emulsion were protected from developing EAE and mice that did develop EAE had mild disease. Conversely, 100% of the mice treated with MOG^{35-55} in CFA alone had severe paralytic EAE. The vaccine

induced tolerance even when MOG^{35-55} was present at a 75:1 molar excess to GMCSF-MOG. Similar results were obtained in SJL mice with GMCSF-PLP. For example, mice that received GMCSF-PLP mixed in the $PLP^{139-151}$ and CFA emulsion had reduced EAE scores associated with partial tail paralysis while mice that did not receive GMCSF-PLP had severe EAE associated with partial hind limb paralysis. These results showed that GMCSF-NAg vaccines exhibited dominant inhibitory action in inflammatory environments (187).

GMCSF-NAg inhibited both TH1-driven and TH17-dominated EAE. GMCSF-MOG ameliorated TH17-directed disease in *Infgr1*$^{-/-}$ mice when administered directly in the CFA and MOG^{35-55} emulsion. Additionally, GMCSF-MOG was an effective therapeutic and ameliorated EAE induced via the adoptive transfer of encephalitogenic TH1-skewed T cells (187).

Overall, GMCSF-NAg vaccines were found to be robust vaccines that induced tolerance in both rat and murine models of EAE. GM-CSF was a tolerogenic fusion partner when combined with three separate encephalitogenic peptides (MBP, MOG, and PLP). GMCSF-NAg elicited tolerogenic memory responses that persisted after vaccination. GMCSF-NAg vaccines where highly effective in inflammatory environments and as therapeutic interventions. These finding suggest that GM-CSF is an effective tolerogenic adjuvant that targets self-antigens to myeloid APC for enhanced antigen presentation that favors tolerogenic outcomes.

1.9 The hypothesis

We hypothesize that the GM-CSF domain of GMCSF-NAg fusion proteins acts as an adjuvant by targeting the NAg for enhanced antigen presentation on myeloid APC and by amplifying tolerogenic or immunogenic responses that are directed by the NAg domain based on the TCR-antigen recognition efficiency. We hypothesize that vaccines comprised of GM-CSF

and self-antigens will result in low-affinity/ efficiency T cell responses that favor Tregs and tolerance, while vaccines comprised of GM-CSF and foreign-antigens will result in high-affinity/ efficiency T cell responses and favor Tcons and immunity.

1.10 The rational

The use of GM-CSF as a tolerogenic adjuvant is intriguing because GM-CSF has classically been considered a pro-inflammatory cytokine and has been used as an immunogenic adjuvant in several vaccine formulations. GM-CSF was designated a pro-inflammatory cytokine because of the ability of GM-CSF to potentiate several autoimmune diseases. For example, GM-CSF-deficient mice are profoundly resistant to the development of EAE, myocarditis, and rheumatoid arthritis (194-196). Similarly, treatment of mice with neutralizing mAb against GM-CSF decreases the severity of disease in models of psoriasis, rheumatoid arthritis, allergic disease, nephritis, and EAE (194, 197-201). Additionally, treatment of mice with recombinant GM-CSF has been shown to exacerbate both EAE and rheumatoid arthritis (194, 202). GM-CSF has also been implicated in the development of many autoimmune diseases in humans because patients with rheumatoid arthritis and MS have increased levels of GM-CSF at the site of inflammation (203, 204). Evidence suggests that GM-CSF promotes the activation and maturation of myeloid cells which, in turn, drive autoimmune inflammation. Stimulation of myeloid APC such as DC, macrophages, monocytes with GM-CSF increases the expression of MHCII, the co-stimulatory molecules CD80, CD86, and CD40, as well as increases the production of inflammatory cytokines leading to enhanced T cell responses (205). GM-CSF can prompt myeloid APC to produce IL-23 and IL-12 which support the differentiation of pathogenic TH17 and TH1 cells respectively (206). GM-CSF can also recruit monocytes, macrophages, and granulocytes to the site of inflammation while concurrently promoting cell survival needed to

drive inflammation (207). However, the inflammatory response is dependent on the myeloid cell subset, dose of GM-CSF, and the presence of other inflammatory mediators because GM-CSF can also stimulate immunosuppressive rDC and myeloid-derived suppressor cells (201, 208).

GM-CSF has been incorporated into cancer, viral, and bacterial vaccine platforms in an effort to increase vaccine immunogenicity. Several of these vaccine platforms exist including, protein-based vaccines that incorporate GM-CSF as a free cytokine or as a fusion partner with target antigens, DNA-based vaccines that include both GM-CSF and antigen expression vectors, and cell-based vaccines which utilize GM-CSF expressing cancer cells (209-212). Of the numerous vaccines devised, Provenge has had the most clinical success and was the first and is currently the only FDA approved therapeutic cancer vaccine. Provenge was designed to treat prostate cancer and is a fusion protein comprised of GM-CSF and prostate acid phosphatase. Provenge is applied *ex vivo* to patient PBMCs which are then reinfused into the patient to achieve cancer rejection. While Provenge has therapeutic activity, the vaccine is relatively weak and has a 3 year survival rate of 31.7% as compared to 21.7% in the placebo treated control group (213). GM-CSF-based vaccines have had mixed success rates in clinical trials and a number of these vaccines have inadvertently induced varying levels of immunosuppression (214). For example, clinical trials testing metastatic carcinoma and melanoma cancer vaccines found that the addition of GM-CSF suppressed antigen-specific T cell responses as compared to vaccine formulations that lacked GM-CSF (215, 216).

In contrast to the pro-inflammatory roles, GM-CSF also has anti-inflammatory properties which have been relatively overlooked. For example, administering recombinant GM-CSF decreases disease severity in animal models of myasthenia gravis, thyroiditis, graft versus host disease, and type I diabetes (217-221). Additionally, decreased levels of GM-CSF are associated

with increased susceptibility to type 1 diabetes and systemic lupus erythematosus (222, 223). GM-CSF has been shown to induce myeloid suppressor cells and rDC which in turn can increase Treg populations and suppress autoimmune responses (138, 201). GM-CSF induced rDC can expand Tregs through low-efficiency antigen presentation as well as expand Tregs in an antigen-independent mechanism through the expression of OX40L and Jagged-1 to resolve autoimmunity. Myeloid-derived suppressor cells induced Tregs via the expression of IL-10 and TGF-β. Additionally, GM-CSF-induced myeloid-derived suppressor cells break down arginine and produce reactive oxygen species as well as nitric oxide which prevent T cell proliferation (224). Therefore, GM-CSF does not simply conform to being either a pro-inflammatory or anti-inflammatory cytokine.

Our lab has routinely demonstrated that fusion proteins comprised of GM-CSF and myelin peptides (MBP, MOG, and PLP) act in an anti-inflammatory manner and confer profound resistance to EAE (185, 187, 190). These findings are in opposition to the pro-inflammatory roles of GM-CSF and in accordance with the anti-inflammatory properties. Therefore, we hypothesized that GM-CSF is conducive for both tolerance and immunity and may simply act as a response amplifier, suggesting that other stimuli direct the overall outcome. In the case of GM-CSF-based vaccines the antigen component may represent the directing stimulus which determines if these vaccines induce tolerance or immunity.

Evidence suggests that high-efficiency antigen recognition events favor Tcon responses and immunity, while low-efficiency antigen recognition favors Treg responses and tolerance (225-228). High-efficiency T cell responses lead to increased activation and co-stimulation which drive APC maturation and effector T cell differentiation while low-efficiency responses result in diminished co-stimulation and favor rDC and Treg responses (229-231). The efficiency

of antigen recognition is dependent, in part, on the affinity of the $CD4^+$ T cells to its cognate antigen when presented on MHCII. TCR selection in the thymus controls the relative affinity range in which a T cell can recognize either self-antigens or foreign-antigens. T cell recognition of self-antigens is limited to a lower affinity range because of negative thymic selection, whereas T cell recognition of foreign-antigens are higher affinity due to positive thymic selection (8, 232-235). Therefore, we hypothesized that vaccines comprised of GM-CSF and self-antigens would result in low-affinity/ efficiency T cell responses favoring Tregs and tolerance, while GM-CSF in combination with foreign-antigens will result in high-affinity/ efficiency responses that favor Tcons and immunity.

Previous research showed that GMCSF-MOG fusion proteins were an effective pretreatment and therapeutic interventions in C57BL/6 mice that prevented EAE (187, 190). The evidence that GMCSF-MOG was effective as a pretreatment and induced immunological memory suggested that GMCSF-MOG may prompt lasting tolerogenic responses through the induction of Tregs. Indeed, GMCSF-MOG-induced tolerance was dependent on GMCSF-MOG-induced Tregs because depletion of Tregs in GMCSF-MOG treated mice with PC61 an anti-CD25 mAb abrogated tolerance to EAE. Therefore, we sought to determine the parameters which permitted GM-CSF to act as a tolerogenic adjuvant to elicit Tregs and tolerance.

The studies detailed here provide evidence that the antigen recognition efficiency directs the effects of GM-CSF fusion proteins towards either tolerance or immunity. These studies utilized TCR transgenic OTII mice which recognize $OVA^{323-337}$ as a high-efficiency foreign antigen, and 2D2 mice which recognize MOG^{35-55} as a low-efficiency self-antigen and NFM^{13-37} as a high-affinity self-antigen. In the contexts of these studies, NFM^{13-37} acted as a surrogate "foreign" antigen because NFM failed to elicit central tolerance and allowed the aberrant

formation of high-affinity self-reactive T cells (236-238). Both OTII and 2D2 mice were crossed with FIG mice (OTII-FIG and 2D2-FIG) which express a GFP reporter of FOXP3 expression and allowed Tregs to be identified based on GFP expression.

The low-efficiency GMCSF-MOG vaccine elicited a robust Treg response in 2D2-FIG mice and increased the percent of Tregs ~15-25 fold and number of Tregs ~2-3 fold over control vaccines comprised of GM-CSF + MOG^{35-55} and saline. Covalent linkage of GM-CSF to MOG^{35-55} was required for Treg induction because a vaccine comprised of equal molar dose of GM-CSF and MOG^{35-55} as separate molecules did not exhibit Treg-inductive activity. The GMCSF-MOG-induced Treg population was apparent within 3 days of vaccination, was sustained over several weeks, and presented systemically with high frequencies of Tregs in the blood, spleen, and lymph nodes. GMCSF-MOG-induced Tregs had a canonical Treg phenotype and expressed FOXP3, CD25, LAP, and Neuropilin, as well as displayed a memory phenotype that was $CD44^{high}$ $CD62L^{low}$. GMCSF-MOG vaccination not only augmented the Treg compartment but also reduced the total number of $CD3^+$ T cells, decreased the 2D2 TCR on a per cell basis, and increased the percent of aberrant $CD4^-$ T cells which was consistent with a desensitized MOG^{35-55}-specific T cell repertoire. The tolerogenic vaccine did not exclusively require the draining lymphatics, or skin resident immunocytes because subcutaneous and intravenous injection of GMCSF-MOG were equally effective for the induction of $FOXP3^+$ Tregs. Booster vaccination with GMCSF-MOG elicited increased numbers and percentages of Tregs and maintained the preceding vaccine-induced Treg population. Importantly, GMCSF-MOG elicited Tregs in inflammatory environments when mixed in the immunogenic adjuvants CFA and alum. GMCSF-MOG-induced Tregs were immunosuppressive and prevented the proliferation of naïve 2D2-FIG T cells *in vitro*.

The ability of GMCSF-antigen fusion proteins to induce Treg was dependent upon the efficiency of the T cell antigen recognition because vaccination of 2D2-FIG and OTII-FIG mice with the high-efficiency GMCSF-NFM and GMCSF-OVA vaccines, respectively, did not elicit Tregs but favored Tcon responses. The high-efficiency GMCSF-NFM vaccine elicited robust Tcon recall response *ex vivo* and activated the CD40L/CD40 costimulation pathway *in vitro*. In contrast, the low-efficiency GMCSF-MOG vaccine elicited Treg responses *in vivo* and lacked sufficient TCR signal strength to activate the CD40L/CD40 pathway *in vitro*. Therefore we hypothesized that the strength of T cell-APC cross talk through CD40L/CD40 pathway may represent a critical junction that controls Treg/ Tcon responses. In order to determine if CD40L/CD40 pathway controlled Tcon and Treg response *in vivo*, mice were pretreated with an agonistic anti-CD40 mAb to activate the CD40L/CD40 pathway or were treated with a control mAb and subsequently treated with the low-efficiency GMCSF-MOG vaccine. Pretreatment of mice with an agonistic anti-CD40 significantly reduced the percentages and numbers of Tregs per μl of blood following vaccination with GMCSF-MOG as compared to mice treated with the control mAb. Therefore, high-efficiency antigen recognition led to CD40L/CD40 activation which directed Tcon responses while low-efficiency antigen recognition precluded CD40L/CD40 activation and elicited Treg responses. This study revealed that low-efficiency antigen recognition can be partially dominant over concurrent high-efficiency antigen recognition. In 2D2-FIG mice, the GMCSF-MOG vaccine induced Tregs even when directly mixed with the GMCSF-NFM vaccine which favored Tcon responses.

Interestingly, GMCSF-MOG appeared to expand pre-existing Tregs because GMCSF-MOG-induced Treg emergence was dependent on the level of pre-existing Tregs. Specifically, Treg induction with GMCSF-MOG was delayed by ~1 week in 2D2-FIG-*Rag1*$^{-/-}$ mice, which

lacked pre-existing Tregs, as compared to 2D2-FIG mice exhibited a pre-existing Treg pool. In accordance with these findings pre-existing Tregs were also required for GMCSF-NAg induced tolerance. Both GMCSF-MOG and GMCSF-NFM were encephalitogenic in Treg-deficient 2D2-FIG-*Rag1*$^{-/-}$ mice but not in Treg sufficient 2D2-FIG mice. Additionally, GMCSF-MOG was an effective prophylactic in Treg-sufficient C57BL/6 mice and prevented MOG$^{35-55}$/CFA-induced EAE. Overall, these studies provide evidence that GM-CSF acts as a tolerogenic adjuvant when paired with low-efficiency self-peptides that fall below the CD40L/CD40 triggering threshold. Thus, inefficient TCR ligation and subimmunogenic CD40L/CD40 activation establish antigen-specific tolerance through the expansion of pre-existing Treg populations.

CHAPTER 2

MATERIALS AND METHODS

2.1 Mice

C57BL/6J (000664), B6.SJL-Ptprc^{a} Pepc^{b}/BoyJ (CD45.1 002014), B6.Cg-*Foxp3*^{tm2Tch}/J (FIG Foxp3-IRES-GFP 006772), B6.129S7-*Rag1*^{tm1Mom}/J (*Rag1*$^{-/-}$ 002216), C57BL/6-Tg(Tcra2D2,Tcrb2D2)1Kuch/J (2D2 MOG$^{35-55}$ and NFM$^{13-37}$ -specific TCR transgenic 006912), and B6.Cg-Tg(TcraTcrb)425Cbn/J (OTII OVA$^{323-339}$-specific TCR transgenic 004194) mouse strains were obtained from the Jackson Laboratory (Bar Harbor, ME) and were housed and bred in the Department of Comparative Medicine at East Carolina University Brody School of Medicine. 2D2-FIG, CD45.1-2D2-FIG, 2D2-FIG-*Rag1*$^{-/-}$ and OTII-FIG mice were obtained through intercross breeding. PBMCs from 2D2 mice were routinely screened by FACS analysis for 2D2 TCR expression with antibodies specific for Vβ11 and Vα3.2. OTII mice were routinely screened by FACS analysis for OTII TCR expression with antibodies specific for Vβ5.1/5.2 and Vα2. The congenic CD45.1 allele was maintained as at least a single copy as determined by FACS analysis of PBMCs using antibodies specific for CD45.1 and CD45.2. Foxp3-IRES-GFP (FIG) mice were screened via PCR by use of forward (CAC CTA TGC CAC CCT TAT CC) and reverse (ATT GTG GGT CAA GGG GAA G) primers. GFP expression from FIG mice was used as a surrogate marker of FOXP3 expression in these studies. Animal care and use was performed in accordance with approved animal use protocols and guidelines of the East Carolina University Institutional Animal Care and Use Committee.

2.2 Reagents and recombinant proteins

Synthetic peptides MOG$^{35-55}$ (MEVGWYRSPFSRVVHLYRNGK), NFM$^{13-37}$

(RRVTETRSSFSRVSGSPSSGFRSQS), and $OVA^{323-339}$ (ISQAVHAAHAEINEAGR) were obtained from Genscript (Piscataway, NJ). Monoclonal antibodies FGK4.5 (rat anti-mouse CD40 IgG2a) and 2A3 (rat anti-trinitrophenol IgG2a) were purchased from BioXcell (West Lebanon, NH). Derivation, expression, purification, and bioassay of the murine GM-CSF and GMCSF-MOG fusion proteins were described in previous studies (164, 190). These fusion proteins as well as GMCSF-OVA and GMCSF-NFM were comprised of the murine GM-CSF cytokine as the N-terminal domain, the amino acid sequence comprising the relevant antigenic peptide domain, and an 8-histidine C-terminus. GM-CSF contained the 8-histidine tag C-terminus but did not contain an antigenic peptide domain. GMCSF-MOG, GMCSF-NFM, and GMCSF-OVA contained MOG^{35-55}, NFM^{13-37}, and $OVA^{323-339}$ peptides, respectively. These fusion proteins did not contain linkers in the GM-CSF/ antigenic peptide/ 8-histidine-tag junctions. These recombinant proteins were isolated from stably-transfected human embryonic kidney (HEK) cells or from Chinese hamster ovary (CHO-S) cells. The fusion proteins were purified by incubation of Ni-NTA Agarose beads with expression supernatant under agitation for 1 hour followed by bead collection in column and extensive washing of the resin bed (50 mM NaH_2PO_4, 500 mM NaCl, with 10, 20, or 60 mM imidazole, pH 8.0). Recombinant proteins were eluted with 250 mM imidazole (pH 8.0) and were concentrated and diafiltrated in Amicon Ultra-15 centrifugal filter devices (EMD Millipore, Billerica, MA). Protein quantity was assessed by absorbance at 280 nm, and purity was assessed by SDS-PAGE. Bioactivity of each fusion protein preparation was determined by the ability of the GM-CSF domain to drive proliferation of bone marrow cells, and the antigenic peptide domain to drive proliferation of 2D2 T cells (MOG^{35-55} and NFM^{13-37}) and OTII T cells ($OVA^{323-339}$). Recombinant rat TGF-β1 was expressed by use of HEK cells and purified as previously described (189). Recombinant rat IL-2 was derived from a

baculovirus expression system as previously described (239). Hybridomas secreting the PC61-5.3 mAb or a rat IgG1 isotype control were described previously (240). Hybridoma cells were cultured in supplemented DMEM in C2011 hollow fiber cartridges (FiberCell Systems, Inc., Frederick, MD). Hybridoma supernatants were clarified at 7,200 x g, precipitated with 50% ammonium sulfate, and dissolved in PBS. MAb preparations were purified on protein G agarose columns. Antibody was eluted with 200 mM glycine at pH 3.0 and immediately neutralized by 1M Tris buffer of pH 9.0. The purity of the antibody was verified by SDS-PAGE.

2.3 Flow cytometric analyses of lymphocytes, splenocytes, and PBMCs

Blood was collected from the submandibular vein into 200 µl of sodium citrate (130 mM). Inguinal lymph nodes and spleen were dissected from mice and placed into 10 ml of HBSS. Dissected lymph nodes and spleen were pressed through a wire mesh screen and a 70 µm cell strainer (Corning, NY) to obtain single-cell suspensions. Cells were washed in 3 ml HBSS with 2% heat-inactivated FBS and stained with designated cocktails of fluorochrome-conjugated antibodies for 1 hour at 4°C in the dark. After staining whole blood, erythrocytes (RBC) were lysed with 1:10 HBSS for 20 seconds at 4°C followed by addition of 2X PBS. Alternatively, RBCs were lysed by incubating samples for 10 mins on ice with 3 ml of ammonium chloride lysis buffer (150 mM NH_4Cl, 10 mM $NaHCO_3$, 1.2 mM EDTA- pH 7.2). Lysis was repeated when necessary. Samples were then washed 1 time with HBSS + 2% FBS and were analyzed on a Becton-Dickson LSRII flow cytometer (San Jose, CA) with FlowJo software (Ashland, OR). In designated experiments, reference 'counting' beads were added to samples immediately before flow cytometric analysis (AccuCount blank particles or FITC-, PE-, or APC-conjugated EasyComp fluorescent particles 3.0-3.4 µm, Spherotech, Lake Forest, IL). The use of reference beads enabled comparisons of absolute cell numbers among different samples. For intercellular

staining of FOXP3 and Ki67, blood was collected, and RBCs were lysed as previously described. PBMC were fixed for 10 minutes using 2% paraformaldehyde (PFA) and were fixed/ permeabilized with 1 mL of ice cold 100% methanol for 30 minutes. Cells were then stained with antibody cocktails against both surface markers and intercellular targets for 30 mins at room temp. Cells were extensively washed between PFA, methanol, and staining treatments using PBS + 2% FBS. Fluorochrome-conjugated mAbs were obtained from BioLegend and included CD3-BV421, PE/Dazzle 594, or PE (17A2 or 145-2C11), CD4-BV785, PE, or APC (GK1.5), CD25-BV421 or APC (PC61), CD40-PE (MR1), CD44-BV421 (IM7), CD45-BV785 (30-F11), CD45.1-APC or BV421 (A20), CD45.2-APC (104), CD62L-APC (MEL-14), FOXP3-AF488 (MOPC-21), Ki67-APC (16A8), TCR-Vα2-APC (B20.1), TCR-Vα3.2-PE (RR3-16), TCR-Vβ11-PE or AF647 (KT11), TCR-Vβ5.1,5.2-PE (MR9-4), Neuropilin-PE (3E12), LAP-PE (TW7-16B4), and Trinitrophenol-KLH-PE (HTK888). In order to stain CD40L, T cells were stimulated with antigen for 4 hours and subsequently incubated with 10 µg/mL anti-mouse CD40L-PE (Armenian Hamster IgG, MR1) or the isotype control anti-mouse Trinitrophenol-KLH-PE (Armenian Hamster IgG, HTK888) for an additional 2 hours at 37°C. Cultures were then processed and surface stained as previously described.

2.4 *In vitro* Treg suppression and antigen-specific response assays

To measure antigen-specific proliferation, 2D2 or OTII T cells (2.5×10^4/well) were cultured with irradiated splenocytes (3000 rads, 2.0×10^5 cells/well) in the presence of designated antigen concentrations. To measure GM-CSF activity, C57BL/6 bone marrow cells were cultured with designated concentrations of GM-CSF or GM-CSF fusion proteins. To determine if GMCSF-MOG-induced Tregs were suppressive, 2D2-FIG mice were subcutaneously vaccinated with 4 nmoles of GMCSF-MOG in saline to induce Tregs. On day 7, splenocytes

were harvested and GFP^{high} ($FOXP3^{high}$) Tregs were FACS purified with the Becton-Dickson FACSAria Fusion (San Jose, CA). Tresponder cells (Tresp) were isolated from a naïve 2D2-FIG mouse using untouched $CD4^+$ MACS system (Miltenyi Biotech, Bergisch Gladbach, Germany). Tregs were mixed with Tresp and activated with 1 x 10^5 irradiated C57BL/6 splenocytes, and 1 µM MOG^{35-55}. In order to assess vaccine-induced antigen-recall, 2D2-FIG mice were vaccinated with GMCSF-MOG, GMCSF-NFM, or saline and splenocytes were harvested 7 days later. $CD4^+$ T cells were isolated using anti-CD4 (L3T4) MACS system (Miltenyi Biotech, Bergisch Gladbach, Germany). Purified $CD4^+$ T cells (25,000) from vaccinated mice were activated with 2 x 10^5 irradiated C57BL/6 splenocytes and designated concentrations of MOG^{35-55} or NFM^{13-37}. Cultures were pulsed with 1 µCi [^{3}H] thymidine (6.7 Ci/mmol, New England Nuclear, Perkin Elmer, Waltham, MA, USA) during the last 24 h of a 72-h culture. Cultures were harvested onto filters by use of a Tomtec Mach III harvester (Hamden, CT, USA). [^{3}H] thymidine incorporation into DNA was measured by use of a Perkin Elmer MicroBeta2 liquid scintillation counter.

2.5 Generation and maintenance of Treg and Tcon lines

Naïve splenocytes were harvested from 2D2-FIG mice and activated at a density of 2 × 10^6 cells a ml in complete RPMI for 3 days with 1 µM MOG^{35-55} and for Treg cultures with 10 nM TGF-β. After activation T cells were passaged every 3–4 days with rat IL-2. T cell lines were periodically reactivated every 2–4 weeks with MOG^{35-55}, irradiated splenocytes from C57BL/6 mice and for Treg lines with 1 nM TGF-β. Anti-CD25 antibody PC61 (10 µg/ml; 65 nM) was included in Treg cultures in order to stabilize and enrich Tregs as previously described (241). Cells were acid washed with pH 5.0 complete RPMI to remove PC61 before adoptive transfer.

2.6 Induction and assessment of EAE in C57BL/6 mice

CFA (Incomplete Freund's Adjuvant with 4 mg/ml heat-killed Mycobacterium tuberculosis H37Ra, BD Biosciences, Franklin Lakes, NJ) was mixed 1:1 with MOG^{35-55} in phosphate-buffered saline. The CFA/antigen mixture was emulsified by sonication. EAE was elicited by injection of 200 μg MOG^{35-55} in a total volume of 100 μl emulsion via three SC injections of 33 μl across the lower back. Each mouse received separate intraperitoneal injections (200 or 400 nanograms i.p.) of Pertussis toxin (Ptx; EMD Millipore, Billerica, MA) in PBS on days 0 and 2. All immunizations were performed under isoflurane anesthesia (Abbott Laboratories, Chicago, IL). Mice were assessed daily for clinical score and body weight. The following scale was used to score the clinical signs of EAE: 0, no disease; 0.5, partial paralysis of tail without ataxia; 1.0, flaccid paralysis of tail or ataxia but not both; 2.0, flaccid paralysis of tail with ataxia or impaired righting reflex; 3.0, partial hind limb paralysis marked by inability to walk upright but with ambulatory rhythm in both legs; 3.5, same as above but with full paralysis of one leg; 4.0, full hindlimb paralysis; 5.0, total hindlimb paralysis with forelimb involvement or moribund. A score of 5.0 was designated a humane endpoint and mice were euthanized.

2.7 Induction and assessment of EAE in 2D2-FIG-*Rag1*$^{-/-}$ mice

Mice were vaccinated with 4 nmoles of GMCSF-MOG or GMCSF-NFM in 200 μL of saline. Vaccines were given subcutaneously in two locations (100 μL each) on the hind back. Mice were assessed daily for clinical score and body weight. The following scale was used to score the clinical signs of EAE: 0, no disease; 0.5, partial paralysis of tail without ataxia; 1.0, flaccid paralysis of tail or ataxia or bladder dysfunction but not combined; 2.0, flaccid paralysis of tail with ataxia or impaired righting reflex; 3.0, partial hind limb paralysis or impaired reflexes associated with foot clasping or disequilibrium with head tilt; 3.5, partial hind limb paralysis

with full paralysis of one leg; 4.0, full hindlimb paralysis; 5.0, total hindlimb paralysis with forelimb involvement or moribund. A score of 5.0 was designated a humane endpoint and mice were euthanized.

2.8 EAE analysis and statistics

EAE incidence was the number of EAE-afflicted mice compared to the total group size. Maximal scores were calculated as the most severe EAE score for each mouse. Mice that did not exhibit EAE had a score of zero, and these scores were included in the group average. Mice that exhibited humane endpoints as assessed by body weight loss, body score, or clinical score of 5.0 were subjected to humane euthanasia and were omitted from scoring thereafter. Time-course graphs portrayed daily mean maximal scores. Cumulative and maximal EAE scores were analyzed by either a Mann-Whitney U Test (two groups) or the Kruskal-Wallis Test (greater than two groups). To calculate percent maximal weight loss, 100% body weight was assigned as the maximal body weight obtained on day 0 and daily body weights were calculated for each day after normalization to the day 0 value. The minimum body weight was defined as the lowest body weight after normalization to the day 0 value until the end of the experiment. Maximal weight loss was calculated by subtraction of the normalized minimum value from the day 0 value. Negative weight loss values represented weight gain. Weight loss was analyzed by two-tailed Student's t-test. Kruskal-Wallis Test significance values were adjusted by the Bonferroni correction for multiple test. Mean EAE and weight loss data were shown with the standard error of the mean (SEM). A two-way repeated measures ANOVA was used to determine daily statistical significance.

2.9 Preparation of GMCSF-MOG in saline, alum, and CFA

Vaccines containing GMCSF-MOG, GMCSF-OVA, GMCSF-NFM, GM-CSF, MOG^{35-55}, or GM-CSF + MOG^{35-55} were administered at a dosage of either 2 or 4 nmoles as designated in the figure legends. CFA-based vaccines were prepared with equal parts of CFA and vaccine proteins/ peptides (in PBS) for a total injection volume of 100 µl. The CFA/ vaccine mixture was emulsified by sonication and injected via two SC injections of 50 µl across the back hindquarters. Conversely, vaccines in saline (no extrinsic adjuvant) were prepared in 200 µl of PBS and were administered SC by two injections of 100 µl each in the back hindquarters. Vaccines administered intravenously (IV) were given in 100 µl of PBS and injected retro-orbitally. Alum-based vaccines were prepared by mixing equal volumes of Alhydrogel adjuvant (InvivoGen) and vaccine proteins/ peptides (in PBS) for a total injection volume of 150 µl per mouse. The alum/ vaccine mixture was incubated for 1 hour on ice with continuous agitation to allow the protein/peptide to attach to the alum gel. The vaccine was administered SC by two injections of 75 µl each in the back hindquarters.

2.10 Statistical analysis

Unless designated otherwise, comparisons among three or more groups were analyzed by use of ANOVA, which was interpreted with a Holm-Sidak multiple comparisons test. Pairwise comparisons were analyzed by two-tailed t-tests for data that passed Normality (Shapiro-Wilk) and Equal Variance (Brown-Forsythe) tests. A P-value < 0.05 was considered significant. Error bars represent standard error of the mean (SEM) unless designated otherwise.

CHAPTER 3

RESULTS

A GMCSF-NEUROANTIGEN TOLEROGENIC VACCINE ELICITS SYSTEMIC LYMPHOCYTOSIS OF $CD4^+$ $CD25^{HIGH}$ $FOXP3^+$ REGULATORY T CELLS IN MYELIN-SPECIFIC TCR TRANSGENIC MICE CONTIGENT UPON LOW-EFFICIENCY T CELL ANTIGEN RECEPTOR RECOGNITION.

These studies were previously published in Frontiers in Immunology.

Moorman CD, Curtis AD, 2nd, Bastian AG, Elliott SE, Mannie MD. A GMCSF-Neuroantigen Tolerogenic Vaccine Elicits Systemic Lymphocytosis of CD4(+) CD25(high) FOXP3(+) Regulatory T Cells in Myelin-Specific TCR Transgenic Mice Contingent Upon Low-Efficiency T Cell Antigen Receptor Recognition. *Frontiers in immunology* (2018) 9:3119. doi: 10.3389/fimmu.2018.03119. PubMed PMID: 30687323; PubMed Central PMCID: PMC6335336.

3.1 Abstract

Previous studies showed that single-chain fusion proteins comprised of GM-CSF and major encephalitogenic peptides of myelin, when injected subcutaneously in saline, were potent tolerogenic vaccines that suppressed experimental autoimmune encephalomyelitis (EAE) in rats and mice. These tolerogenic vaccines exhibited dominant suppressive activity in inflammatory environments even when emulsified in Complete Freund's Adjuvant (CFA). The current study provides evidence that the mechanism of tolerance was dependent upon vaccine-induced regulatory $CD25^+$ T cells (Tregs), because treatment of mice with the Treg-depleting anti-CD25 mAb PC61 reversed tolerance. To assess tolerogenic mechanisms, we focused on 2D2-FIG mice, which have a transgenic T cell repertoire that recognizes myelin oligodendrocyte glycoprotein peptide MOG^{35-55} as a low-affinity ligand and the neurofilament medium peptide NFM^{13-37} as a high-affinity ligand. Notably, a single subcutaneous vaccination of GMCSF-MOG in saline elicited a major population of $FOXP3^+$ Tregs that appeared within 3 days, was sustained over several weeks, expressed canonical Treg markers, and was present systemically at high frequencies in the blood, spleen, and lymph nodes. Subcutaneous and intravenous injections of GMCSF-MOG were equally effective for induction of $FOXP3^+$ Tregs. Repeated booster vaccinations with GMCSF-MOG elicited FOXP3 expression in over 40% of all circulating T cells. Covalent linkage of GM-CSF with MOG^{35-55} was required for Treg induction whereas vaccination with GM-CSF and MOG^{35-55} as separate molecules lacked Treg-inductive activity. GMCSF-MOG elicited high levels of Tregs even when administered in immunogenic adjuvants such as CFA or alum. Conversely, incorporation of GM-CSF and MOG^{35-55} as separate molecules in CFA did not support Treg induction. The ability of the vaccine to induce Tregs was dependent upon the efficiency of T cell antigen recognition, because vaccination of 2D2-FIG or

OTII-FIG mice with the high-affinity ligands GMCSF-NFM or GMCSF-OVA (Ovalbumin323-339), respectively, did not elicit Tregs. Comparison of 2D2-FIG and 2D2-FIG-*Rag1*$^{-/-}$ strains revealed that GMCSF-MOG may predominantly drive Treg expansion because the kinetics of Treg emergence was a function of pre-existing Treg levels. In conclusion, these findings indicate that the antigenic domain of the GMCSF-NAg tolerogenic vaccine is critical in setting the balance between regulatory and conventional T cell responses in both quiescent and inflammatory environments.

3.2 Depletion of FOXP3$^+$ CD25$^+$ Tregs with the anti-CD25 mAb PC61 reversed tolerogenic vaccination.

We hypothesized that GMCSF-based tolerogenic vaccines mediated tolerance via induction of CD25^{high} FOXP3$^+$ Tregs (Figure 3.1). To address this question, we pretreated C57BL/6 mice with 2 nmoles GMCSF-MOG (A) or saline (B) on days -21, -14, and -7 and then administered the anti-CD25 PC61 mAb or a an IgG1 isotype control mAb on days -4 and -2 to deplete CD25$^+$ FOXP3$^+$ Tregs in vivo (242). Mice were then subjected to active induction of EAE on day 0. Pretreatment with the anti-CD25 PC61 mAb but not the isotype control antibody eliminated circulating CD25$^+$ Tregs (data not shown). Pretreatment with the anti-CD25 PC61 mAb reversed the suppressive action of the tolerogenic vaccine such that the PC61-treated mice acquired full susceptibility to EAE and showed a chronic course of paralytic EAE equivalent to mice in the control groups (Figure 3.1A, B). PC61 had no effect on mice vaccinated with saline, presumably because Tregs played a minimal role in mice that were fully susceptible to EAE (Figure 3.1B). These results were mirrored by maximal weight loss: (a) 20.3% ± 4.6%, (b) 6.7% ± 4.2%, (c) 31.3% ± 1.0%, and (d) 26.4% ± 4.2%; b versus c, d, $p < 0.004$. In conclusion, the GMCSF-MOG vaccine elicited CD25$^+$ Tregs that were required for the inhibitory action of the

tolerogenic vaccine. Thus, these data revealed a causal link between GMCSF-MOG vaccination, $CD25^+$ Tregs, and tolerance induction in EAE.

3.3 GMCSF-MOG elicited a robust $FOXP3^+$ Treg response in 2D2-FIG mice.

To address whether GMCSF-MOG expanded MOG-specific Tregs, we used 2D2-FIG mice that had a transgenic MOG-specific T cell repertoire and a GFP reporter of FOXP3 expression. 2D2-FIG mice were vaccinated SC with 4 nmoles of GMCSF-MOG, GM-CSF + MOG^{35-55}, MOG^{35-55}, GM-CSF in saline or with saline alone (Figure 3.2). A 'day 0' baseline revealed that Tregs comprised less than 1.5% of all circulating T cells in naïve 2D2-FIG mice. By day 7 after vaccination with GMCSF-MOG, $FOXP3^+$ Tregs comprised approximately 30% of all circulating T cells whereas mice vaccinated with control vaccines "GM-CSF + MOG^{35-55}", MOG^{35-55} alone, GM-CSF alone, or saline had baseline levels of Tregs (<1.5%) (Figure 3.2A). Previous research showed that covalent linkage of GM-CSF and NAg was required for the tolerogenic activity of GMCSF-MOG (164, 185, 190). Covalent linkage of GM-CSF to MOG^{35-55} was also required for induction of $FOXP3^+$ Tregs (Figure 3.2A). Time course studies revealed that GMCSF-MOG vaccination increased Treg percentages to 27% of the circulating $CD4^+$ T cell pool by day 7 and that significant percentages of these Tregs were maintained through days 14 (22%) and 21 (12%) (Figure 3.2B, top). Thus, after the initial vaccine-mediated inductive event, Treg percentages gradually attenuated throughout the remainder of the experiment.

GMCSF-MOG vaccination resulted in an increased percentage of $CD4^{(-)}$ $CD3^+$ Tcon cells, such that 30% of the circulating Tcon cells lacked CD4 expression as compared to 5% of T cells in control groups on days 7, 14, and 21 (Figure 3.2B, bottom). The absolute number of $CD4^{(-)}$ T cells/ μl of blood however was unchanged among all vaccine groups but the absolute number of $CD4^+$ T cells was significantly diminished in mice that received GMCSF-MOG

(~400/ µl blood) as compared to control groups "GMCSF + MOG^{35-55}" or saline (~2000/ µl of blood) (Figure 3.2D, top). These data indicate the GMCSF-MOG acted indirectly to increase percentages of $CD4^{(-)}$ T cells by depleting $CD4^{+}$ T cells rather than expanding the $CD4^{(-)}$ T cell subset. Thus, GMCSF-MOG primarily affected the most reactive T cells (i.e., the $CD4^{+}$ subset rather than the relatively nonreactive $CD4^{(-)}$ subset).

GMCSF-MOG vaccination also reduced the percentages of circulating $CD3^{+}$ T cells per total PBMCs by approximately 2.5 fold (~ 7% $CD3^{+}$ T cells) compared to a baseline of 16-20% T cells in control groups that received "GM-CSF + MOG^{35-55}" or saline (Figure 3.2C, middle). GMCSF-MOG selectively eliminated MOG- specific $V\beta11^{+}$ (2D2 TCRβ) $CD3^{+}$ Tcon cells (~300/ µl of blood) as compared to control groups (~2000/ µl of blood), whereas $V\beta11^{(-)}$ $CD3^{+}$ T cells numbers remained unchanged (Figure 3.2D, middle). Thus, GMCSF-MOG exhibited antigen specificity by depleting NAg-reactive $V\beta11^{+}$ T cells while sparing nonspecific $V\beta11^{(-)}$ T cells.

GMCSF-MOG vaccination resulted in approximately 140 Tregs/ µl of blood compared to 50-60 Tregs/ µl of blood in control groups (Figure 3.2C, top). GMCSF-MOG also selectively expanded the number of $V\beta11^{+}$ Tregs compared to control groups whereas $V\beta11^{(-)}$ Tregs numbers were unchanged (Figure 3.2D, bottom). These data indicated that at least two factors accounted for the elevated percentages of Tregs (Figure 3.2C, bottom), including an increase in the absolute numbers of circulating Tregs and a decrement in the absolute numbers of Tcon cells. Overall, these data indicate that GMCSF-MOG effectively targeted MOG^{35-55} to myeloid APC to expand MOG-specific $CD4^{+}$ Tregs and deplete $CD4^{+}$ MOG-specific Tcon cells while preserving $CD4^{(-)}$ Tcon cells.

3.4 GMCSF-MOG elicited a system-wide FOXP3$^+$ Treg lymphocytosis in lymph nodes, spleen, and blood.

GMCSF-MOG primed a system-wide Treg response in that the vaccine elicited high frequencies of FOXP3$^+$ Tregs in the spleen, draining inguinal lymph nodes, and blood (Figure 3.3A). 2D2-FIG mice were vaccinated with GMCSF-MOG or "GMCSF + MOG^{35-55}" on day 0, PBMC were analyzed on day 4, and lymphoid organs were analyzed on days 5 and 6. GMCSF-MOG vaccination induced high percentages of FOXP3$^+$ Tregs in all three compartments including approximately 22%, 15%, and 7% of all T cells in PBMC, spleen, and lymph nodes, respectively (Figure 3.3A, C, E). Mice that received the control vaccine "GM-CSF + MOG^{35-55}" had relatively low frequencies of FOXP3$^+$ Tregs (approximately 1%, 4%, and 2% Tregs in PBMC, spleen, and lymph nodes, respectively). GMCSF-MOG increased the total number of Tregs as compared to the "GM-CSF + MOG^{35-55}" control vaccine (Figure 3.3B, D). GMCSF-MOG vaccination resulted in approximately 4.5 x 10^6 Tregs as compared to 1.0 x 10^6 Tregs per spleen in "GM-CSF + MOG" vaccinated mice. Similarly, GMCSF-MOG induced approximately 1.2 x 10^6 Tregs in the inguinal lymph nodes as compared to 0.2 x 10^6 Tregs in control nodes. These results indicate that SC vaccination with GMCSF-MOG in saline elicited Treg responses throughout the secondary lymphoid organs and the circulation.

3.5 Booster vaccination of GMCSF-MOG maintained circulating levels of FOXP3$^+$ Tregs.

Booster immunizations were used to assess whether repeated immunization of GMCSF-MOG elicited sustained Treg responses. 2D2-FIG mice were given three injections (days 0, 7, 14), two injections (days 7, 14), or one injection (day 14) of GMCSF-MOG (Figure 3.4). On day -1, baseline FOXP3$^+$ Tregs as a percentage of total CD3$^+$ T cells in PBMC were less than 1.5% for all 16 mice (Figure 3.4A). Vaccination with GMCSF-MOG elicited circulating FOXP3$^+$

Tregs by day 4 with a range of 5-29%. By day 11, mice receiving 2 immunizations exhibited percentages of Tregs ranging from 27-49% of all circulating T cells whereas mice receiving 1 immunization exhibited Treg percentages ranging from 6-32%. Percentages of circulating Tregs on day 18 ranged from 26-42% (3 injections, 3x), 33-50% (2 injections, 2x), 12-44% (single injection, 1x), and ~1% for saline treated mice. Major $FOXP3^+$ subpopulations were noted in both transgenic $V\beta11^+$ T cells and nontransgenic $V\beta11^{(-)}$ populations whereas $FOXP3^+$ T cells were exclusively $CD4^+$ (Figure 3.4B). Major populations of $V\beta11^{(-)}$ Treg were attributed to the overall loss of $CD3^+$ Tcon cells, resulting in elevated percentage but not numbers of $V\beta11^{(-)}$ Tregs. Elevated percentages of $FOXP3^+$ T cells in vaccinated mice mirrored increased numbers of $FOXP3^+$ T cells per µl of blood (Figure 3.4C). As measured by $FOXP3^+$ Treg frequencies or absolute numbers, the disappearance of circulating Tregs occurred at similar rates in the 3x, 2x, and 1x vaccine groups. Thus, multiple boosters maintained Tregs in circulation during repeated immunizations. For example, the 3x vaccination group showed a longer duration of Treg presence in the circulation compared to the 1x vaccination group. However, after the last vaccination on day 14, Tregs disappeared from the blood at similar rates during the next 2-3 weeks.

GMCSF-MOG (1x, 2x, and 3x) resulted in the down-regulation of TCRα/β on a per cell basis (Figure 3.4D). Diminished expression of TCR Vβ11 expression however did not rebound to baseline levels during this time span. Rather, lower levels of TCR-Vβ11 expression instead appeared to represent a new set-point for the 2D2 repertoire. These findings indicated that GMCSF-MOG not only elicited a major $FOXP3^+$ Treg population but also desensitized T cell antigen recognition among the Tcon repertoire.

3.6 GMCSF-MOG induced a FOXP3^{+} population with a canonical Treg phenotype.

To determine the phenotype of GMCSF-MOG-induced Tregs, 2D2-FIG mice were vaccinated SC with GMCSF-MOG or "GM-CSF + MOG^{35-55}" in saline. PBMC were analyzed on day 4 for CD44, CD62L, CD25, LAP, Neuropilin, and Ki67 expression (Figure 3.5A-B). GMCSF-MOG vaccinated mice exhibited significantly increased numbers and percentages of $CD44^{high}$ $CD62L^{low}$, LAP^{high}, $CD25^{high}$, and $Neuropilin^{high}$ Tregs in blood compared to control mice (Figure 3.5C-D). For example, in GMCSF-MOG vaccinated mice, ~8% of total T cells expressed a FOXP3^{+} $CD44^{high}$-$CD26L^{low}$ phenotype compared to ~1% in control mice (Figure 3.5D). GMCSF-MOG vaccination also increased the percentages of T cells that expressed a FOXP3^{+}, LAP^{high} (14%), $CD25^{high}$ (18%), or $Neuropilin^{high}$ (22%) phenotype compared to control mice in which less than 2% of the T cells were Tregs positive for any of the respective markers (Figure 3.5D). Interestingly, the two treatment groups did not differ in the percentages of Tregs that expressed these markers within the Treg pool, aside from a modest decrease (~13 %) in $Neuropilin^{high}$ Tregs in GMCSF-MOG treated mice (Figure 3.5E). GMCSF-MOG vaccination also increased the number and percentages of T cells that were $CD44^{high}$ Tregs compared to control mice (Figure 3.5F-G), whereas GMCSF-MOG vaccination increased percentages but not numbers of T cells that were $CD44^{high}$ Tcon cells, a discrepancy that reflected the generalized loss of Tcon cells. GMCSF-MOG vaccination increased both Treg and Tcon intracellular staining for Ki67, a marker of cell division, compared to control mice although Ki67 expression was upregulated 5-fold in Tregs versus 2-fold in Tcon cells (Figure 3.5H). These data showed that GMCSF-MOG-induced Tregs have a phenotype similar to pre-existing Tregs and that GMCSF-MOG favors the expansion of MOG-specific Tregs over MOG-specific Tcon cells.

3.7 The antigenic domain of GMCSF-antigen fusion proteins was a major parameter for Treg induction.

A major question was whether the GM-CSF domain or the antigenic domain of GMCSF-antigen fusion proteins represented the predominant variable polarizing T cells into the Treg lineage. To assess this issue, GMCSF-MOG and GMCSF-OVA were compared for Treg induction in MOG-specific (2D2-FIG) versus OVA-specific (OTII-FIG) mice. GMCSF-MOG and GMCSF-OVA were exquisitely specific in stimulating proliferation by MOG-specific T cells and OVA-specific T cells, respectively (Figure 3.6A-B). As expected, given that MOG represented a self-antigen and OVA represented a foreign antigen in mice, the antigenic activity of GMCSF-MOG and MOG^{35-55} in 2D2-FIG T cell cultures was substantially less potent than the respective GMCSF-OVA and $OVA^{323-339}$ responses of OTII-FIG T cells. That is, 2D2 T cell responses to GMCSF-MOG and MOG^{35-55} were at least 100-fold less potent than those of OTII T cells to GMCSF-OVA and $OVA^{323-339}$, respectively. Thus, MOG^{35-55} represented a low-affinity or inefficient T cell epitope whereas $OVA^{323-339}$ represented a relatively high-affinity, high-efficiency T cell epitope in the respective systems. Both GMCSF-MOG and GMCSF-OVA displayed enhanced antigen potency as compared to their respective peptide counterparts, MOG^{35-55} and $OVA^{323-339}$, which most likely reflected antigenic targeting to myeloid APC via GM-CSF and the GM-CSF receptor (CD116, CD131).

To assess induction of Tregs, GMCSF-MOG, GMCSF-OVA, or control vaccines GM-CSF (2D2-FIG) or saline (OTII-FIG) were used to vaccinate 2D2-FIG or OTII-FIG mice (Figure 3.6C-E). As expected, GMCSF-MOG vaccination caused a significant induction of absolute numbers and percentages of MOG-specific Tregs in 2D2-FIG mice (Figure 3.6C), including an average of 55% Tregs per the total $CD3^+$ T pool by day 4 (Figure 3.6E, right panel). GMCSF-

MOG however did not significantly elicit Tregs in OTII-FIG mice, which verified that specific T cell antigen recognition was a requirement for induction of Tregs (Figure 3.6D). In contrast, GMCSF-OVA vaccination of OTII-FIG or 2D2-FIG mice did not reliably elicit significant increases in the absolute numbers or percentage of Tregs compared to control mice (Figure 3.6C, D). These data indicated that specific T cell antigen recognition, although required in the GMCSF-MOG/ 2D2-FIG system, was not sufficient for induction of Tregs in the GMCSF-OVA/ OTII-FIG system. These findings indicated that T cell antigen recognition was necessary but not sufficient for induction of Tregs. Rather, the quality of T cell antigen recognition was the critical parameter polarizing the Treg/ Tcon balance, in that the low efficiency ligand MOG^{35-55} in GMCSF-MOG was best adapted to support induction of Tregs. These experiments revealed that intrinsic qualities of the antigen covalently attached to the GM-CSF fusion partner played a key role in Treg induction.

The GM-CSF domain of GMCSF-MOG was also critical for induction of Tregs because the synthetic MOG^{35-55} peptide did not independently elicit Tregs (Figures 3.2, 3.3, 3.5). Rather, the covalently-linked GM-CSF and MOG^{35-55} domains were both required for efficient induction of Tregs. Interestingly, GM-CSF alone (i.e., GM-CSF, GMCSF-MOG in OTII mice, GMCSF-OVA in 2D2 mice) resulted in increased numbers and percentages of Tregs (2-10%) as compared to saline (< 2% Tregs). However, these increases were transient (day 4) and were modest when compared to the effect of GMCSF-MOG vaccine in 2D2-FIG mice (Figure 3.6E). These findings are consistent with previous studies showing that GM-CSF alone increased Treg proliferation in rodent models of autoimmune disease (218, 219, 221, 243, 244).

3.8 Induction of Tregs by GMCSF-MOG was associated with inefficient TCR ligation.

To test whether low-efficiency TCR ligands are optimal for induction of Tregs, we devised an alternative experimental system based on the observation that the 2D2 TCR recognizes two distinct NAg, including MOG^{35-55} as a low affinity antigen and NFM^{13-37} as a high affinity antigen (245, 246). We derived an expression system for GMCSF-NFM, which exhibited GM-CSF activity equivalent to that of GMCSF-MOG, GMCSF-OVA and GM-CSF in bone marrow proliferation assays (Figure 3.7A). Each recombinant protein induced equivalent proliferation responses with a half-maximal stimulation in the 10 – 100 pmolar range. These assays confirmed that C-terminal antigenic domains did not affect potency of the GM-CSF cytokine. To measure activity of the antigenic domain, GMCSF-MOG, GMCSF-NFM, MOG^{35-55}, and NFM^{13-37} were compared in 2D2 T cell proliferative assays (Figure 3.7B). GMCSF-NFM exhibited the highest potency (half-maximal stimulation at approximately 320 pM). GMCSF-NFM was approximately 10-fold more potent that NFM^{13-37} and was several orders of magnitude more active than either GMCSF-MOG or MOG^{35-55}.

To assess induction of Tregs, GMCSF-MOG, GMCSF-NFM, or saline were used to vaccinate 2D2-FIG mice, and PBMCs were analyzed on day 4 for Treg induction. GMCSF-MOG induced high percentages of $FOXP3^+$ Tregs in the $CD4^+$ T cell pool. Importantly, GMCSF-NFM lacked activities necessary for induction of Tregs (~1%) (Figure 3.7C). GMCSF-MOG induced a sustained Treg response as shown by high percentages of Tregs on day 5 (30%), day 12 (25%), and day 19 (20%) and increased numbers of Tregs/ μl of blood on day 5 (130/ μl) and day 12 (180/ μl). In contrast, GMCSF-NFM did not affect Treg numbers or percentages during the 19 days of the experiment (Figure 3.7D, E). These data support the hypothesis that GMCSF-antigen fusion proteins containing high-efficiency TCR ligands lack activities required

for the robust induction of $FOXP3^+$ Tregs. Although GMCSF-MOG and GMCSF-NFM differed qualitatively in activities needed for the induction of Tregs, both vaccines caused activation of the 2D2-FIG T cell repertoire as shown by the increased percentages of $CD62L^{low}$ $CD44^{high}$ T cells (Figure 3.7G). Both vaccines also caused the diminution of the 2D2 Tcon repertoire (Figure 3.7F), which may represent a separate mechanism of tolerance.

3.9 The Treg-inductive activity of GMCSF-MOG remained intact when administered in pro-immunogenic adjuvants.

Previous studies showed that GMCSF-MOG and GMCSF-PLP(139-151) imposed tolerogenic outcomes at relatively low doses even when emulsified with the respective encephalitogenic peptide in CFA in the C57BL/6 and SJL models of EAE (187). These data indicated that GMCSF-NAg exerted operational tolerance even in strong pro-inflammatory environments. For example, inclusion of 1 nmole GMCSF-MOG with 77.5 nmoles of MOG^{35-55} in CFA strongly inhibited incidence, severity, and duration of EAE compared to mice immunized with the CFA/ MOG^{35-55} emulsion without GMCSF-MOG. These data raised the important question of whether GMCSF-MOG would retain Treg inductive capacity in adjuvant primed proinflammatory environments.

To assess this question, GMCSF-MOG was prepared in saline, alum, or CFA and injected into 2D2-FIG mice (Figure 3.8A, B). Alum vaccine formulations incorporated GMCSF-MOG, GM-CSF, MOG^{35-55}, or saline into the alum adjuvant. A single vaccination of GMCSF-MOG/ CFA, GMCSF-MOG/ alum, and GMCSF-MOG in saline elicited high percentages of circulating Tregs that persisted through the 21-day assessment (Figure 3.8B). On day 7, the GMCSF-MOG/ alum and GMCSF-MOG/ saline vaccines elicited higher Treg percentages than GMCSF-MOG/ CFA although these differences disappeared by days 14 and 21 (Figure 3.8B). On day 11

GMCSF-MOG in saline and GMCSF-MOG/ alum both elicited high percentages of Tregs while GMCSF/ alum, MOG^{35-55} / alum, and saline/ alum did not elicit significant Treg responses (Figure 3.8C). These findings are consistent with the concept that low-efficiency T cell antigen recognition events are integrated within the confines of an immunological synapse and can support Treg induction without regard to local inflammatory environmental cues.

A related question was whether incorporation of GMCSF-MOG into CFA would relieve the strict requirement for covalent coupling of GM-CSF and NAg, because the two domains would be physically sequestered in the same antigenic depot. Vaccine formulations in CFA included GMCSF-MOG, "GMCSF + MOG^{35-55}", MOG^{35-55}, or saline in CFA. GMCSF-MOG/ CFA induced a significant Treg response whereas the other CFA-based vaccine formulations including "GMCSF + MOG^{35-55}" in CFA lacked robust Treg inductive capability (Figure 3.8D). These data indicate that GMCSF-MOG exerted a dominant Treg response even within the context of a CFA adjuvant-primed lymphatic drainage. However, co-localization of independent GM-CSF and NAg molecules in the same adjuvant-based antigenic depot did not relieve the requirement for covalent cytokine-NAg linkage. These data suggest that a continued requirement of GMCSF-NAg linkage is needed for Treg induction during and/ or after the immunological processing of the CFA antigenic depot.

3.10 Subcutaneous and intravenous routes of GMCSF-MOG administration drive robust Treg responses.

The observation that SC GMCSF-MOG vaccination elicited the highest Treg frequencies in the blood (30-40%) rather than the spleen (13-15%) or lymph nodes (6%) raised questions whether the Treg inductive response required a classical lymphatic drainage (Figure 3.3). The expectation was that SC injection of GMCSF-MOG would target MOG^{35-55} to myeloid APC in the

draining lymphatics at the site of inoculation and that sensitization of the Treg response would occur in the draining lymphatics. Conversely, IV administration of GMCSF-MOG would predictably bypass the lymphatic drainage and instead introduce NAg directly into the blood, spleen, lung, and liver. To assess this question, the optimal route of GMCSF-MOG administration was tested by comparing SC or IV injections in 2D2-FIG mice. Notably, either route was equally effective. Administration of GMCSF-MOG via either SC and IV route caused robust Treg responses marked by ~25% Tregs (of the total $CD4^+$ T cell population) as compared to mock (saline) vaccination (3% Tregs) when assessed on day 12 (Figure 3.9A, B). Both SC and IV vaccination also resulted in increased percentages of activated 2D2 T cells marked by high expression levels of CD44 and low levels of CD62L (Figure 3.9A, E). Although both SC and IV administration of GMCSF-MOG caused the activation of both Treg and Tcon subsets, the vaccine preferentially drove the expansion Tregs in both cases. Mice vaccinated by either route had significantly increased levels of Treg per µl of blood (~180) as compared to saline (~60) (Figure 3.9C) and reduced percentages and numbers of circulating $CD3^+$ T cells (~900) as compared to saline (~8000) (Figure 3.9D). These results indicate that neither cutaneous APC nor draining lymphatics are required for GMCSF-MOG-mediated Treg induction.

3.11 Vaccine-induced kinetics controlling Treg emergence was a function of pre-existing Treg levels.

A central question was whether tolerogenic GMCSF-MOG vaccination required pre-existing Tregs to stage the rapid and predominant $FOXP3^+$ Treg response that occurred in 3-4 days among the circulating MOG-specific repertoire. That is, did GMCSF-MOG drive expansion of pre-existing Tregs or did GMCSF-MOG induce de novo differentiation of Tregs from naïve T cell precursors? To gain insight into this question, 2D2-FIG-*Rag1*$^{-/-}$ mice were

derived because these mice largely lack FOXP3^{+} Tregs of either thymic or peripheral origin. TCR transgenic Rag1$^{-/-}$ naïve T cells however have the capacity to differentiate into iTregs/ pTregs (i.e., inducible Tregs, peripheral Tregs) upon TGF-β signaling during cellular activation.

As expected, naïve 2D2-FIG-*Rag1*$^{-/-}$ mice exhibited a substantial 120-fold reduction in Treg percentages in that 2D2-FIG-*Rag1*$^{-/-}$ mice averaged 0.007% Tregs compared to 0.845% 2D2-FIG Tregs in the circulating CD4^{+} pool (Figure 3.10A). These data indicated that 2D2-FIG-*Rag1*$^{-/-}$ mice had profound reductions in Tregs but were not devoid of Tregs. Notably, 2D2-FIG-*Rag1*$^{-/-}$ mice exhibited substantially delayed kinetics in response to tolerogenic GMCSF-MOG, which elicited 1% and 30% Tregs in 2D2-FIG-*Rag1*$^{-/-}$ and 2D2-FIG mice respectively by day 5 (Figure 3.10C, Top). In accordance, 2D2-FIG-Rag1$^{-/-}$ mice and 2D2-FIG mice averaged 4 and 150 Tregs per µl of blood respectively (Figure 3.10C, bottom) on day 5. By day 12 however, GMCSF-MOG vaccinated 2D2-FIG-*Rag1*$^{-/-}$ mice had high numbers and percentages of circulating Tregs that closely approximated the circulating Treg population in 2D2-FIG mice (~20% Tregs, Figure 3.10C). Mice injected with saline or "GM-CSF + MOG" control vaccines did not exhibit significant increases in Tregs (Figure 3.10B). The delayed Treg induction in 2D2-FIG-*Rag1*$^{-/-}$ mice was not due to deficient exposure to MOG35-55 because GMCSF-MOG caused equivalent decrements in circulating Tcon numbers and equivalent elevations in CD44^{high} CD62L^{low} T cell numbers (per µl of blood) in both mouse strains by day 12 (Figure 3.10D).

Collectively, these data are consistent with the proposition that GMCSF-MOG vaccination selectively amplifies pre-existing Tregs to stage the rapid accumulation of Tregs. However, these data did not exclude the possibility that GMCSF-MOG may also drive de novo differentiation of naïve T cells into Tregs, perhaps abetted by pre-existing Tregs. Notably, when given sufficient time, GMCSF-MOG has sufficient tolerogenic efficacy to elicit large Treg

populations in both 2D2-FIG-*Rag1*$^{-/-}$ and 2D2-FIG mice. These data reveal that the tolerogenic activity of GMCSF-MOG does not require clonotypic diversity in the T cell repertoire or an intact B cell repertoire because 2D2-FIG-*Rag1*$^{-/-}$ mice lack endogenous TCR-alpha chain rearrangements and are largely devoid of B cells.

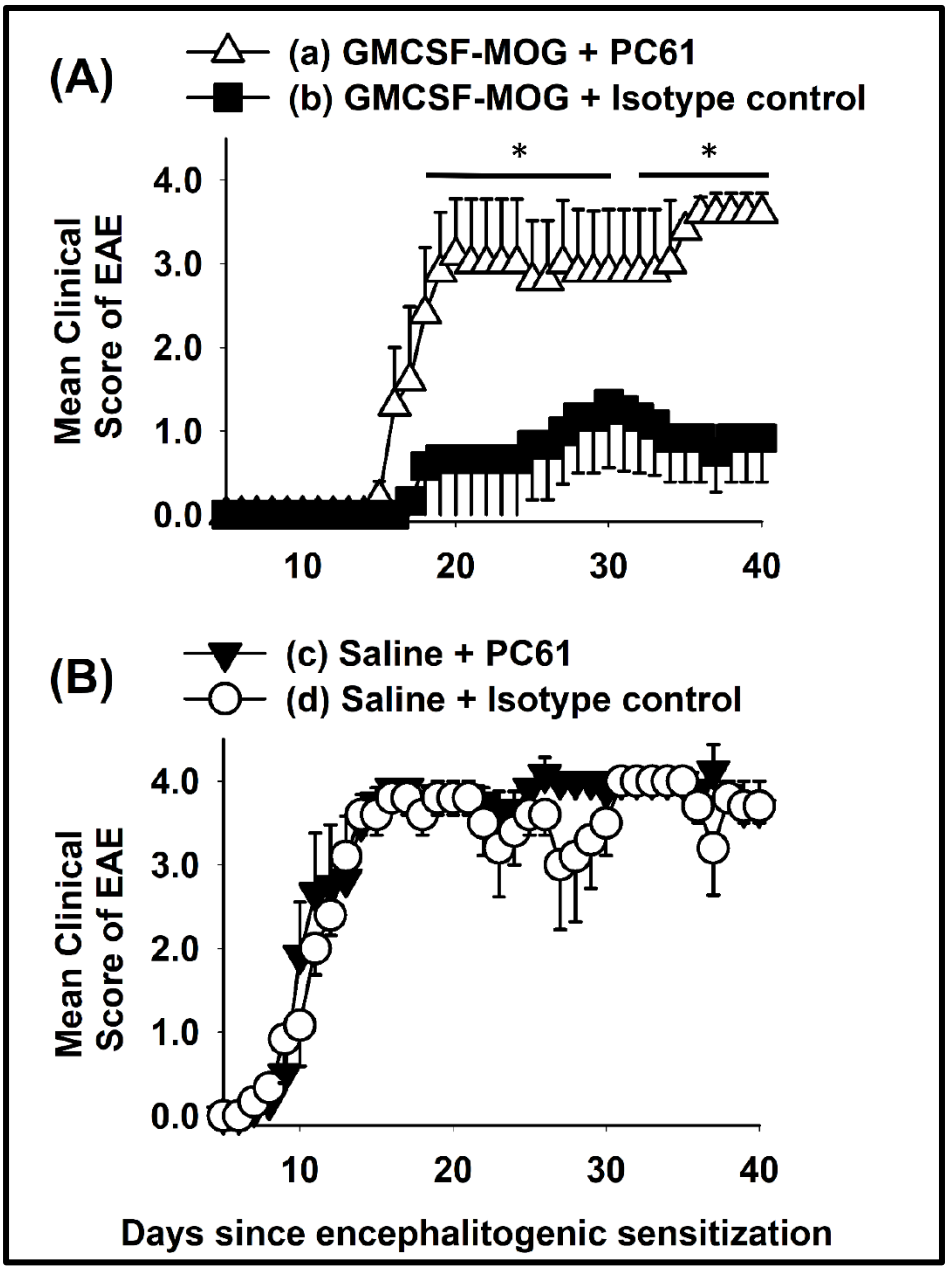
(A)
(a) GMCSF-MOG + PC61
(b) GMCSF-MOG + Isotype control
*
*
Mean Clinical Score of EAE
4.0
3.0
2.0
1.0
0.0
10
20
30
40
(B)
(c) Saline + PC61
(d) Saline + Isotype control
Mean Clinical Score of EAE
4.0
3.0
2.0
1.0
0.0
10
20
30
40
Days since encephalitogenic sensitization

Figure 3.1: Depletion of CD25$^+$ Tregs with the anti-CD25 mAb PC61 reversed tolerogenic vaccination. C57BL/6 mice were treated with 2 nmoles GMCSF-MOG **(A)** or saline **(B)** on days −21, −14, and −7. Mice were administered either 250 μg of the anti-CD25 PC61 mAb or 250 μg of a rat IgG1 isotype control mAb on days −4 and −2. On day 0, all mice were immunized with 200 μg MOG35-55 emulsified in CFA. Mice received 200 ng of Ptx toxin i.p. on days 0 and 2. Shown are the daily mean clinical EAE scores through the end of the experiment on day 40 (*$p <$ 0.05). Differences between (a) and (b) were analyzed using a two-way repeated measures ANOVA. Incidence of EAE was; (a) 5 of 5, (b) 3 of 6, (c) 6 of 6, and (d) 5 of 5. Mean maximal scores were; (a) 4.0 ± 0.0, (b) 1.3 ± 0.8, (c) 4.3 ± 0.2, and (d) 4.0 ± 0.0 (non-parametric ANOVA (b) vs. (a, c, d), $p \leq 0.012$). Error bars represent ± SEM.

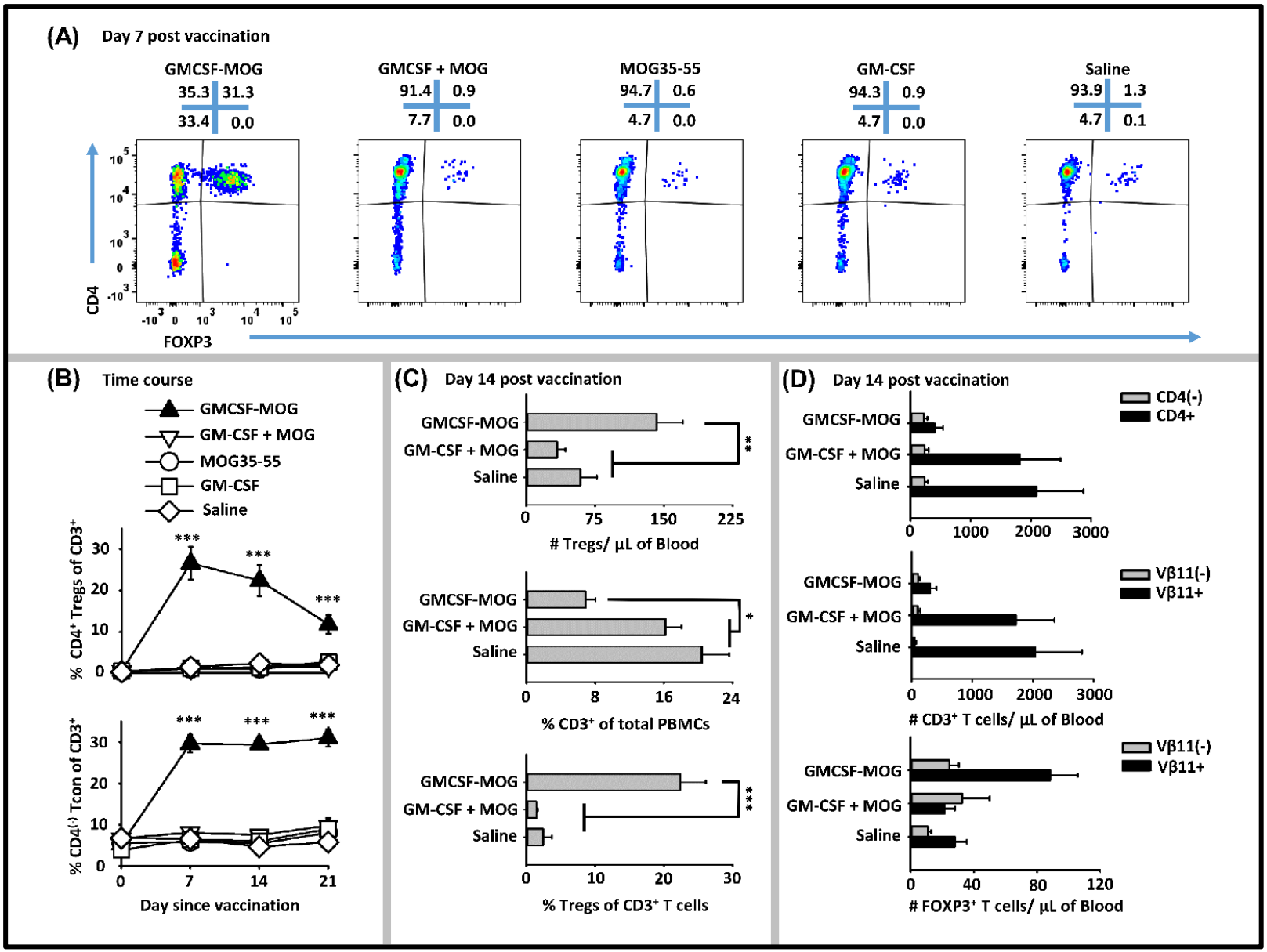
(A)
Day 7 post vaccination
GMCSF-MOG
35.3
31.3
33.4
0.0
GMCSF + MOG
91.4
0.9
7.7
0.0
MOG35-55
94.7
0.6
4.7
0.0
GM-CSF
94.3
0.9
4.7
0.0
Saline
93.9
1.3
4.7
0.1
CD4
FOXP3
(B)
Time course
GMCSF-MOG
GM-CSF + MOG
MOG35-55
GM-CSF
Saline
% CD4+ Tregs of CD3+
% CD4(-) Tcon of CD3+
Day since vaccination
(C)
Day 14 post vaccination
GMCSF-MOG
GM-CSF + MOG
Saline
Tregs/ µL of Blood
% CD3+ of total PBMCs
% Tregs of CD3+ T cells
(D)
Day 14 post vaccination
CD4(-)
CD4+
Vβ11(-)
Vβ11+
CD3+ T cells/ µL of Blood
FOXP3+ T cells/ µL of Blood

Figure 3.2: GMCSF-MOG elicited FOXP3$^+$ Tregs in 2D2-FIG mice. On day 0, 2D2-FIG mice (n = 4/group) were vaccinated with GMCSF-MOG, the combination of GM-CSF + MOG35-55, MOG35-55 alone, GM-CSF alone, or saline. All injections were SC in saline at a dose of 4 nmoles. PBMCs were assayed for CD45, CD3, CD4, GFP (FOXP3), Vβ11 (2D2 TCRβ) by flow cytometry on days −1, 7, 14, and 21. Shown are **(A)** representative dot plots (day 7 time-point) from each treatment group gated on CD3$^+$ T cells and analyzed for CD4 (y-axis) and FOXP3 (x-axis) expression. **(B)** The percentages of CD4$^+$ FOXP3$^+$ Tregs (top) and CD4$^{(-)}$ FOXP3$^{(-)}$ Tcon cells (bottom) among total CD3$^+$ T cells are shown before vaccination (day 0) and for day 7, 14, and 21 time-points. Shown **(C)** are the total number of FOXP3$^+$ Tregs per μl of blood (top) and percentages of CD3$^+$ T cells among CD45$^+$ leukocytes (middle) and FOXP3$^+$ Tregs among CD3$^+$ T cells (bottom) on day 14. Shown **(D)** are the number of CD3$^+$ CD4$^+$ and CD3$^+$ CD4$^{(-)}$ T cells per μl of blood (top) and the CD3$^+$ Vβ11$^+$ and CD3$^+$ Vβ11$^{(-)}$ T cells per μl of blood (middle) as well as the numbers of Vβ11$^+$ FOXP3$^+$ and Vβ11$^{(-)}$ FOXP3$^+$ Tregs (bottom) on day 14. Statistical significance was analyzed by use of a one-way ANOVA (*$p < 0.05$, **$p < 0.01$, ***$p < 0.001$). These data are representative of three independent experiments. Error bars represent ± SEM.

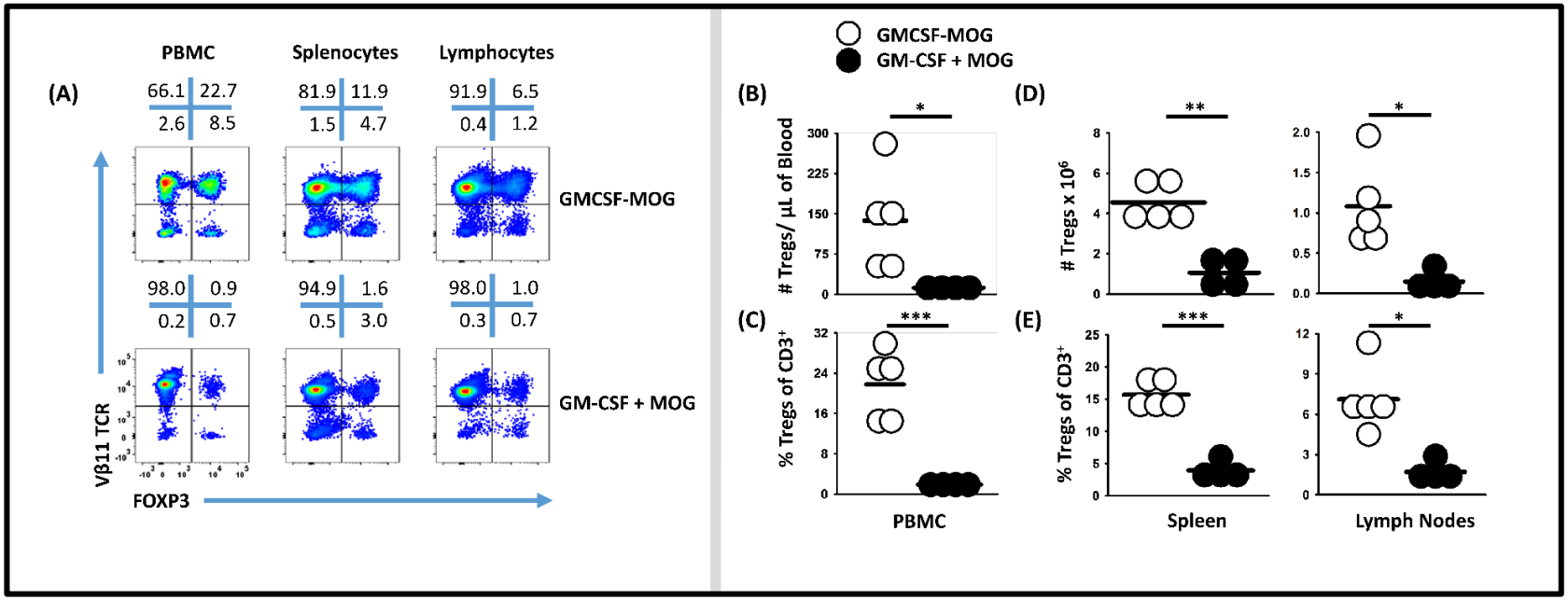
(A)
PBMC
Splenocytes
Lymphocytes
66.1
22.7
2.6
8.5
81.9
11.9
1.5
4.7
91.9
6.5
0.4
1.2
GMCSF-MOG
98.0
0.9
0.2
0.7
94.9
1.6
0.5
3.0
98.0
1.0
0.3
0.7
GM-CSF + MOG
Vβ11 TCR
FOXP3
GMCSF-MOG
GM-CSF + MOG
(B)
Tregs/ µL of Blood
(C)
% Tregs of CD3+
PBMC
(D)
Tregs x 10^6
(E)
% Tregs of CD3+
Spleen
Lymph Nodes

Figure 3.3: Subcutaneous administration of GMCSF-MOG in saline elicited FOXP3$^+$ Tregs in lymph nodes, spleen, and blood. On day 0, 2D2-FIG mice (n = 4–5/group) were vaccinated with 4 nmoles of GMCSF-MOG or 4 nmoles GM-CSF + 4 nmoles MOG35-55. PBMC were analyzed on day 4, and draining inguinal lymph nodes and spleen were analyzed on days 5 and 6. **(A)** Representative dotplots of CD3 gated T cells from the peripheral blood, lymph nodes, and spleen were analyzed for Vβ11 (2D2 TCRβ) (y-axis) and FOXP3 (x-axis). Shown are numbers of Tregs per μl of blood **(B)**, percentages of Tregs among the total CD3$^+$ T cells **(C)**, as well as the total numbers **(D)** and percentages **(E)** of Tregs among the total CD3$^+$ T cells in the spleen and lymph nodes. Each dot represents a single mouse. The bar represents the mean. Statistical significance was analyzed by use of a one-tailed t-test (*$p < 0.05$, **$p < 0.01$, ***$p < 0.001$). These data are representative of three independent experiments.

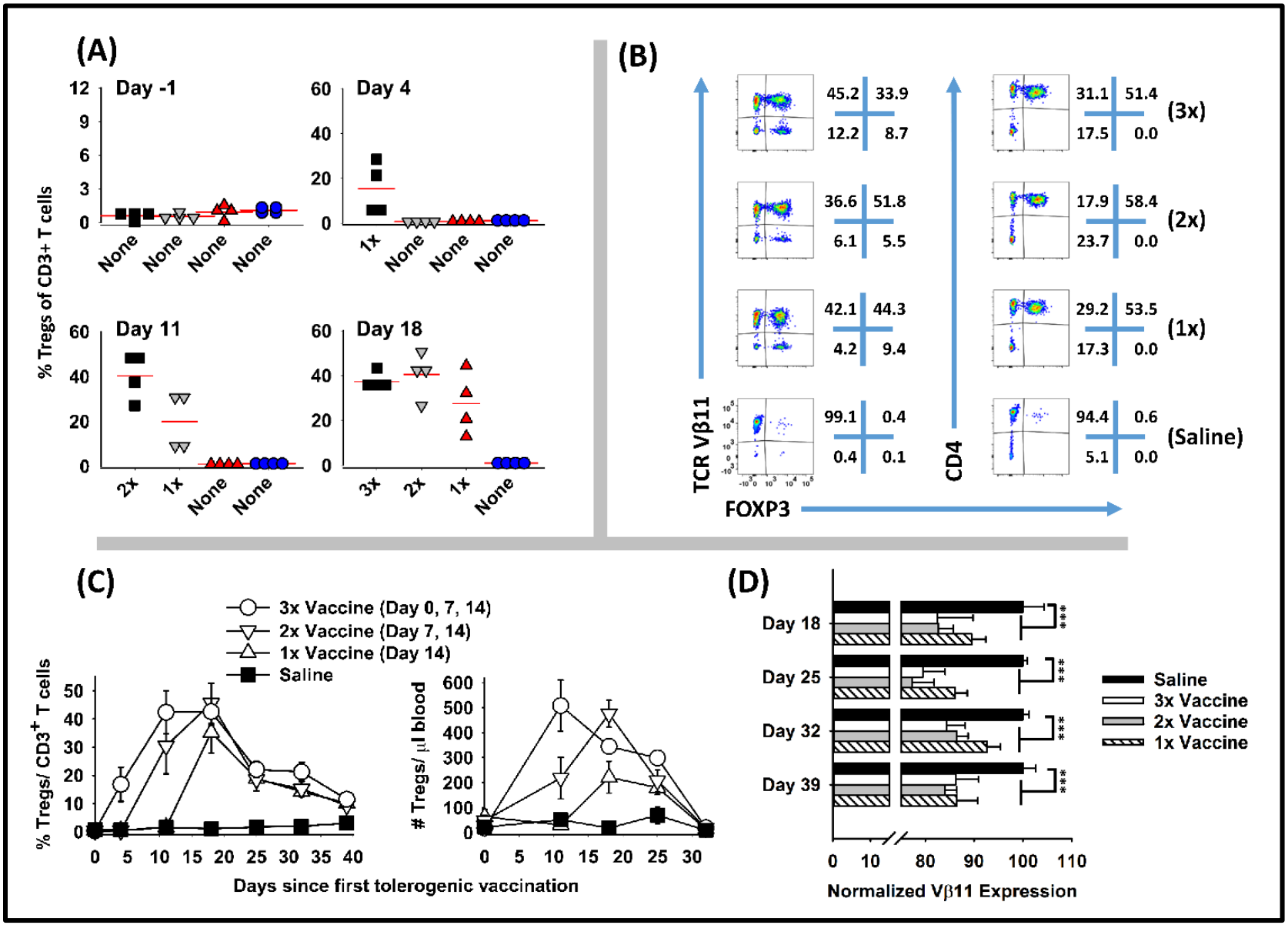
(A)
Day -1
Day 4
Day 11
Day 18
% Tregs of CD3+ T cells
None
1x
2x
3x
(B)
TCR Vβ11
FOXP3
CD4
45.2 33.9 12.2 8.7
31.1 51.4 17.5 0.0
(3x)
36.6 51.8 6.1 5.5
17.9 58.4 23.7 0.0
(2x)
42.1 44.3 4.2 9.4
29.2 53.5 17.3 0.0
(1x)
99.1 0.4 0.4 0.1
94.4 0.6 5.1 0.0
(Saline)
(C)
3x Vaccine (Day 0, 7, 14)
2x Vaccine (Day 7, 14)
1x Vaccine (Day 14)
Saline
% Tregs/ CD3+ T cells
# Tregs/ μl blood
Days since first tolerogenic vaccination
(D)
Day 18
Day 25
Day 32
Day 39
Saline
3x Vaccine
2x Vaccine
1x Vaccine
Normalized Vβ11 Expression

Figure 3.4: Booster vaccines with GMCSF-MOG maintained circulating levels of Tregs. 2D2-FIG mice were injected with 4 nmoles of GMCSF-MOG or saline on days 0, 7, and 14. One group received three GMCSF-MOG vaccinations (3x), one group received saline on day 0 and vaccine on days 7 and 14 (2x), one group received saline on days 0 and 7 and vaccine on day 14 (1x), and one group received saline on days 0, 7, and 14 (n = 4/group). T cells in peripheral blood were assayed for CD45, CD3, CD4, GFP (FOXP3), Vβ11 (2D2 TCRβ) expression on days −1, 4, 11, 18, 25, 32, and 39. **(A)**PBMC were assessed for percentages of $FOXP3^+$ Tregs among total $CD3^+$ T cells on day −1, 4, 11, and 18. **(B)** For day 18, Vβ11 (y-axis) or CD4 (y-axis) expression is shown as a function of FOXP3 expression (x-axis) among $CD3^+$ T cells. **(C)** Percentages and numbers (per μl blood) of $FOXP3^+$ Tregs are shown for $CD3^+$ T cells collected on days −1, 4, 11, 18, 25, 32, and 39. For % Tregs, the 1x, 2x, and 3x groups were significantly different from saline on days 18, 25, 32, and 39. For numbers of Tregs/μl of blood, significant differences were noted on days 18 and 25 ($p < 0.05$). **(D)** The MFI of Vβ11 expression among $Vβ11^+$ T cells is shown for PBMC samples collected on days 18, 25, 32, and 39. Statistical significance was analyzed by use of a one-way ANOVA (***$p < 0.001$). Error bars represent ± SEM.

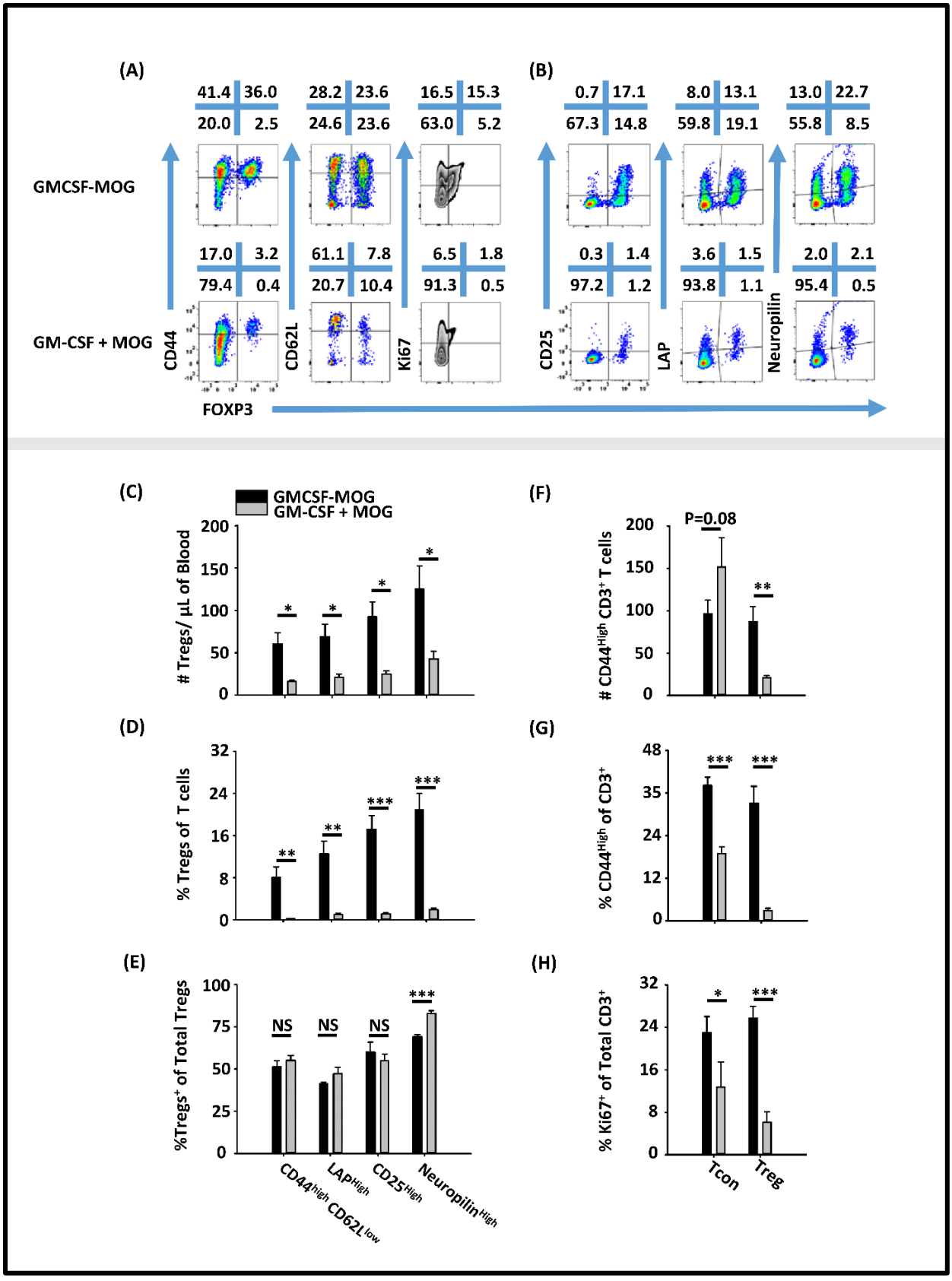
(A)
(B)
GMCSF-MOG
GM-CSF + MOG
CD44
CD62L
Ki67
FOXP3
CD25
LAP
Neuropilin
41.4 36.0
20.0 2.5
28.2 23.6
24.6 23.6
16.5 15.3
63.0 5.2
17.0 3.2
79.4 0.4
61.1 7.8
20.7 10.4
6.5 1.8
91.3 0.5
0.7 17.1
67.3 14.8
8.0 13.1
59.8 19.1
13.0 22.7
55.8 8.5
0.3 1.4
97.2 1.2
3.6 1.5
93.8 1.1
2.0 2.1
95.4 0.5
(C)
GMCSF-MOG
GM-CSF + MOG
Tregs/ µL of Blood
(D)
% Tregs of T cells
(E)
%Tregs+ of Total Tregs
NS
CD44high CD62Llow
LAPHigh
CD25High
NeuropilinHigh
(F)
P=0.08
# CD44High CD3+ T cells
(G)
% CD44High of CD3+
(H)
% Ki67+ of Total CD3+
Tcon
Treg

Figure 3.5: GMCSF-MOG induced a FOXP3$^+$ T cell population with a canonical Treg phenotype. On day 0, 2D2-FIG (*n* = 4–5/group) mice were vaccinated subcutaneously with 4 nmoles of GMCSF-MOG or 4 nmoles GM-CSF + 4 nmoles MOG35-55. PBMCs were analyzed on day 4. Shown **(A)** are representational dotplots of CD3$^+$ T cells analyzed for CD44, CD62L, and Ki67 expression (y-axis) and **(B)** CD4$^+$ T cells analyzed for CD25, LAP, and Neuropilin vs. FOXP3 expression (x-axis). Shown are numbers of Tregs per μl of blood **(C)** or percentages of Tregs **(D)** that express CD44^{high}CD62L^{low}, LAP, CD25, or Neuropilin among total T cells **(D)** or among Tregs **(E)**. Shown are the Treg and Tcon cell numbers per μl of blood **(F)** and percentages of CD44^{high} Tcons or Tregs among CD3$^+$ T cells **(G)**. Shown are **(H)** percentages of Ki67$^+$ Tregs or Tcons among CD3$^+$ T cells. Statistical significance was analyzed by use of a one-tailed *t*-test (*$p < 0.05$, **$p < 0.01$, ***$p < 0.001$). These data are representative of two independent experiments. Error bars represent ± SEM.

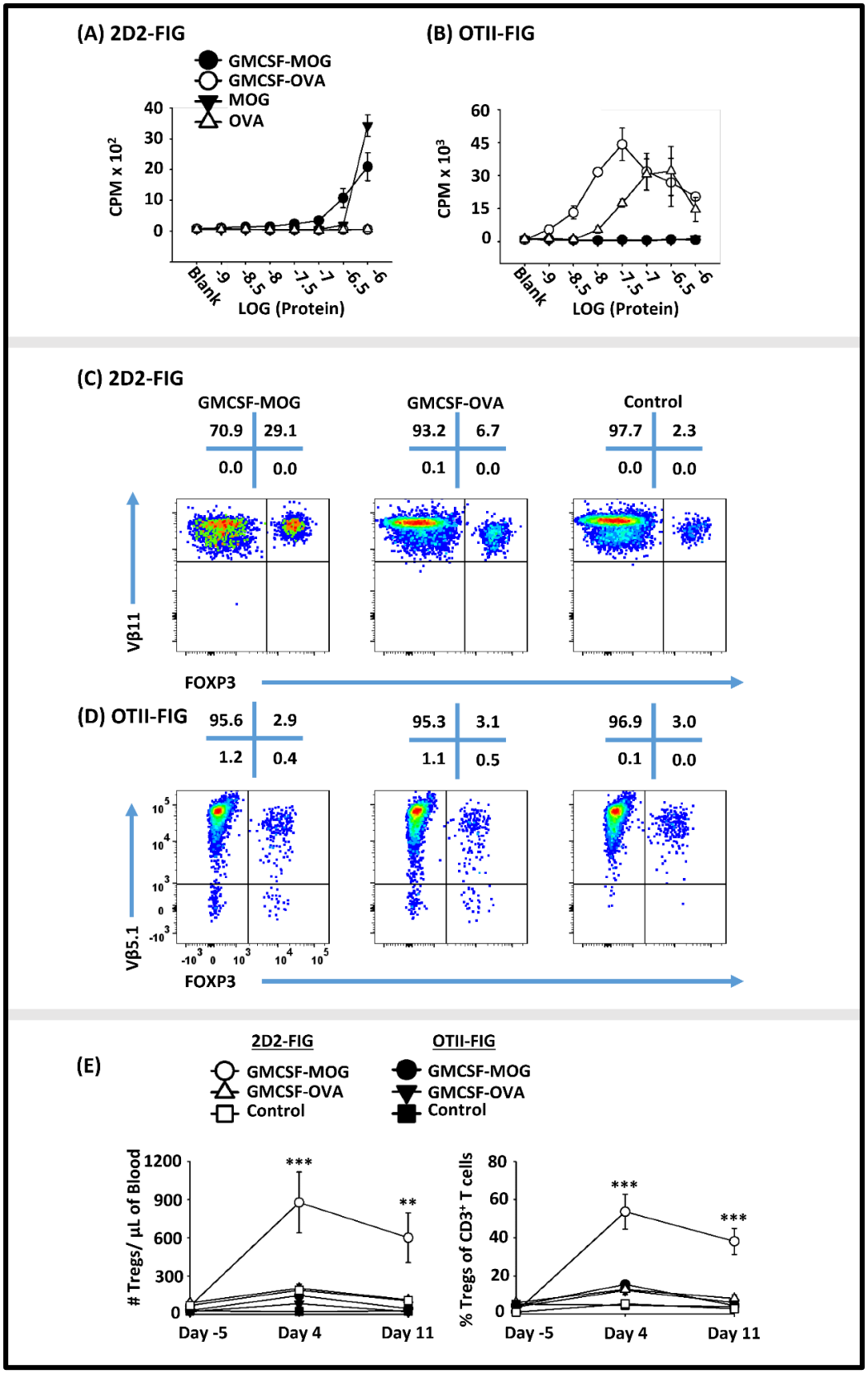
(A) 2D2-FIG
GMCSF-MOG
GMCSF-OVA
MOG
OVA
CPM x 10²
40
30
20
10
0
Blank
-9
-8.5
-8
-7.5
-7
-6.5
-6
LOG (Protein)
(B) OTII-FIG
CPM x 10³
60
45
30
15
0
Blank
-9
-8.5
-8
-7.5
-7
-6.5
-6
LOG (Protein)
(C) 2D2-FIG
GMCSF-MOG
70.9
29.1
0.0
0.0
GMCSF-OVA
93.2
6.7
0.1
0.0
Control
97.7
2.3
0.0
0.0
Vβ11
FOXP3
(D) OTII-FIG
95.6
2.9
1.2
0.4
95.3
3.1
1.1
0.5
96.9
3.0
0.1
0.0
Vβ5.1
FOXP3
(E)
2D2-FIG
GMCSF-MOG
GMCSF-OVA
Control
OTII-FIG
GMCSF-MOG
GMCSF-OVA
Control
Tregs/ µL of Blood
1200
900
600
300
0
***
**
Day -5
Day 4
Day 11
% Tregs of CD3+ T cells
80
60
40
20
0
***
***
Day -5
Day 4
Day 11

Figure 3.6: GMCSF-MOG Treg induction was dependent upon the antigenic domain. Twenty-five thousand 2D2 T cells **(A)** or OTII T cells **(B)** from continuous T cell lines were cultured with 100,000 irradiated splenocytes and designated concentrations (x-axis) of GMCSF-MOG, GMCSF-OVA, MOG35-55, or OVA323-339. Cultures were pulsed with 1 μCi of [^{3}H] thymidine during the last 24 h of a 3-day culture, and counts per minute (CPM, y-axis) were measured on day 3. **(C–E)** On day 0, 2D2-FIG or OTII-FIG (n = 3–4/group) were subcutaneously vaccinated with either 4 nmoles of GMCSF-MOG, 4 nmoles GMCSF-OVA, or with saline (OTII-FIG) or GM-CSF + MOG35-55 (2D2-FIG). PBMCs were assayed on days −5, 4, and 11 for CD3, CD4, Vβ11 (2D2 TCRβ), Vβ5.1 (OTII TCRβ) and FOXP3 expression. Representative dotplots of 2D2-FIG **(C)** and OTII-FIG **(D)** PBMCs were analyzed for Vβ11 or Vβ5.1 (y-axis) respectively and FOXP3 (x-axis) among CD3$^+$ T cells. Shown **(E)** are Treg numbers per μl of blood and Treg percentages of total CD3$^+$ T cells on days −5, 4, and 11. Statistical significance was analyzed by use of a one-way ANOVA (**$p < 0.01$, ***$p < 0.001$). These data are representative of three independent experiments. Error bars represent ± SD (A, B) or SEM (E).

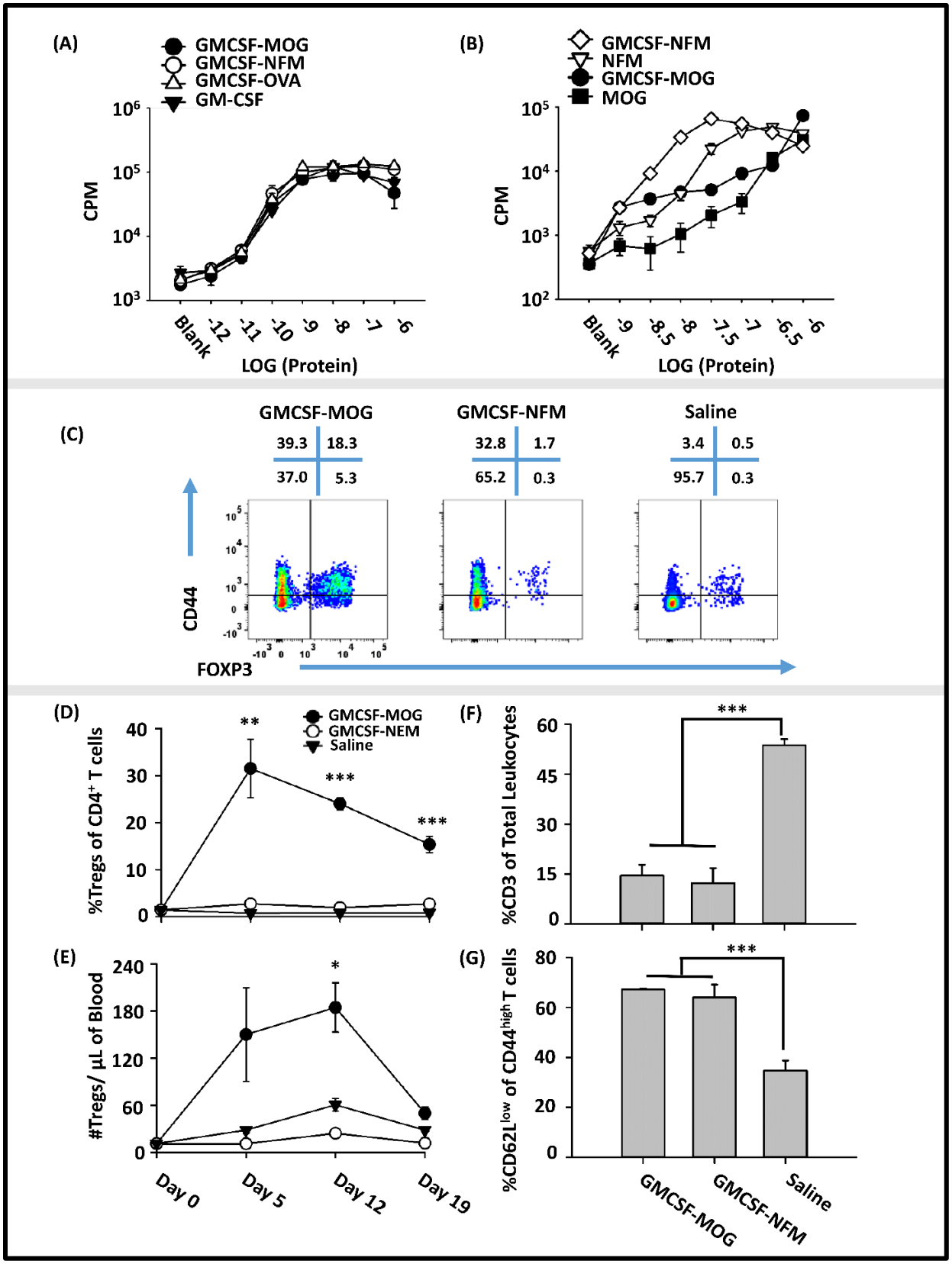
(A)
GMCSF-MOG
GMCSF-NFM
GMCSF-OVA
GM-CSF
CPM
LOG (Protein)
(B)
GMCSF-NFM
NFM
GMCSF-MOG
MOG
CPM
LOG (Protein)
(C)
GMCSF-MOG
GMCSF-NFM
Saline
39.3
18.3
37.0
5.3
32.8
1.7
65.2
0.3
3.4
0.5
95.7
0.3
CD44
FOXP3
(D)
GMCSF-MOG
GMCSF-NEM
Saline
%Tregs of CD4+ T cells
(E)
#Tregs/ µL of Blood
Day 0
Day 5
Day 12
Day 19
(F)
%CD3 of Total Leukocytes
(G)
%CD62Llow of CD44high T cells
GMCSF-MOG
GMCSF-NFM
Saline

Figure 3.7: Induction of Tregs by GMCSF-MOG was associated with inefficient TCR ligation. (A) Designated concentrations (x-axis) of GM-CSF, GMCSF-MOG, GMCSF-NFM, or GMCSF-OVA were incubated with 100,000 C57BL/6 bone marrow cells for 3 days. **(B)** 25,000 2D2 T cells were cultured with 100,000 irradiated splenocytes with designated concentrations (x-axis) of GMCSF-MOG, GMCSF-NFM, MOG35-55, or NFM13-37. **(A, B)** Cultures were pulsed with 1 μCi of [^{3}H] thymidine during the last 24 h of a 3-day culture. **(C–G)** On day 0, 2D2-FIG mice were subcutaneously vaccinated with either 4 nmoles of GMCSF-MOG (n = 5), 4 nmoles GMCSF-NFM (n = 3), or saline (n = 3). PBMCs were assayed on 5, 12, and 19 for CD3, CD4, Vβ11 (2D2 TCRβ), CD44, CD62L, and GFP (FOXP3) expression. The pre-day 0 bleed was derived from the average Treg percentages among $CD4^+$ T cells and the average number of Tregs per μl of blood (N = 50 mice from 3 independent experiments). **(C)** On day 12, PBMCs from GMCSF-MOG, GMCSF-NFM, or saline treated mice were analyzed for CD44 (y-axis) and FOXP3 (x-axis) among $CD3^+$ $CD4^+$ T cells. Shown **(D, E)** are Treg numbers per μl of blood and Treg percentages among $CD4^+$ T cells on days 5, 12, and 19. Shown are percentages of $CD3^+$ T cells among total $CD45^+$ leukocytes **(F)** and percentages of $CD62L^{low}$ cells among $CD44^{high}CD3^+$ $CD4^+$ T cells **(G)** on day 12. Statistical significance was analyzed by use of a one-way ANOVA (*$p < 0.05$, **$p < 0.01$, ***$p < 0.001$). These data are representative of three independent experiments. Error bars represent ± SD (A, B) or SEM (D-G).

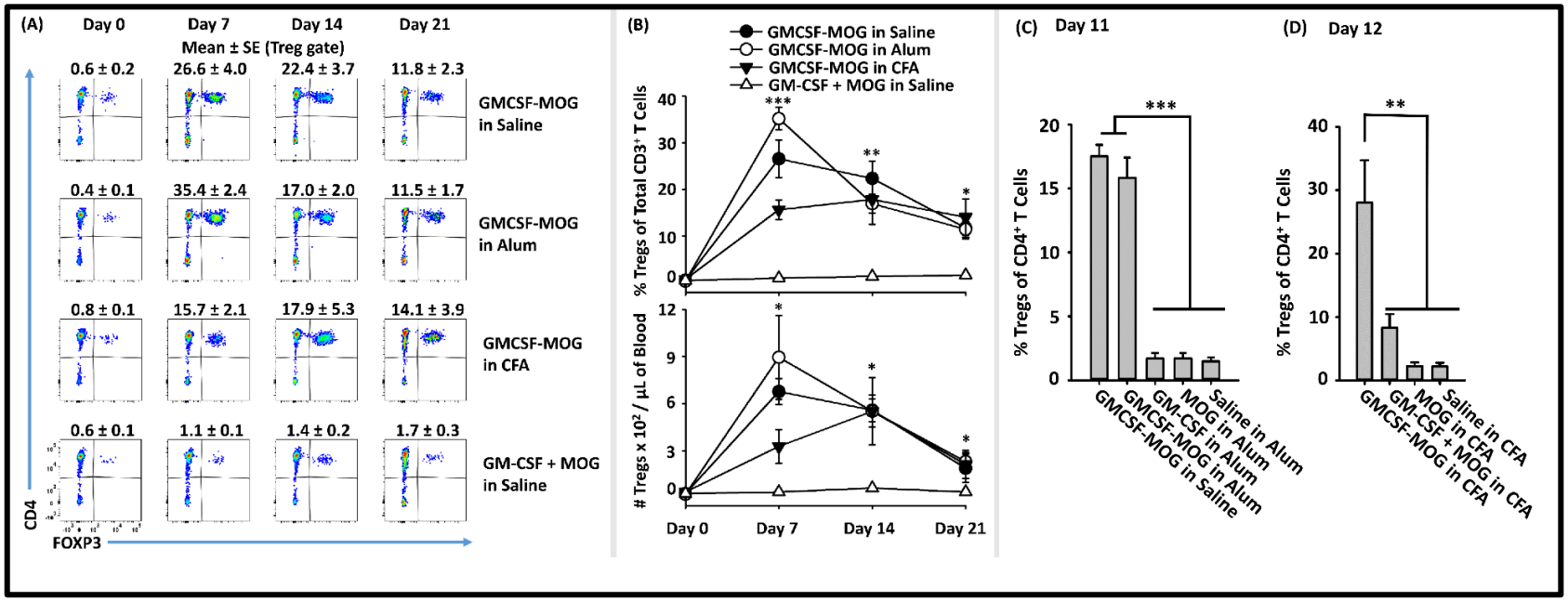
(A)
Day 0
Day 7
Day 14
Day 21
Mean ± SE (Treg gate)
0.6 ± 0.2
26.6 ± 4.0
22.4 ± 3.7
11.8 ± 2.3
GMCSF-MOG in Saline
0.4 ± 0.1
35.4 ± 2.4
17.0 ± 2.0
11.5 ± 1.7
GMCSF-MOG in Alum
0.8 ± 0.1
15.7 ± 2.1
17.9 ± 5.3
14.1 ± 3.9
GMCSF-MOG in CFA
0.6 ± 0.1
1.1 ± 0.1
1.4 ± 0.2
1.7 ± 0.3
GM-CSF + MOG in Saline
CD4
FOXP3
(B)
GMCSF-MOG in Saline
GMCSF-MOG in Alum
GMCSF-MOG in CFA
GM-CSF + MOG in Saline
% Tregs of Total CD3+ T Cells
# Tregs x 10² / µL of Blood
Day 0
Day 7
Day 14
Day 21
(C) Day 11
% Tregs of CD4+ T Cells
GMCSF-MOG in Saline
GMCSF-MOG in Alum
GM-CSF in Alum
MOG in Alum
Saline in Alum
(D) Day 12
% Tregs of CD4+ T Cells
GMCSF-MOG in CFA
GM-CSF + MOG in CFA
MOG in CFA
Saline in CFA

Figure 3.8: The Treg-inductive activity of GMCSF-MOG remained intact when administered in pro-immunogenic adjuvants. (A, B) On day 0, 2D2-FIG mice (n = 4/group) were or were not vaccinated with GMCSF-MOG in saline, alum, or CFA, and PBMCs were obtained on days 0, 7, 14, and 21. All injections were SC at a dose of 4 nmoles. **(A)** CD3+ T cells were analyzed for CD4 (y-axis) and FOXP3 (x-axis) expression. Percentages of CD4+ FOXP3+ Tregs are designated at the top of each dotplot. Shown **(B)** are percentages of FOXP3+ Tregs among CD3+ T cells (top) and Treg numbers per μl of blood (bottom) on days 0, 7, 14, and 21. **(C)** On day 0, 2D2-FIG mice (n = 4/group) were vaccinated with 4 nmoles of GMCSF-MOG, GM-CSF, MOG35-55, or saline in 100 μl of alum, and blood was analyzed on day 11 for Treg percentages among CD4+ T cells. **(D)** On day 0, 2D2-FIG mice (n = 4/group) were vaccinated with 4 nmoles of GMCSF-MOG, GM-CSF + MOG, MOG35-55, or saline in CFA and blood was analyzed on day 12 for Treg percentages among CD4+ T cells. Statistical significance was analyzed by use of a one-way ANOVA (*$p < 0.05$, **$p < 0.01$, ***$p < 0.001$). These data are representative of three independent experiments. Error bars represent ± SEM.

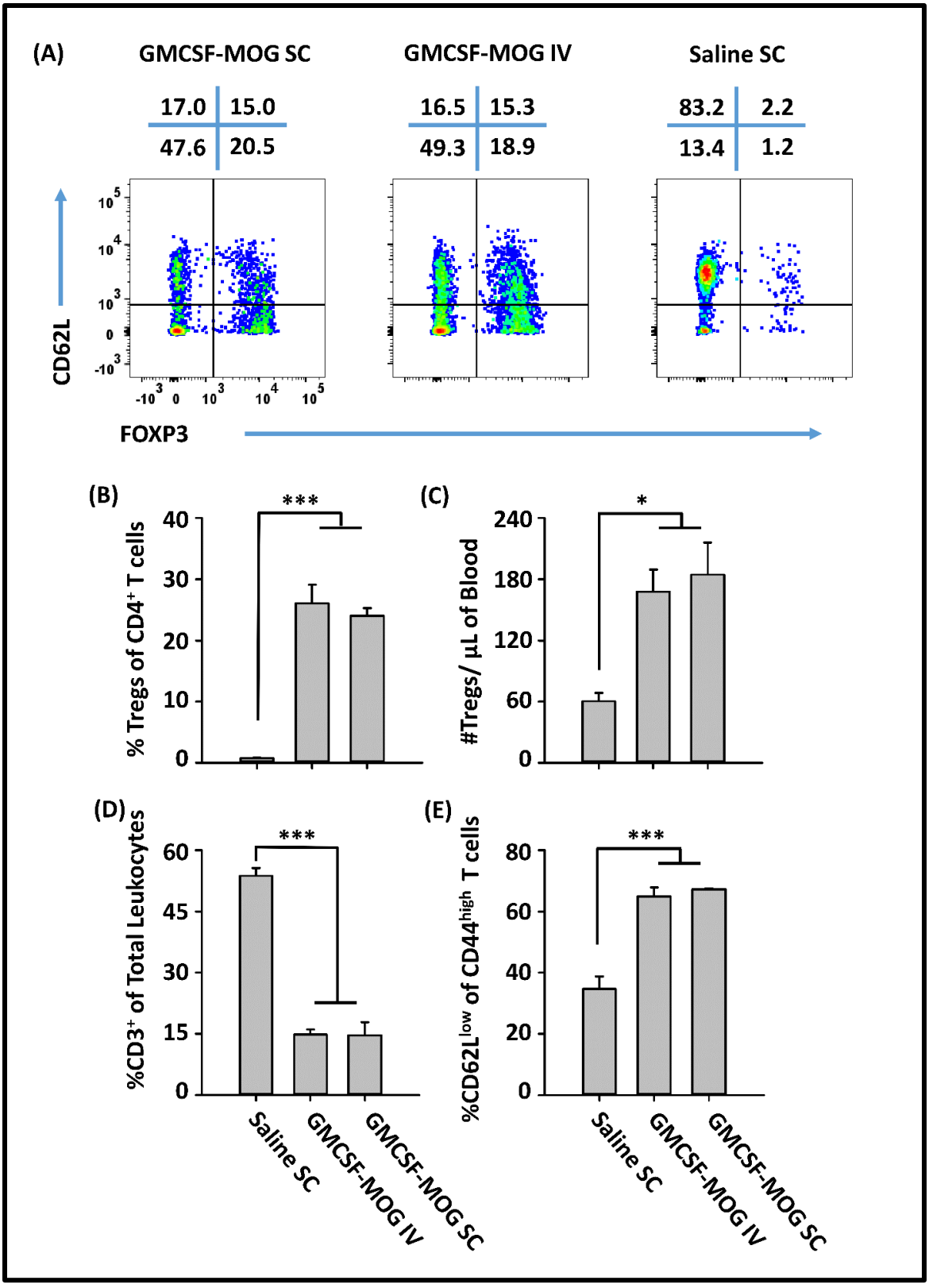
(A)
GMCSF-MOG SC
GMCSF-MOG IV
Saline SC
17.0
15.0
47.6
20.5
16.5
15.3
49.3
18.9
83.2
2.2
13.4
1.2
CD62L
FOXP3
(B)
% Tregs of CD4+ T cells
***
(C)
#Tregs/ µL of Blood
*
(D)
%CD3+ of Total Leukocytes
***
(E)
%CD62Llow of CD44high T cells
***
Saline SC
GMCSF-MOG IV
GMCSF-MOG SC

Figure 3.9: GMCSF-MOG induced Tregs when administered intravenously. On day 0, 2D2-FIG mice were vaccinated with 4 nmoles of GMCSF-MOG intravenously via the retro-orbital route (n = 5) or by SC (n = 5) injection or were vaccinated SC with saline alone (n = 3). Blood was analyzed on day 12. **(A)** $CD3^+$ $CD4^+$ $CD44^{high}$ T cells were analyzed for CD62L expression (y-axis) and FOXP3 (x-axis). The percentages of each quadrant are designated at the top of each dotplot. Shown **(B)** are the percentages of $FOXP3^+$ Tregs among total $CD3^+$ $CD4^+$ T cells and **(C)** total numbers of $FOXP3^+$ Tregs per μl of blood. Shown **(D)** are percentages of $CD3^+$ T cells among total leukocytes in the blood. Shown **(E)** are the percentages of $CD62L^{low}$ T cells among $CD44^{high}$ $CD3^+$ $CD4^+$ T cells. Mean percentages of $CD44^+$ T cells in the $CD3^+$ $CD4^+$ T cell pool for the "GMCSF-MOG IV" and "GMCSF-MOG SC" groups (61% ± 4%, 54% ± 4%, respectively) were significantly different from those for the saline group (6% ± 1%) ($p \leq 0.001$). Statistical significance was analyzed by use of a one-way ANOVA (*$p < 0.05$, ***$p < 0.001$). These data are representative of two independent experiments. Error bars represent ± SEM.

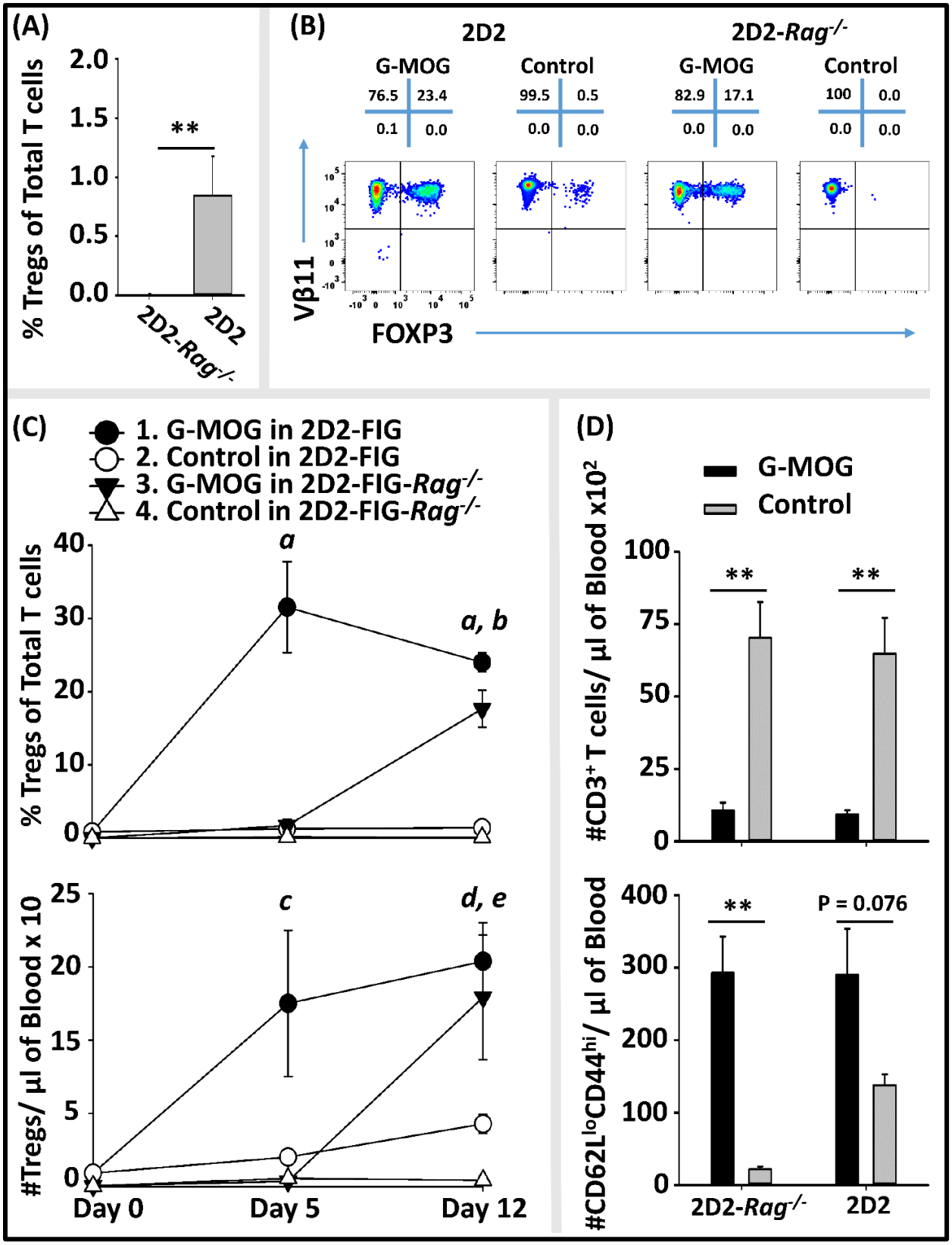
(A)
% Tregs of Total T cells
2.0
1.5
1.0
0.5
0.0
**
2D2-Rag-/-
2D2
(B)
2D2
2D2-Rag-/-
G-MOG
Control
G-MOG
Control
76.5
23.4
0.1
0.0
99.5
0.5
0.0
0.0
82.9
17.1
0.0
0.0
100
0.0
0.0
0.0
Vβ11
FOXP3
(C)
1. G-MOG in 2D2-FIG
2. Control in 2D2-FIG
3. G-MOG in 2D2-FIG-Rag-/-
4. Control in 2D2-FIG-Rag-/-
% Tregs of Total T cells
40
30
20
10
0
a
a, b
#Tregs/ µl of Blood x 10
25
20
15
5
0
c
d, e
Day 0
Day 5
Day 12
(D)
G-MOG
Control
#CD3+ T cells/ µl of Blood x10²
100
75
50
25
0
**
**
#CD62LloCD44hi/ µl of Blood
400
300
200
100
0
**
P = 0.076
2D2-Rag-/-
2D2

Figure 3.10: Pre-existing FOXP3$^+$ MOG-specific Tregs are associated with rapid expansion of Tregs following GMCSF-MOG (G-MOG) vaccination. (A) Shown are percentages of circulating FOXP3$^+$ Tregs in the CD3$^+$ CD4$^+$ T cell pool of naïve untreated 2D2-FIG (n = 13) and 2D2-FIG-*Rag1*$^{-/-}$ (n = 19) mice. **(B–D)** On day 0, 2D2-FIG (n = 5) and 2D2-FIG-*Rag1*$^{-/-}$ (n = 4) mice were vaccinated subcutaneously with 4 nmoles of GMCSF-MOG or with control vaccines (saline alone in 2D2-FIG mice or "4 nmoles GM-CSF + 4 nmoles MOG35-55" in 2D2-FIG-*Rag1*$^{-/-}$ mice). PBMCs were analyzed on day 5 and 12. **(B)** Shown are representative dotplots of CD3$^+$ CD4$^+$ T cells analyzed for FOXP3 expression (x-axis) and Vβ11 (y-axis) on day 12 post vaccination. **(C)** Shown are percentages (top) and numbers (bottom) of FOXP3$^+$ Tregs in the CD4$^+$ T cell pool on days 5 and 12. Group sizes for day 0 were supplemented with historical data (2D2-FIG mice, total n = 50 and n = 13; and 2D2-FIG-*Rag1*$^{-/-}$ mice, n = 19 and n = 10) for calculation of average Treg percentages and Tregs per µl of blood, respectively. **(D)** Shown are the number of CD3$^+$ T cells (top) and the number of CD62L^{low} CD44^{high} T cells (bottom) per µl of blood on day 12. Statistical significance was analyzed by use of a one-way ANOVA. Pairwise comparisons were performed by use of the Holm-Sidak method (**$p < 0.01$). Statistically significant ($p < 0.05$) pairwise comparisons for **(C)**; *a*, 1 vs. 2, 3, and 4; *b*, 3 vs. 2 and 4; *c*, 1 vs. 4; *d*, 1 vs. 2 and 4; *e*, 3 vs. 4. These data are representative of three independent experiments. Error bars represent ± SEM.

CHAPTER 4

RESULTS

A SINGLE-CHAIN GMCSF-MOG TOLEROGENIC VACCINE ELICITS WEAK ANTIGEN RECOGNITION EVENTS BELOW THE CD40L TRIGGERING THRESHOLD TO EXPAND PRE-EXISTING $CD4^+$ $CD25^+$ $FOXP3^+$ TREGS THAT INHIBIT EXPERIMENTAL AUTOIMMUNE ENCEPHALOMYELITIS (EAE).

4.1 Abstract

Tolerogenic vaccines represent antigen-specific interventions designed to re-establish self-tolerance and thereby alleviate inflammatory autoimmune diseases such as Multiple Sclerosis. Tolerogenic vaccines comprised of single-chain GM-CSF-neuroantigen (NAg) fusion proteins were shown in previous studies to be effective prophylactic and therapeutic interventions that inhibited disease in multiple rodent models of experimental autoimmune encephalomyelitis (EAE). GMCSF-NAg inhibited EAE in both quiescent and inflammatory environments by a mechanism associated with low-efficiency T cell receptor (TCR)-antigen engagement and accumulation of $CD4^+$ $CD25^+$ $FOXP3^+$ regulatory T cells (Tregs). This study focused on GMCSF-MOG (myelin oligodendrocyte glycoprotein 35-55/ MOG^{35-55}) and GMCSF-NFM (neurofilament medium 13-37/ NFM^{13-37}) which engaged the transgenic 2D2 T cell antigen receptor with either low or high efficiencies to elicit Treg versus conventional T cell (Tcon) responses, respectively. The purpose was to assess mechanisms by which tolerogenic vaccination translates low-efficiency TCR recognition into the expansion of tolerogenic Tregs to counterbalance high-efficiency TCR recognition and autoimmunity. This study provided evidence that the high-efficiency GMCSF-NFM vaccine elicited memory Tcon responses in association with activation of the CD40L/ CD40 costimulatory system. In contrast, the low-efficiency GMCSF-MOG vaccine lacked sufficient TCR signal strength that was needed to elicit the CD40L/ CD40 pathway and instead elicited Tregs by a mechanism that was impaired by a CD40 agonist. GMCSF-MOG appeared to elicit Tregs in the absence and in opposition to the CD40L/ CD40 pathway because GMCSF-MOG elicited durable and robust Treg responses even when co-delivered with the GMCSF-NFM immunogenic vaccine. GMCSF-MOG not only induced robust circulating Treg responses in naive 2D2-FIG mice, but GMCSF-MOG also

induced sustained decreases in Vβ11 (2D2 TCRβ), CD3, and CD62L as well as sustained increases in CD44 expression in Tcon subsets. GMCSF-MOG inhibited EAE in wildtype mice but appeared to require pre-existing Tregs for induction of tolerance because subcutaneous injection of GMCSF-MOG without adjuvants was pathogenic rather than tolerogenic in 2D2-FIG-*Rag1*$^{-/-}$ mice, which lack pre-existing Tregs. In contrast, GMCSF-MOG lacked pathogenic activity in Treg-sufficient 2D2-FIG mice. Overall, this study provided evidence that GMCSF-MOG elicited tolerogenic Treg-mediated responses that were delimited by the CD40L triggering threshold and were largely mediated by expansion of pre-existing Treg pools.

4.2 The high-efficiency antigen NFM$^{13-37}$ but not the low-efficiency antigen MOG$^{35-55}$ elicited CD40L and CD25 expression in 2D2-FIG splenocytes.

Previous studies showed that the low-efficiency GMCSF-MOG vaccine favored Treg induction while the high-efficiency GMCSF-NFM vaccine did not elicit Treg responses in 2D2-FIG mice. We hypothesized that high-efficiency antigen recognition would lead to increased levels of T cell-APC crosstalk through the CD40L/CD40 co-stimulatory pathway and would thereby favor Tcon responses. In contrast, we hypothesized that low-efficiency antigen recognition would be insufficient to activate the CD40L/CD40 co-stimulatory pathway and would favor Treg responses. Therefore, we investigated if high-efficiency NFM$^{13-37}$ or GMCSF-NFM antigens elicited increased levels of CD40L and the T cell activation marker CD25 as compared to low-efficiency antigens MOG$^{35-55}$ and GMCSF-MOG in 2D2-FIG splenocytes.

In vitro, 2D2-FIG splenocytes were incubated with 32 nM – 3.2 μM of GMCSF-MOG, MOG$^{35-55}$, GMCSF-NFM, or NFM$^{13-37}$ and after 6 hours, CD40L and CD25 expression were analyzed (Figure 4.1). The high-efficiency ligands NFM$^{13-37}$and GMCSF-NFM increased the percent of CD40L^{+} T cells from ~3% (blank) to ~20-35% (3.2 uM) compared to T cells treated

with the isotype control (~2-4%) (Figure 4.1 A, C). Furthermore, the high-efficiency ligands NFM^{13-37} and GMCSF-NFM increased the percent of $CD25^+$ T cells from ~4% (blank) to 16-33% (3.2 uM) compared to T cells treated with 32 nM – 3.2 μM of GM-CSF (~2-4%) (Figure 4.1B, D). The low-efficiency ligands MOG^{35-55} and GMCSF-MOG did not elicit CD40L (Figure 4.1A, C) or CD25 (Figure 4.1B, D) expression at the measured concentrations (32 nM- 3.2 μM). Interestingly, GMCSF-NFM induced a lower percentage of $CD40L^+$ and $CD25^+$ T cells as compared to NFM^{13-37}-treated 2D2-FIG splenocytes which may be a result of GM-CSF-induced T cell suppression through the IFN-γ/NO axis (Figure 4.1A-D) (187). These findings are consistent with the concept that antigen recognition efficiency controls the level of CD40L/CD40 activation. Therefore, high-efficiency but not low-efficiency antigens provide sufficient TCR stimulation to drive the robust activation of the CD40L/CD40 co-stimulatory pathway.

4.3 GMCSF-NFM induced an antigen-recall response in 2D2-FIG mice.

The high-efficiency GMCSF-NFM vaccine precluded Treg induction in 2D2-FIG mice. However, it was unclear whether the vaccine elicited memory Tcon responses or tolerogenic responses that resulted in T cell apoptosis or anergy. Because the GMCSF-NFM vaccine stimulated robust CD40L expression *in vitro* we hypothesized that GMCSF-NFM vaccines would favor the formation of memory Tcons. To address this question, 2D2-FIG mice were vaccinated with 4 nmoles of GMCSF-NFM, GMCSF-MOG, or saline and splenocytes were harvested and analyzed 8 days post vaccination for CD3, CD4, FOXP3, Vβ11, and CD44 expression. As expected, GMCSF-MOG vaccination resulted in the highest percentages of $V\beta11^+$ Tregs in the spleen, where 32% of the total $CD3^+$ $CD4^+$ T cells were $FOXP3^+$ Tregs as compared to ~1% in saline and ~3% in GMCSF-NFM vaccinated 2D2-FIG mice (Figure 4.2A). Interestingly, GMCSF-MOG vaccination resulted in higher percentages of $CD44^{high}$ T cells

where 41% of the $CD3^+$ $CD4^+$ T cells were $CD44^{high}$ as compared to 16% in GMCSF-NFM treated 2D2-FIG mice (Figure 4.2B). The antigen-specific recall response was measured by activating purified $CD4^+$ T cells from GMCSF-MOG, GMCSF-NFM, and saline vaccinated 2D2-FIG mice with 200,000 irradiated C57BL/6 splenocytes and various concentrations 1 nM - 10 uM of MOG^{35-55} or NFM^{13-37}. The subsequent T cell proliferative responses were measured by [^{3}H]thymidine incorporation (Figure 4.2C, D). T cells from GMCSF-NFM-treated mice had increased proliferative responses when re-stimulated with 1 µM – 10 µM of MOG^{35-55} as compared to T cells derived from GMCSF-MOG or saline treated mice (Figure 4.2C). Likewise, T cells derived from GMCSF-NFM treated mice had an increased memory response and exhibited twice the amount of proliferation when re-stimulated with 320 nM – 10 µM of NFM^{13-37} as compared to T cells derived from GMCSF-MOG or saline treated mice (Figure 4.2D). T cells from saline and GMCSF-MOG treated mice behaved similarly and had low levels of proliferation in response to 1 µM – 10 µM of MOG^{35-55} and 32 nM – 10 µM of NFM^{13-37} (Figure 4.2C, D). Therefore GMCSF-MOG treated mice had 2.5 fold more $CD44^{high}$ T cells as compared to GMCSF-NFM treated mice yet exhibited T cell responses that were similar to naïve T cells from saline treated mice. The reduced proliferation was most likely due to the increased percent of immunosuppressive GMCSF-MOG-induced Tregs (Figure 4.2A). These results show that GMCSF-NFM induced a strong effector memory T cell response while GMCSF-MOG had reduced T cell proliferation that was comparable to naïve T cell.

4.4 APC activation with anti-CD40 partially abrogated Treg induction by GMCSF-MOG.

The low-efficiency TCR ligands MOG^{35-55} and GMCSF-MOG were insufficient for the activation of the CD40L/CD40 pathway and instead resulted in Treg induction. Here we investigated if Treg induction with the low-efficiency GMCSF-MOG vaccine could be abolished

through the independent activation of the CD40L/CD40 pathway. To test this possibility, the agonistic anti-CD40 mAb was used to pre-activate APC *in vivo* (Figure 4.3). The agonist anti-CD40 mAb (FGK4.5) or control mAb (2A3) was injected (i.p. 100 µg) into 2D2-FIG mice on days -2 and 0 followed by vaccination with GMCSF-MOG on day 0. PBMCs were analyzed on day 3 and lymph nodes were analyzed on day 4. As expected, anti-CD40 treatment caused APC activation *in vivo*, as shown by an increase in the median MHCII expression on both $CD11b^+$ cells (>2 fold) and B cells (> 3 fold) as compared to control mAb-treated mice (Figure 4.3A, C). Treatment with anti-CD40 also increased the total number of $MHCII^+$ cells and $CD11b^+$ cells in the lymph nodes (Figure 4.3D, E).

As predicted, pretreatment of mice with the agonistic anti-CD40 mAb diminished the Treg-inductive activities of GMCSF-MOG, in that anti-CD40-treated mice had significantly lower percentages of Tregs and fewer Tregs per µl of blood than mice treated with the control mAb (Figure 4.3B, F, G). On day 3, after vaccination with GMCSF-MOG, anti-CD40-treated mice had similar numbers of Tregs (~5-10 Tregs per µl of blood) as the pre-bleed (day -8) and had fewer Tregs than control mAb-treated mice (~26 Treg per µl of blood; Figure 4.3G). Anti-CD40-treated mice exhibited ~12% Tregs in the $CD3^+$ T cell pool compared to ~25% in control mAb-treated mice (Figure 4.3 F). Mice treated with anti-CD40 also had >2 fold decrease in the ratio of $CD44^{high}$ Tregs/ $CD44^{high}$ Tcons as a number and percent of total $CD3^+$ T cells in PBMCs and lymph nodes (data not shown). These data indicate that activation of CD40L/CD40 pathway impairs the induction of Tregs with GMCSF-MOG and favors Tcon responses.

4.5 The low-efficiency GMCSF-MOG vaccine induced Tregs when mixed directly with the high-efficiency GMCSF-NFM vaccine in 2D2-FIG mice.

We next asked whether low or high-efficiency antigen recognition events would dominate T cell lineage decisions when both the low and high-efficiency antigens were concurrently presented in the same draining lymphatics. To address this question, the low-efficiency GMCSF-MOG vaccine was mixed with the high-efficiency GMCSF-NFM vaccine and subcutaneously injected into 2D2-FIG mice. Individual vaccine responses were determined by vaccinating 2D2-FIG mice with 4 nmoles of GMCSF-MOG, GMCSF-NFM, or saline. The vaccine dose was controlled by administering 2 nmoles GMCSF-MOG + 2 nmoles GMCSF-NFM (Figure 4.4A, B) for a total of 4 nmoles antigen or by administering 4 nmoles of GMCSF-MOG + 4 nmoles GMCSF-NFM (Figure 4.4C-M) for a total of 8 nmoles antigen.

As expected 4 nmoles of GMCSF-MOG resulted in significant Treg induction with an average of ~30% (day 5), ~23% (day 12) and ~15% (day 19) in Figure 4.4A and ~15% (day 7), and ~12% (day 15) in Figure 4.4C of the total circulating $CD4^+$ T cells differentiating into $FOXP3^+$ Tregs in 2D2-FIG mice. GMCSF-NFM did not result in Treg expansion on the days analyzed and had Treg percentages comparable to pre-vaccination levels seen on day 0 (~1%; Figure 4.4A, C). The mix of GMCSF-MOG + GMCSF-NFM resulted in a significant increase in Tregs as compared to GMCSF-NFM alone and about half the Treg response of mice treated with GMCSF-MOG alone. GMCSF-MOG + GMCSF-NFM treated mice resulted in an average ~12% (day 5), ~14% (day 12) and ~10% (day 19) in Figure 4.4A and ~8% (day 7) and ~10% (day 15) in Figure 4.4C of the total circulating $CD4^+$ T cells differentiating into $FOXP3^+$ Tregs. Numbers of Tregs per μl of blood paralleled the percent of Tregs where GMCSF-MOG vaccination resulted in the highest numbers of Tregs, followed by GMCSF-MOG + GMCSF-NFM which

displayed intermediate levels, and lastly by GMCSF-NFM which failed to induce Tregs (Figure 4.4C, D).

GMCSF-MOG, GMCSF-NFM, and GMCSF-MOG + GMCSF-NFM vaccination resulted in a 2-5 fold reduction in the total number of circulating $CD3^+$ T cells per μl of blood as compared to saline vaccinated mice (Figure 4.4F). Thus, antigen stimulation resulted in the decreased circulation of 2D2 T cells in the blood. The $CD4^+$ T cells from GMCSF-MOG and GMCSF-MOG + GMCSF-NFM treated mice had decreased Vβ11 (2D2 TCRβ), CD3, and CD62L expression as well as increased CD44 expression on a per cell basis as compared to GMCSF-NFM and saline treated mice (Figure 4.4G-N). Therefore, GMCSF-MOG selectively led to the downregulation of Vβ11 and CD3 expression as well as induced a memory phenotype of $CD44^{high}$ $CD62L^{low}$ in $CD4^+$ T cells. Together these data suggested that the low-efficiency GMCSF-MOG vaccine exerted partial dominance and generated Treg responses even when administered with the high-efficiency GMCSF-NFM vaccine. Furthermore, phenotypic changes associated with low-efficiency GMCSF-MOG vaccination were fully dominant over the high-efficiency GMCSF-NFM vaccine phenotype.

4.6 GMCSF-MOG led to increased percentages of $CD44^{high}$ T cells.

Unexpectedly, the low-efficiency GMCSF-MOG vaccine engendered higher percentages of lasting $CD44^{high}$ memory T cells as compared to the high-efficiency GMCSF-NFM vaccine in 2D2-FIG mice. These findings were surprising because the GMCSF-NFM vaccine activated the CD40L/CD40 co-stimulatory pathway which typically supports T cell activation and memory T cell differentiation. 2D2-FIG mice were vaccinated with 4 nmoles of GMCSF-MOG (n=10), GMCSF-NFM (n=3), or with saline (n=3). PBMCs were analyzed for the percent of $CD44^{high}$ T cells (Figure 4.5A, D), $CD44^{high}$ Tcons (Figure 4.5B, D), and $CD44^{high}$ $FOXP3^+$ Tregs (Figure

4.5C, D) of the total $CD3^+$ $CD4^+$ T cells on days 5, 12, and 19. The baseline (day 0) CD44 expression was derived from $CD3^+$ $CD4^+$ T cells from naïve 2D2-FIG mice (n=23; Figure 4.5A-C). Treatment with GMCSF-MOG increased the percentage of $CD44^{high}$ T cells where ~55% of the total $CD3^+$ $CD4^+$ T cells expressed CD44 on day 5 and were maintained at ~50-55% on days 12 and 19 (Figure 4.5A). Conversely, GMCSF-NFM treated mice exhibited reduced levels of $CD44^{high}$ T cells where ~25% of the total $CD3^+$ $CD4^+$ T cells expressed CD44 on day 5 and were maintained at ~20-30% on days 12 and 19 (Figure 4.5A) The total percent of $CD44^{high}$ T cell in GMCSF-MOG vaccinated mice was due to an increase in the percent of both $CD44^{high}$ Tcons (35-43%; Figure 4.5B) and $CD44^{high}$ Tregs (11-20%; Figure 4.5C). However, the GMCSF-NFM vaccine only increased the percent of $CD44^{high}$ Tcons (~20-30%; Figure 4.5B) and had no impact on $CD44^{high}$ Tregs (1-2%; Figure 4.5C). Analysis of 4 independent experiments analyzing PBMCs expression of CD44 on $CD3^+$ $CD4^+$ T cells from GMCSF-MOG (n=18) and GMCSF-NFM (n=16) treated 2D2-FIG mice (Figure 4.5E) showed that both the GMCSF-MOG and GMCSF-NFM vaccines initially induce similar percentages of $CD44^{high}$ T cells. Both GMCSF-MOG and GMCSF-NFM treated mice had ~55-65% $CD44^{high}$ $CD3^+$ $CD4^+$ T cells on day 4. Therefore, 2D2-FIG mice treated with the GMCSF-NFM vaccine displayed transient CD44 expression because of the reduced CD44 expression (~20-30%) seen on days 5, 12, and 19 (Figure 4.5 A-D) These data confirmed that GMCSF-MOG vaccination led to higher percentages of $CD44^{high}$ T cells including both Tcons and Tregs while GMCSF-NFM vaccination induced transient and reduced percentages of $CD44^{high}$ Tcons and had no effect on the percentage of $CD44^{high}$ Tregs.

4.7 The tolerogenic activity of GMCSF-MOG was contingent upon pre-existing Tregs.

Next we wanted to determine if GMCSF-MOG-induced Tregs were functional and could suppress MOG-specific T cell responses. 2D2-FIG mice were vaccinated with 4 nmoles of GMCSF-MOG to induce Tregs. Splenocytes were harvested 7 days post vaccination and GMCSF-MOG-induced Tregs were FACS purified. *In vitro*, GMCSF-MOG-induced Tregs were mixed at various ratios with purified naïve $CD4^+$ 2D2-FIG Tresponders cells (Tresp) and activated with irradiated C57BL/6 splenocytes and 1 μM MOG^{35-55}. T cell proliferation was measured by [^{3}H]thymidine incorporation (Figure 4.6). GMCSF-MOG-induced Tregs were functional and suppressed ~80% of the total T cell proliferation as compared to the proliferation of Tresp alone at a ratio of 1:4 (Tregs: Tresp) (Figure 4.6A, B). GMCSF-MOG-induced Tregs were functional at the highest ratio tested (1:32) and suppressed ~20% of the total T cell response (Figure 4.6A). These data showed that GMCSF-MOG-induced Tregs were immunosuppressive and prevented the proliferation of MOG^{35-55}-specific Tresp cells.

Previous research showed that 2D2-FIG-*Rag1*$^{-/-}$ mice had reduced homeostatic Treg populations and delayed Treg responses following vaccination with GMCSF-MOG as compared to 2D2-FIG mice. The delayed Treg response was attributed to a model in which GMCSF-MOG vaccination expanded pre-existing Tregs. Thus, Treg induction with the GMCSF-MOG vaccine was delayed in 2D2-FIG-*Rag1*$^{-/-}$ mice because of the minute Treg starting population. We next wanted to determine if pre-existing Tregs were required for the tolerogenic activity of GMCSF-MOG.

First we tested if GMCSF-MOG vaccination would prevent encephalitogenic priming with MOG^{35-55}/CFA in C57BL/6 mice which have normal Treg frequencies and a wild type T cell repertoire. C57BL/6 mice were pretreated on days -21, -14, and -7 with 2 nmoles of either

GMCSF-MOG (n=8) or GMCSF-OVA (n=7) and subsequently challenged with 200 μg MOG^{35-55} in CFA on day 0 and treated with 400 ng of Ptx on days 0 and 2 (Figure 4.6C, D). C57BL/6 mice pretreated with GMCSF-MOG were protected from developing EAE and 2 of 8 mice showed mild signs of EAE with a mean maximum score of 0.57 ± 0.57 while 7 of 7 mice treated with GMCSF-OVA came down with severe EAE with a mean maximum score of 3.9 ± 0.09 (Figure 4.6C, Table 4.1). Mice treated with GMCSF-MOG vaccine also maintained their bodyweight throughout the experiment while mice treated with GMCSF-OVA lost significant portion of their bodyweight (Figure 4.6D). These results showed that GMCSF-MOG was an effective pretreatment and prevented encephalitogenic priming in C57BL/6 mice which have wild type Treg repertoire.

We next tested the effects of the GMCSF-MOG vaccine in the Treg deficient 2D2-FIG-*Rag1*$^{-/-}$ mice. 2D2-FIG-*Rag1*$^{-/-}$ and 2D2-FIG mice were vaccinated on days 0 and 20 with 4 nmoles of GMCSF-MOG, GMCSF-NFM, GMCSF-MOG + GMCSF-NFM, or saline and clinical EAE scores and weight were monitored through day 41 (Figure 4.6E-F). No immunizing adjuvants such as CFA or Ptx were used in these experiments. GMCSF-MOG and GMCSF-NFM induced EAE in Treg-deficient 2D2-FIG-*Rag1*$^{-/-}$ mice but not in Treg sufficient 2D2-FIG mice (Figure 4.6E). The GMCSF-MOG vaccine induced EAE in 3 of 6 2D2-FIG-*Rag1*$^{-/-}$ mice with a mean maximum EAE score of 1.7 ± 0.8 while the GMCSF-NFM vaccine induced EAE in 5 of 6 2D2-FIG-*Rag1*$^{-/-}$ mice with a mean maximum EAE score of 2.6 ± 0.5 (Table 4.1). 2D2-FIG-*Rag1*$^{-/-}$ mice treated with saline did not exhibit clinical signs of EAE. 2D2-FIG mice treated with GMCSF-MOG, GMCSF-NFM, GMCSF-NFM + GMCSF-MOG, and saline did not elicit EAE or induced significant levels of weight loss through the end of the experiment on day 41. GMCSF-MOG and GMCSF-NFM vaccination induced significant weight loss in 2D2-FIG-

Rag1$^{-/-}$ mice as compared to 2D2-FIG mice (Figure 4.6F, G). Saline-treated 2D2-FIG and 2D2-FIG-*Rag1*$^{-/-}$ mice gained similar amounts of weight throughout the experiment (Figure 4.6H). Together these data suggest that pre-existing Tregs are a critical parameter for the clinical outcome of GMCSF-NAg based vaccines.

4.8 GMCSF-MOG preferentially expanded Tregs from a memory T cell pool.

GMCSF-MOG expanded pre-existing Tregs in naïve 2D2-FIG mice through low-efficiency antigen recognition which was integrated through diminished CD40L/CD40 signaling. Here we directly tested if GMCSF-MOG expanded memory Tregs. A mixed congenically marked (CD45.1) Treg and Tcon line (40% Tregs and 60% Tcons) was transferred intravenously into 2D2-FIG-*Rag1*$^{-/-}$ (CD45.2) hosts which were subsequently vaccinated with 4 nmoles of GMCSF-MOG or 4 nmoles GM-CSF + 4 nmoles MOG $^{35-55}$ (Figure 4.7). Interestingly, GMCSF-MOG vaccination expanded the memory T cell population resulting in ~1.5 CD45.1^{+} CD4^{+} T cells per µl of blood as compared to 0.5 cells in GM-CSF + MOG$^{35-55}$ treated 2D2-FIG mice (Figure 4.7B). Likewise, the percentage of CD45.1^{+} CD4^{+} T cells also increased to 0.7% in GMCSF-MOG vaccinated 2D2-FIG mice as compared to < 0.1% in GM-CSF + MOG$^{35-55}$ treated mice. These results differed from GMCSF-MOG vaccination of naïve 2D2-FIG mice in which the total 2D2 T cell population in PBMCs was diminished (Figure 4.4F). GMCSF-MOG vaccination selectively expanded the number of memory Tregs resulting in ~1.3 CD45.1^{+} CD4^{+} Treg cells per µl of blood as compared to 0.3 cells in GM-CSF + MOG$^{35-55}$ treated mice (Figure 4.7D). Likewise, GMCSF-MOG selectively increased the percent of memory Tregs to comprise ~85% of the total CD45.1^{+} CD4^{+} T cells as compared to ~61% in GM-CSF + MOG$^{35-55}$ treated mice (Figure 4.7A, C). Finally, GMCSF-MOG vaccination increased the percent and number (>3 fold) of activated CD45.1^{+} CD4^{+} Tregs which were identified by increased CD44 expression

(Figure 4.7F, G). These data show that GMCSF-MOG selectively expanded and activated memory Tregs.

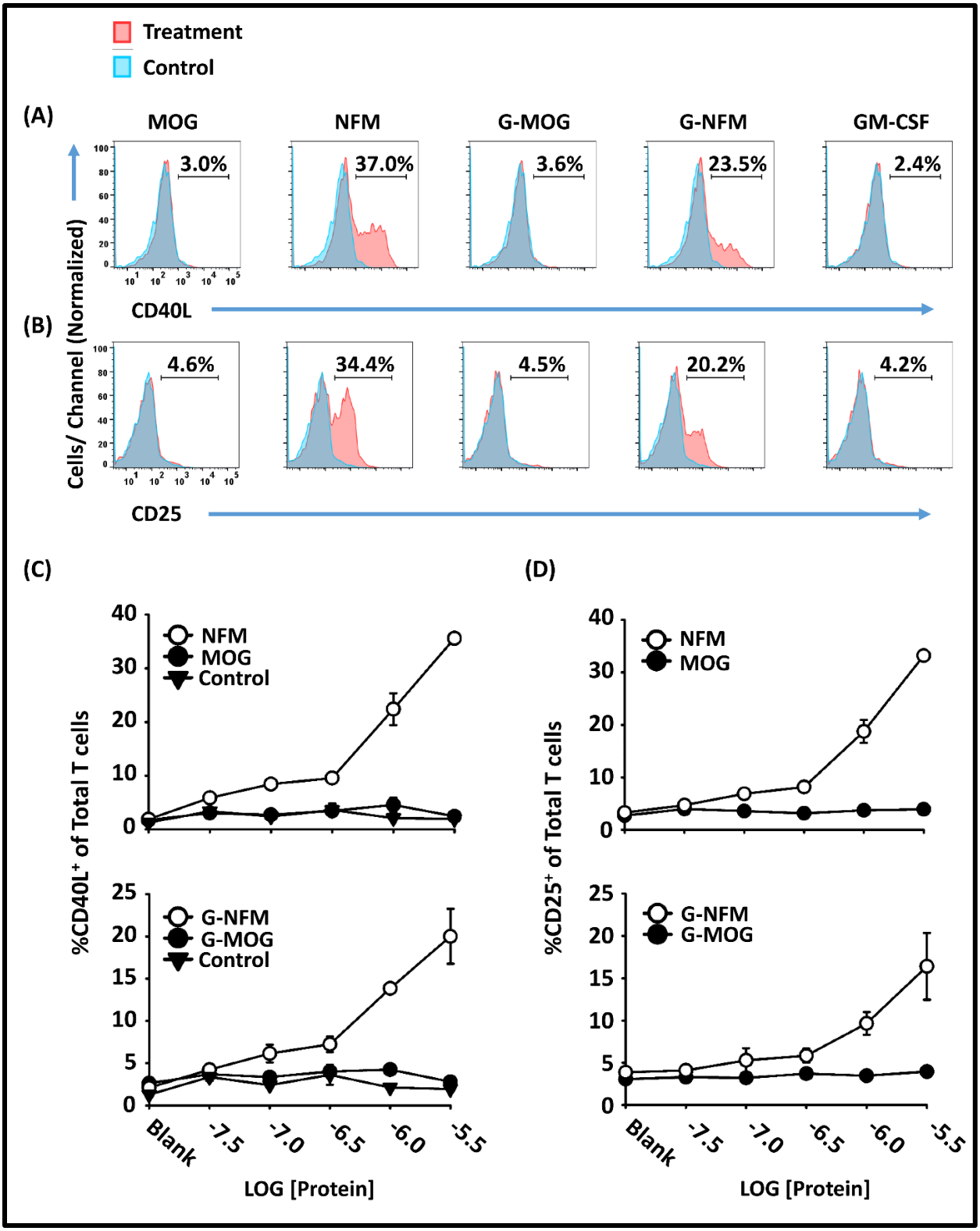
Treatment
Control
(A)
MOG
NFM
G-MOG
G-NFM
GM-CSF
3.0%
37.0%
3.6%
23.5%
2.4%
CD40L
(B)
4.6%
34.4%
4.5%
20.2%
4.2%
Cells/ Channel (Normalized)
CD25
(C)
(D)
NFM
MOG
Control
G-NFM
G-MOG
%CD40L+ of Total T cells
%CD25+ of Total T cells
Blank
-7.5
-7.0
-6.5
-6.0
-5.5
LOG [Protein]

Figure 4.1: The high-efficiency antigen NFM$^{13-37}$ but not the low-efficiency antigen MOG$^{35-55}$ elicited CD40L and CD25 expression in 2D2-FIG splenic T cells. 2D2-FIG splenocytes were cultured with 3.2 μM MOG$^{35-55}$, NFM$^{13-37}$, GMCSF-MOG, GMCSF-NFM, or GM-CSF in duplicate. After 4 hours of culture, 10 μg/ ml PE-conjugated anti-mouse CD40L mAb (Armenian Hamster IgG, MR1) or control PE-conjugated anti-trinitrophenol-KLH mAb (Armenian Hamster IgG, HTK888) were added to cultures and incubated for an additional 2 hours. Cells were then stained for CD3, CD4, and CD25. Shown are representative histograms of CD40L **(A)** and CD25 **(B)** expression (x-axis) of $CD3^+$ $CD4^+$ T cells activated with designated antigens or cytokines. Shown are percentages of $CD40L^+$ **(C)** or $CD25^+$ T cells **(D)** of total $CD3^+$ $CD4^+$ T cell population following culture with designated treatments. Error bars represent ± SD. These data are representative of three independent experiments.

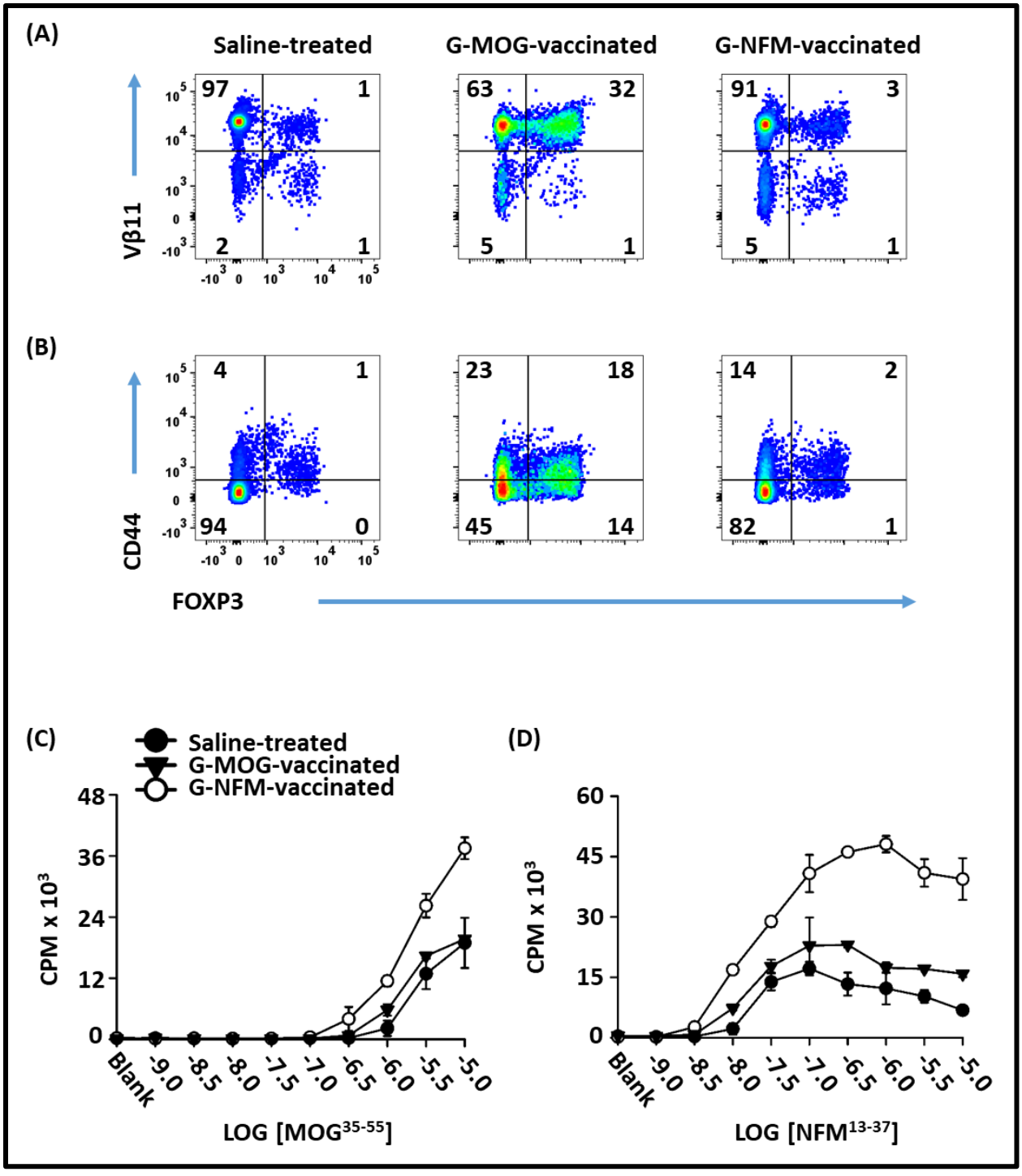
(A)
Saline-treated
G-MOG-vaccinated
G-NFM-vaccinated
Vβ11
97
1
2
1
63
32
5
1
91
3
5
1
(B)
CD44
FOXP3
4
1
94
0
23
18
45
14
14
2
82
1
(C)
Saline-treated
G-MOG-vaccinated
G-NFM-vaccinated
CPM x 10³
48
36
24
12
0
Blank
-9.0
-8.5
-8.0
-7.5
-7.0
-6.5
-6.0
-5.5
-5.0
LOG [MOG35-55]
(D)
CPM x 10³
60
45
30
15
0
LOG [NFM13-37]

Figure 4.2: GMCSF-NFM induced an antigen-recall response in 2D2-FIG mice. **(A-D)** On day 0, 2D2-FIG mice were subcutaneously injected with 4 nmoles of GMCSF-MOG, 4 nmoles of GMCSF-NFM, or saline. On day 8, splenocytes were harvested from vaccinated mice, and $CD4^+$ T cells were purified and analyzed for **(A)** Vβ11 (y-axis), **(B)** CD44 (y-axis) and **(A-B)** FOXP3 expression (x-axis). Purified 2D2-FIG splenic T cells (25,000/ well) from each vaccinated mouse were cultured in duplicate with 200,000 irradiated splenocytes (C57BL/6) and designated concentrations (x-axis) of **(C)** MOG^{35-55} and **(D)** NFM^{13-37}. Cultures were pulsed with 1 μCi of [^{3}H]thymidine during the last 24 h of a 3-day culture. These data are representative of two independent experiments. Error bars represent ± SD.

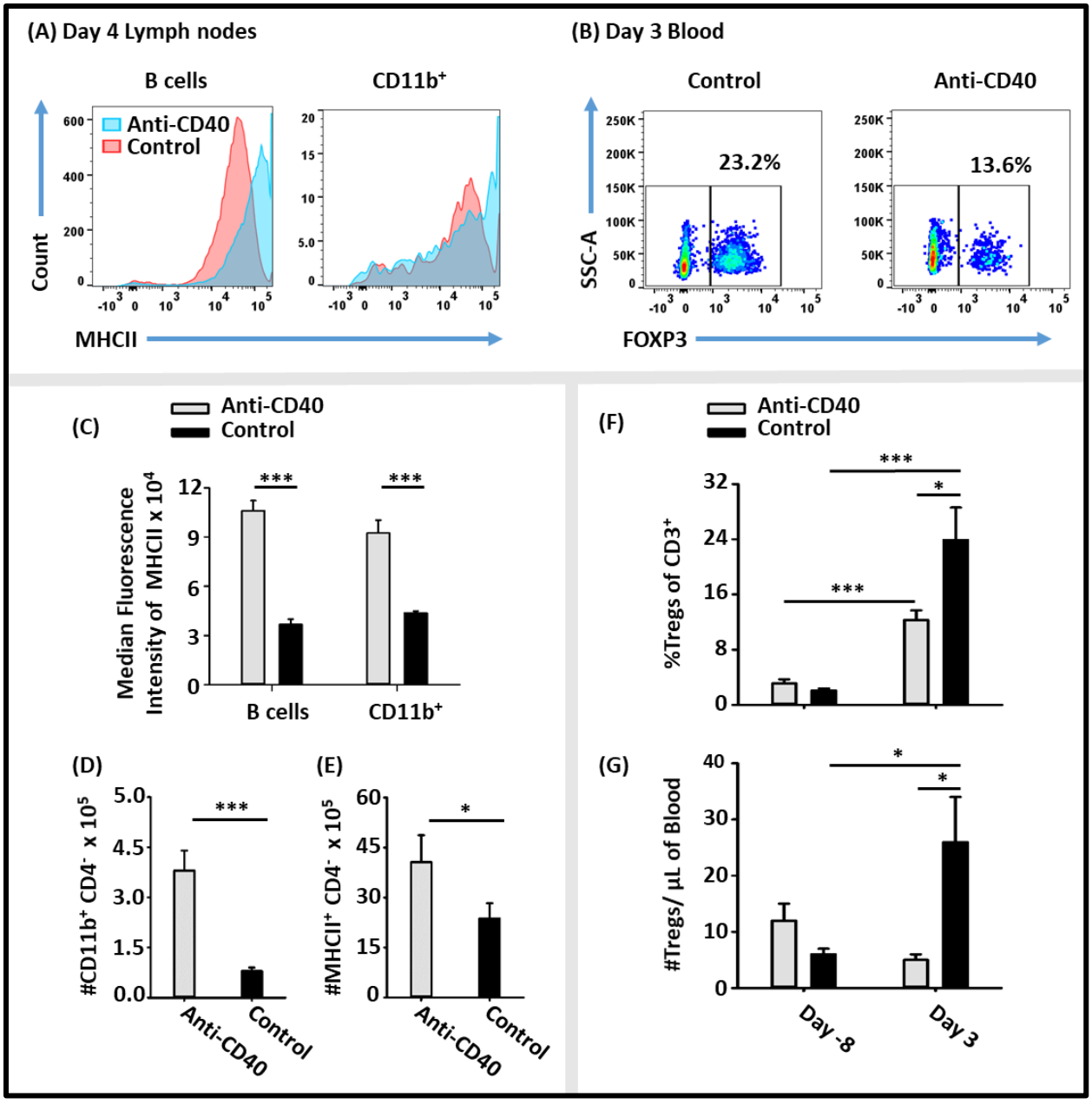
(A) Day 4 Lymph nodes
B cells
CD11b+
Anti-CD40
Control
Count
MHCII
(B) Day 3 Blood
Control
Anti-CD40
23.2%
13.6%
SSC-A
FOXP3
(C)
Anti-CD40
Control
Median Fluorescence Intensity of MHCII x 10^4
B cells
CD11b+
(D)
#CD11b+ CD4- x 10^5
Anti-CD40
Control
(E)
#MHCII+ CD4- x 10^5
Anti-CD40
Control
(F)
Anti-CD40
Control
%Tregs of CD3+
(G)
#Tregs/ µL of Blood
Day -8
Day 3

Figure 4.3: Treatment of mice with an agonistic anti-CD40 mAb inhibited vaccine-induced accumulation of Tregs. On day -2 and 0, 2D2-FIG mice (n = 7/group) were injected i.p. with 100 μg of either anti-CD40 (clone FGK4.5, rat anti-mouse CD40, IgG2a) or control (clone 2A2, rat anti-trinitrophenol, IgG2a) in 500 μl saline. All mice were injected with 4 nmoles of GMCSF-MOG on day 0. PBMC were analyzed on day -8 before vaccination and day 3 post-vaccination for SSC-A, CD3, and FOXP3. Lymph nodes were harvested and analyzed on day 4 for CD4, CD11b, MHCII, and FOXP3. Shown are: **(A)** representative histograms of $CD4^-$, $CD11b^-$ APC (B cells) and $CD11b^+$ APC analyzed for MHCII expression (x-axis) from lymph nodes on day 4; **(B)** representative dot plots of $CD3^+$ T cells analyzed for SSC (y-axis) and FOXP3 (x-axis) from blood on day 3; **(C)** the median fluorescence intensity of $MHCII^+$ of $CD11b^+$ cells and B cells from anti-CD40 and control treated mice; **(D, E)** the number of $CD11b^+$ and $MHCII^+$ cells in the lymph nodes on day 4; and **(F, G)** percentages and numbers of Tregs (per μl of blood) on days -8 and 3. Statistical significance was analyzed using a one-tailed t-test. (*$p<0.05$, ***$p<0.001$). These data are representative of two independent experiments. Error bars represent ± SEM.

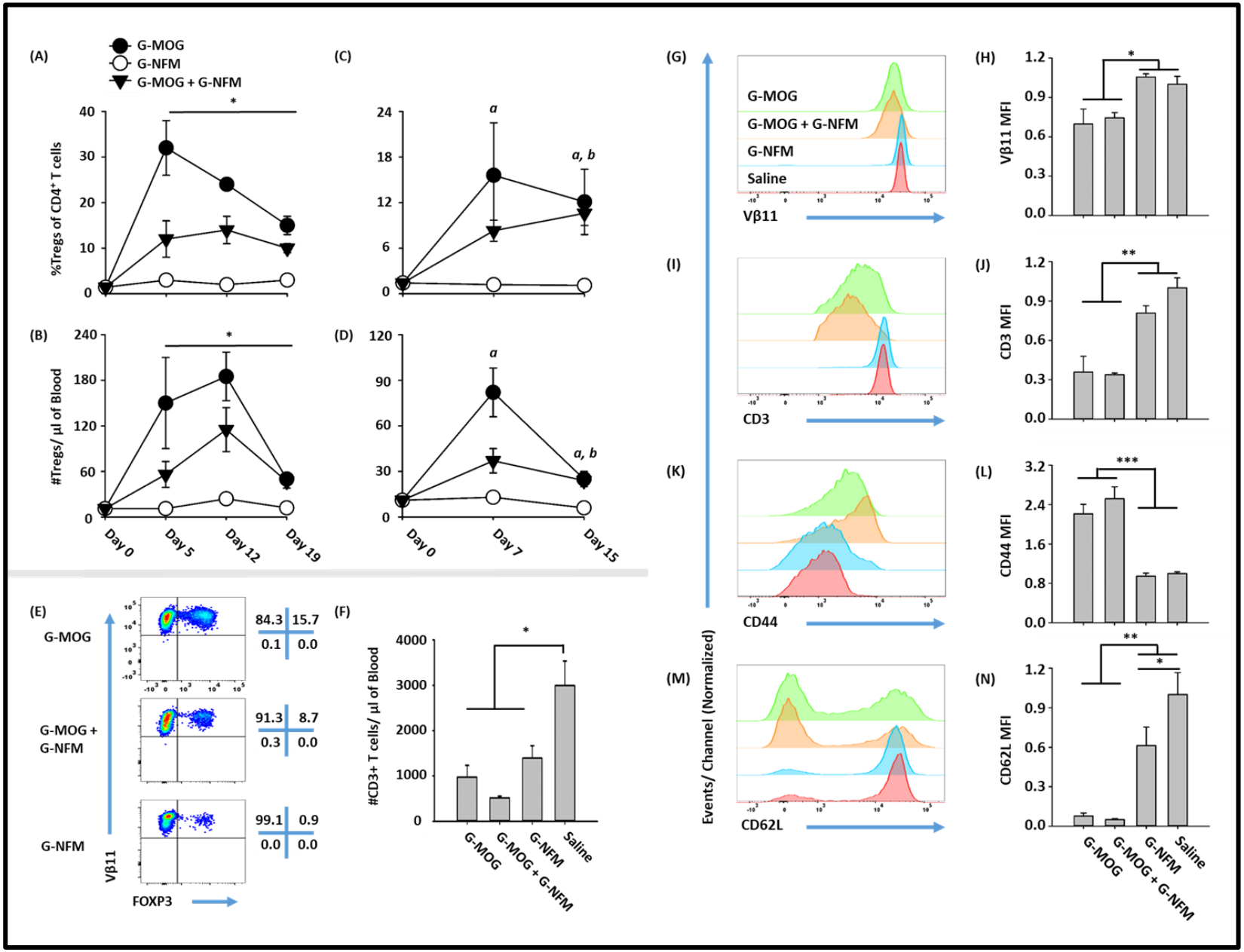
(A)
G-MOG
G-NFM
G-MOG + G-NFM
%Tregs of CD4+ T cells
(B)
#Tregs/ µl of Blood
Day 0
Day 5
Day 12
Day 19
(C)
(D)
Day 0
Day 7
Day 15
(E)
G-MOG
G-MOG + G-NFM
G-NFM
Vβ11
FOXP3
84.3
15.7
0.1
0.0
91.3
8.7
0.3
0.0
99.1
0.9
0.0
0.0
(F)
#CD3+ T cells/ µl of Blood
G-MOG
G-MOG + G-NFM
G-NFM
Saline
(G)
G-MOG
G-MOG + G-NFM
G-NFM
Saline
Vβ11
(H)
Vβ11 MFI
(I)
CD3
(J)
CD3 MFI
(K)
CD44
(L)
CD44 MFI
(M)
Events/ Channel (Normalized)
CD62L
(N)
CD62L MFI
G-MOG
G-MOG + G-NFM
G-NFM
Saline

Figure 4.4: The low-efficiency GMCSF-MOG vaccine induced a robust Treg response even when mixed with the high-efficiency GMCSF-NFM vaccine. **(A - N)** On day 0, 2D2-FIG (n = 3-5) mice were injected with 4 nmoles of GMCSF-MOG, 4 nmoles of GMCSF-NFM, or saline. Separate groups were also injected with either 2 nmoles of GMCSF-MOG + 2 nmoles of GMCSF-NFM **(A, B)** or 4 nmoles of GMCSF-MOG + 4 nmoles GMCSF-NFM **(C-N)**. PBMCs were assayed for CD3, CD4, FOXP3, Vβ11 (2D2 TCR), CD44, and CD62L expression. Shown are **(A, C)** percentages and **(B, D)** numbers (per µl of blood) of $FOXP3^+$ Tregs for $CD3^+$ $CD4^+$ T cells collected on days 0, 5, 12, and 19 **(A, B)** or days 0, 7, and 15 **(C, D)**. Also shown are: **(E)** representative dot plots of $CD3^+$ $CD4^+$ T cells analyzed for Vβ11 (y-axis) and FOXP3 expression (x-axis) on day 7; **(F)** the total number of $CD3^+$ T cells per µl of blood on day 7; representative histograms for **(G)** Vβ11, **(I)** CD3, **(K)** CD44, and **(M)** CD62L expression of $CD3^+$ $CD4^+$ T cells on day 7; and the mean florescent intensity (MFI) of **(H)** Vβ11, **(J)** CD3, **(L)** CD44, and **(N)** CD62L for each group on day 7. **(A, B)** Statistical significance was analyzed by use of a two-way repeated measures ANOVA. The groups G-MOG, "G-MOG + G-NFM", and G-NFM were all statistically significant from each other (*$p < 0.05$). **(C-N)** Statistical significance was analyzed by use of a one-way ANOVA; (*a*) G-MOG vs G-NFM ($p < 0.05$) and (*b*) "G-MOG + G-NFM" vs G-NFM ($p<0.05$). (*$p<0.05$, **$p<0.01$, *** $p<0.001$). Error bars represent ± SEM.

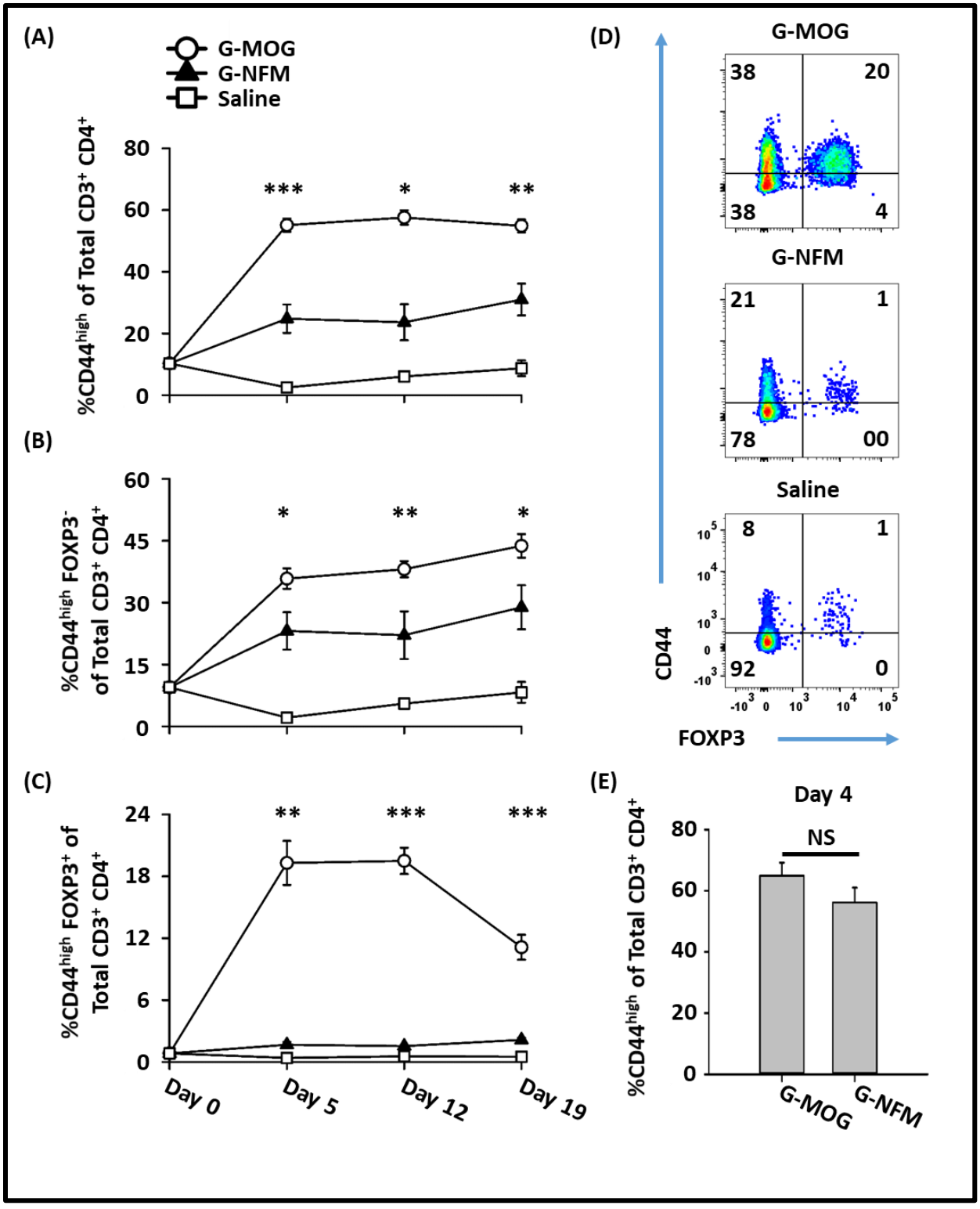
(A)
G-MOG
G-NFM
Saline
%CD44high of Total CD3+ CD4+
80
60
40
20
0
***
*
**
(B)
%CD44high FOXP3- of Total CD3+ CD4+
60
45
30
15
0
*
**
*
(C)
%CD44high FOXP3+ of Total CD3+ CD4+
24
18
12
6
0
**
***
***
Day 0
Day 5
Day 12
Day 19
(D)
G-MOG
38
20
38
4
G-NFM
21
1
78
00
Saline
8
1
92
0
CD44
FOXP3
(E)
Day 4
%CD44high of Total CD3+ CD4+
80
60
40
20
0
NS
G-MOG
G-NFM

Figure 4.5: GMCSF-MOG elicited an increased percent of CD44^{high} T cells. (A-D) 2D2-FIG mice were vaccinated with 4 nmoles of GMCSF-MOG (n=10), 4 nmoles of GMCSF-NFM (n=3), or with saline (n=3). PBMCs were analyzed on day 5, 12, and 19 for CD3, CD4, CD44, and FOXP3 expression. **(A-C)** The day 0 time point was derived from the CD44 expression of CD3^{+} CD4^{+} T cells from naïve 2D2-FIG mice (n=23) and **(E)** represents compiled data of 4 independent experiments analyzing PBMC CD44 expression on CD3^{+} CD4^{+} T cells for GMCSF-MOG (n=18) and GMCSF-NFM (n=16) treated mice on day 4. Shown are; percentages of **(A)** CD44^{high} T cells, **(B)** CD44^{high} Tcon, and **(C)** CD44^{high} Tregs of gated CD3^{+} CD4^{+} T cells on day 0, 5,12, and 19. Shown **(D)** are representative dot plots of CD44 (y-axis) and FOXP3 (x-axis) expression of CD4^{+} CD3^{+} T cells. Shown **(E)** are CD44^{high} T cells, of CD3^{+} CD4^{+} T cells on day 4. Statistical significance was analyzed using a one-way ANOVA. Shown are; **(A, B)** significant differences between the groups GMCSF-MOG, GMCSF-NFM, and saline, and **(C)** statistical differences comparing GMCSF-MOG treatment to both GMCSF-NFM and saline. (*$p<0.05$, **$p<0.01$, *** $p<0.001$). Error bars represent ± SEM.

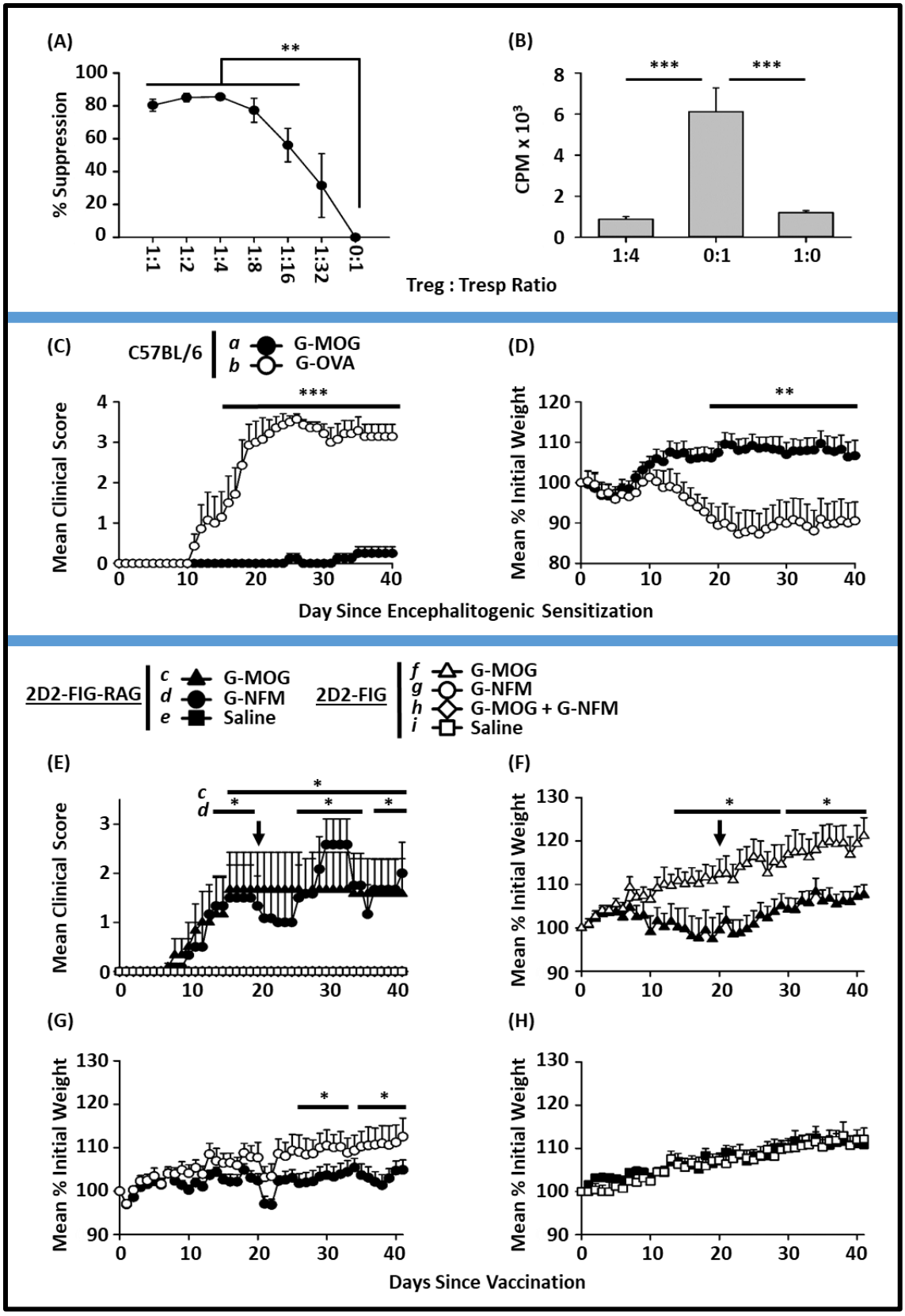
(A)
% Suppression
100
80
60
40
20
0
**
1:1
1:2
1:4
1:8
1:16
1:32
0:1
(B)
CPM x 10³
8
6
4
2
0
***
***
1:4
0:1
1:0
Treg : Tresp Ratio
(C)
C57BL/6
a G-MOG
b G-OVA
Mean Clinical Score
4
3
2
1
0
***
0
10
20
30
40
(D)
Mean % Initial Weight
120
110
100
90
80
**
0
10
20
30
40
Day Since Encephalitogenic Sensitization
2D2-FIG-RAG
c G-MOG
d G-NFM
e Saline
2D2-FIG
f G-MOG
g G-NFM
h G-MOG + G-NFM
i Saline
(E)
Mean Clinical Score
3
2
1
0
c
d
*
*
*
*
0
10
20
30
40
(F)
Mean % Initial Weight
130
120
110
100
90
*
*
0
10
20
30
40
(G)
Mean % Initial Weight
130
120
110
100
90
*
*
0
10
20
30
40
(H)
Mean % Initial Weight
130
120
110
100
90
0
10
20
30
40
Days Since Vaccination

Figure 4.6: The tolerogenic activity of GMCSF-MOG was contingent upon pre-existing Tregs. (A-B) 2D2-FIG mice were vaccinated with 4 nmoles of GMCSF-MOG, and splenic Tregs were purified by flow sorting on day 7. Tregs were added to triplicate cultures of naïve splenic 2D2-FIG T responder (Tresp) cells, 10^5 irradiated C57BL/6 splenocytes, and 1 μM MOG^{35-55} as designated. Cultures were pulsed with 1 μCi of [^{3}H] thymidine during the last 24 hours of a 3-day culture. Shown are **(A)** the percent suppression of maximal MOG-stimulated proliferation and **(B)** the CPM (counts per minute) from cultures containing a 1:4 Treg/ Tresp mixture versus Tregs alone and Tresp alone. **(C, D)** C57BL/6 mice were treated with 2 nmoles GMCSF-MOG (n=8) or GMCSF-OVA (n=7) on days −21, −14, and −7. On day 0, all mice were immunized with 200 μg MOG^{35-55} in CFA and 400 ng of Ptx toxin i.p. on days 0 and 2. Shown **(C)** are the daily mean clinical EAE scores and **(D)** the normalized mean body weight through the end of the experiment on day 40. **(E-H)** 2D2-FIG or 2D2-FIG-*Rag1*$^{-/-}$ mice were treated with 4 nmoles GMCSF-MOG, GMCSF-NFM, "GMCSF-MOG + GMCSF-NFM", or with saline on days 0 and day 20 (arrow). Shown **(E)** are the daily mean clinical EAE scores and **(F-H)** the mean normalized body weight through the end of the experiment on day 41. **(A, B)** Statistical significance was analyzed using a two-tailed t-test. Error bars represent ± SD. **(C-H)** Differences between groups were analyzed using a two-way repeated measures ANOVA. Error bars represent ± SEM. **(C-H)** Significant differences between groups were **(C-D)** (*a*) vs (*b*); **(E)** (*c*) vs (*e-i*) and (*d*) vs (e-*i*); **(F)** (*c*) vs (*f*); and **(G)** (*d*) vs (*g*). **(C, E)** Incidence of EAE was (*a)* 2 of 8, (*b)* 7 of 7, (c*)* 3 of 6, (*d)* 5 of 6, (*e*) 0 of 5, and *(f-i)* 0 of 6. **(C)** Mean maximal scores were (*a*) 0.57 ± 0.57, (*b)* 3.9 ± 0.09, (*c*) 1.7 ± 0.8, (*d*) 2.6 ± 0.5, and (*e-i*) 0.0 ± 0.0. These data are representative of **(C-H)** three or **(A, B)** two independent experiments. *(*p<0.05, **p<0.01, *** p<0.001*).

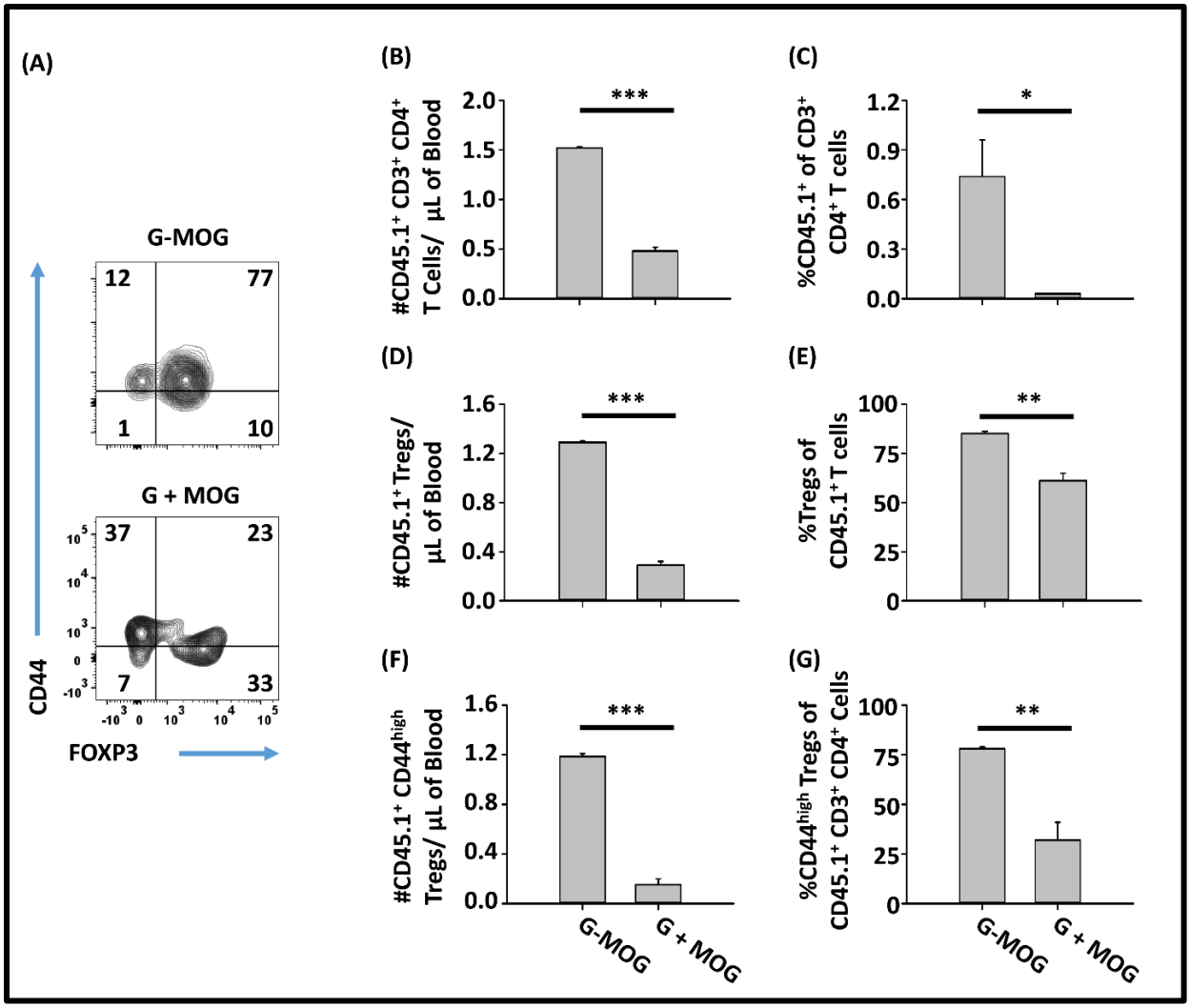
(A)
G-MOG
12
77
1
10
G + MOG
37
23
7
33
CD44
FOXP3
(B)
#CD45.1+ CD3+ CD4+ T Cells/ µL of Blood
***
(C)
%CD45.1+ of CD3+ CD4+ T cells
*
(D)
#CD45.1+ Tregs/ µL of Blood
***
(E)
%Tregs of CD45.1+ T cells
**
(F)
#CD45.1+ CD44high Tregs/ µL of Blood
***
(G)
%CD44high Tregs of CD45.1+ CD3+ CD4+ Cells
**
G-MOG
G + MOG

Figure 4.7: GMCSF-MOG preferentially expanded Tregs from a memory T cell pool. On day 0, a CD45.1-2D2-FIG mixed Treg and Tcon line (40% Tregs and 60% Tcons) was injected intravenously (1.25 x 10^6 cells) into CD45.2 2D2-FIG-RAG mice (n=3). On day 0, 2D2-FIG-RAG mice were vaccinated with 4 nmoles of GMCSF-MOG or 4 nmoles GM-CSF + 4 nmoles MOG^{35-55}. PBMCs were analyzed on day 4 for CD3, CD4, CD45.1, CD44, and FOXP3. Shown are the analyses of donor CD45.1 $CD3^+$ $CD4^+$ T cells including: **(A)** representative dot plots of GMCSF-MOG and "GM-CSF + MOG"-treated mice for CD44 (y-axis) and FOXP3 expression (x-axis) together with **(B, D, F)** cell numbers per µl of blood and **(C, E, G)** percentages of designated cell populations. Statistical significance was analyzed using a two-tailed t-test. (*$p<0.05$, **$p<0.01$, *** $p<0.001$). Error bars represent ± SEM.

Exp.#	Strain	Induction of EAE	Group	Treatment	Incidence of EAE	Average day of EAE onset	Mean cumulative score	Median cumulative score	Mean maximal score	Median maximal score	% Maximal weight loss
1	C57BL/6	Active	*a*	GMCSF-MOG	2 of 8	30.0 ± 5.0	2.1 ± 1.5	0.0	0.3 ± 0.2	0.0	- 0.8 ± 2.1
1	C57BL/6	Active	*b*	GMCSF-OVA	7 of 7	16.2 ± 1.8	81.1 ± 6.9	83.5	3.9 ± 0.1	4.0	17.4 ± 4.1
2	2D2-FIG-RAG	Vaccine	*c*	GMCSF-MOG	3 of 6	11.3 ± 4.5	49.0 ± 22.4	39.0	1.7 ± 0.8	1.5	6.4 ± 4.3
2	2D2-FIG-RAG	Vaccine	*d*	GMCSF-NFM	5 of 6	18.6 ± 10.2	48.3 ± 16.9	45.0	2.6 ± 0.5	3.0	4.4 ± 1.6
2	2D2-FIG-RAG	Vaccine	*e*	Saline	0 of 5	NA	0.0 ± 0.0	0.0	0.0 ± 0.0	0.0	- 2.7 ± 0.9
2	2D2-FIG	Vaccine	*f*	GMCSF-MOG	0 of 6	NA	0.0 ± 0.0	0.0	0.0 ± 0.0	0.0	- 4.0 ± 2.8
2	2D2-FIG	Vaccine	*g*	GMCSF-NFM	0 of 6	NA	0.0 ± 0.0	0.0	0.0 ± 0.0	0.0	- 2.4 ± 1.8
2	2D2-FIG	Vaccine	*h*	GMCSF-MOG + GMCSF-NFM	0 of 6	NA	0.0 ± 0.0	0.0	0.0 ± 0.0	0.0	- 0.7 ± 2.2
2	2D2-FIG	Vaccine	*i*	Saline	0 of 6	NA	0.0 ± 0.0	0.0	0.0 ± 0.0	0.0	- 1.6 ± 0.9

Table 4.1: The tolerogenic activity of GMCSF-MOG was contingent upon pre-existing Tregs. Experiment 1: C57BL/6 mice were treated with 2 nmoles GMCSF-MOG (n=8) or GMCSF-OVA (n=7) on days −21, −14, and −7. On day 0, all mice were immunized with 200 μg MOG^{35-55} in CFA and 400 ng of Ptx toxin i.p. on days 0 and 2. Experiment 2: 2D2-FIG (n=6) or 2D2-FIG-*Rag1*$^{-/-}$ (n=5-6) mice were vaccinated with 4 nmoles GMCSF-MOG, GMCSF-NFM, "GMCSF-MOG + GMCSF-NFM", or with saline on days 0 and day 20. Experiment 1, the % maximum weight loss between days 1-40 was analyzed with a two-tailed Student's t-test. (*a*) versus (*b*), ($p \leq 0.001$). Mean cumulative and maximal scores were analyzed with a Mann-Whitney U Test (*a*) versus (*b*), ($p \leq 0.001$). Experiment 2, the mean cumulative and maximal scores were analyzed with a Kruskal-Wallis Test and adjusted by the Bonferroni correction. Mean cumulative (*d*) versus (*e*), (*f*), (*g*), (h), and (*i*), ($p < 0.01$) and mean maximal scores (*c*) versus (*f*), (*g*), (*h*), and (*i*) ($p < 0.05$) as well as (*d*) versus (*e*), (*f*), (*g*), (*h*), and (*i*), ($p < 0.01$).

CHAPTER 5

DISCUSSION

5.1 GMCSF-NAg vaccines engender tolerance through the induction of Tregs.

Fusion proteins comprised of GM-CSF and immunodominant NAg were potent tolerogenic vaccines that suppressed NAg-induced EAE. GMCSF-NAg tolerogenic vaccines prevented disease when administered as a prophylactic before the onset of EAE and were effective therapeutic interventions that reversed established EAE. These vaccines elicited tolerance in the context of inflammatory environments because GMCSF-NAg vaccines prevented EAE when mixed directly with the encephalitogenic adjuvant of CFA and MOG^{35-55} (185, 187, 190). The studies detailed here provided evidence that GMCSF-NAg stimulated NAg-specific tolerance through the induction of NAg-specific $CD25^+$ $FOXP3^+$ Tregs. First, GMCSF-MOG-induced tolerance was dependent on the vaccine-induced Tregs. Pretreatment of C57BL/6 mice with the GMCSF-MOG vaccine followed by the subsequent injection of the Treg depleting antibody PC61 reversed vaccine-induced tolerance and resulted in severe paralytic EAE. In contrast, C57BL/6 mice pretreated with the GMCSF-MOG vaccine followed by the subsequent injection of a non-specific control mAb were protected from the development of severe paralytic EAE (Figure 3.1). Secondly, the GMCSF-MOG vaccine induced Tregs in MOG-specific TCR transgenic 2D2-FIG mice. A single subcutaneous vaccination of 2D2-FIG mice with GMCSF-MOG in saline, elicited robust Treg responses in which 20-30% of the circulating T cells were $FOXP3^+$ Tregs. The GMCSF-MOG vaccine elicited rapid Treg expansion which was notable within 3 days and persisted for several weeks (Figure 3.2). The GMCSF-MOG vaccine resulted in Treg expansion and not only the mobilization of Treg into the blood because the GMCSF-

MOG vaccine increased the percent of Tregs in the major secondary lymphoid organs including the lymph nodes and spleen (Figure 3.3). Just as GMCSF-MOG induced tolerance in inflammatory environments when mixed directly with CFA, GMCSF-MOG in CFA also induced high percentages of Tregs in 2D2-FIG mice (Figure 3.8). These results provided evidence that GMCSF-NAg vaccines elicit tolerance at least in part by the expansion of NAg-specific Tregs.

5.2 GMCSF-NAg vaccines induce antigen-specific tolerance.

GMCSF-NAg vaccines were antigen-specific therapies that induced NAg-specific tolerance. For example, the GMCSF-MOG but not the GMCSF-PLP vaccine protected C57BL/6 mice from MOG^{35-55} induced EAE. Likewise, GMCSF-NAg vaccines also induced NAg-specific Tregs because GMCSF-MOG but not the GMCSF-OVA vaccine induced Tregs in 2D2-FIG mice which recognized MOG^{35-55} (Figure 3.6). GMCSF-MOG specifically expanded the MOG-specific Tregs because the absolute number of Tregs per μl of blood was increased in the $V\beta11^+$ 2D2 (MOG^{35-55}-specific) T cell repertoire and not in the $V\beta11^-$ $2D2^-$ (MOG^{35-55} non-specific) T cell pool (Figure 3.2). In accordance with these findings, GMCSF-MOG did not elicit Tregs in OTII-FIG mice which recognize $OVA^{323-339}$ (Figure 3.6). Overall these experiments showed that GMCSF-NAg elicited NAg-specific Tregs and NAg-specific tolerance.

5.3 The GM-CSF domain mediates NAg targeting to elicit tolerance.

Previous studies showed that GMCSF-NAg fusion proteins targeted the tethered NAg for enhanced antigen presentation on myeloid APC *in vitro*. For example, a rat GMCSF-MBP fusion protein was ~1000 fold more potent than MBP^{73-87} alone at inducing the proliferation of MBP-specific $CD4^+$ T cells when activated with myeloid APC. The antigen targeting of the GMCSF-MBP fusion protein was mediated by GM-CSF because free GM-CSF but not M-CSF blocked the enhanced antigen response. Furthermore, the targeting was specifically directed to myeloid

APC because GMCSF-MBP did not have increased antigen potency when cultured with $MHCII^+$ blastogenic rat T cells or B cells (164, 185). The murine fusion proteins GMCSF-MOG and GMCSF-PLP also increased the antigen potency as a result of targeting of NAg to myeloid APC. Covalent linkage of GM-CSF and NAg was required for targeting because GM-CSF + NAg as separate molecules lacked targeting activity and had similar antigen potency to NAg alone (185, 187, 190). The studies detailed here also provided evidence that GM-CSF targeted tethered antigens for enhanced antigen presentation. The murine fusion proteins GMCSF-MOG, GMCSF-NFM, and GMCSF-OVA were ~100-1000 fold more potent at stimulating 2D2 T cells (MOG^{35-55} and NFM^{13-37}) and OTII T cells ($OVA^{323-339}$) than the NAg alone when cultured with murine splenocytes (Figure 3.6 and 3.7). Together these results showed that GM-CSF was a fusion partner that loaded NAg into the MHCII antigen processing pathway in myeloid APC.

GMCSF-NAg also appeared to target NAg *in vivo* because covalent linkage of GM-CSF to NAg was required for tolerance, Treg induction, and robust antigenic responses in mice. For example, GMCSF-NAg suppressed EAE whereas control vaccines comprised of the individual vaccine components including GM-CSF + NAg, GM-CSF, and NAg failed to significantly impact the disease course (185, 187, 190). Likewise, the covalently linked GMCSF-MOG vaccine elicited Tregs, increased the percent of activated $CD44^{high}$ and $Ki67^+$ T cells, decreased Vβ11 TCR expression, and decreased $CD3^+$ Tcon circulation in 2D2-FIG mice while the control vaccine of GMCSF + MOG^{35-55} did not elicit detectable T cell responses (Figure 3.2, 3.4 and 3.5). The requirement of covalent linkage could not be overcome through a non-covalent association of GM-CSF and NAg in a CFA emulsion. Only the covalently linked GMCSF-MOG vaccine in CFA elicited a large increase in Treg numbers and percentages while the GM-CSF + MOG^{35-55} vaccine in CFA failed to expand Tregs in 2D2-FIG mice (Figure 3.8). Collectively

these data indicated that GM-CSF introduces the covalently linked NAg into an APC niche that favors tolerogenic outcomes that included the induction of Tregs, depletion of Tcon, and desensitization of the TCR.

Immunosuppressive Tregs have been extensively studied since the discovery of the Treg-specific transcription factor FOXP3. Current evidence suggests that Tregs occupy a distinct niche that is sustained by a specialized milieu of cytokines and antigens that support Treg viability, stability, and functional activity. Evidence suggests that TGF-β and low-level IL-2 comprise the cytokine niche that favors the Treg compartment. IL-2 is required for Treg development and functional activity because mice that are deficient in CD25, part of the IL-2 receptor or IL-2 have decreased levels of Tregs which results in fatal autoimmune disease (247). Low-dose IL-2 specifically maintains the Treg niche because Tregs express superlative levels of CD25 which allows them to outcompete Tcons for IL-2 survival signals (241, 248). Additionally, the cytokine TGF-β maintains the Treg niche by supporting pTreg differentiation and Treg functional activity and stability during antigen activation (249). Tregs require antigenic stimulation for immunosuppressive activity. Therefore, pools of self and extended-self antigens maintain the Treg repertoire diversity and functional activity (250).

In addition to the cytokine and antigen Treg niches, it has also been suggested that there is a Treg-specific APC niche. Evidence suggest that the Treg-APC niche is comprised of myeloid APC that work in concert with the antigen niche to maintain Treg populations. For example, mice depleted of myeloid $CD11c^+$ DC had a 2-fold decrease in the total number and percent of Tregs. The decrement in Treg populations was due to decreased antigen presentation on DC because a CD11c-specific MHCII knockout also led to decreased Treg pools. Furthermore, the lack of myeloid DC and therefore Tregs led to increased incidents of type 1

diabetes in NOD mice (251). Likewise, the transgenic expression of MOG^{35-55} in $CD11c^{+}$ DC protected mice from the development of MOG^{35-55}-indcued EAE. The studies showed the MHCII presentation of MOG^{35-55} on $CD11c^{+}$ DC increased the percentage of MOG^{35-55}-specifc Tregs which in turn reduced the severity of EAE (252). The studies detailed here are consistent with the concept of an APC/antigen Treg niche because GMCSF-NAg selectively loaded NAg into the antigen-processing pathway of myeloid APC which in turn increases NAg-specific Treg populations and protected mice from the development of EAE.

5.4 Low-efficiency antigen recognition induces tolerance in both quiescent and inflammatory environments.

GMCSF-NAg vaccines induced tolerance in quiescent environments when administered as a pretreatment in saline as well as in inflammatory environments when administered in CFA and as a therapeutic intervention (185, 187, 190). These data suggested that antigen presentation of self-peptides on myeloid APC incited tolerance regardless of the immune environment. These observations contradicted the dogma that APC in quiescent environments have tolerogenic activity whereas APC in inflammatory environments support immunogenic responses (253-255). This model lacks a mechanistic rationalization of how tolerance to self-antigens is maintained during immunity. If immune outcomes were simply based on the immune environment, one would expect that inflammatory immune responses to pathogens, especially during chronic infections, would routinely lead to autoimmunity which is not the case. Likewise, the paradigm that immature APC support Treg differentiation whereas mature DC support the Tcon lineage is flawed. Both immature and mature APC have been shown to support Treg and Tcon responses depending on the experimental model (256-258). In accordance, the GMCSF-NAg vaccines were effective tolerogens when mixed with CFA which induces both inflammation and APC

maturation (187). Therefore, the tolerogenic activity of GMCSF-NAg is likely independent of the level of APC maturation and local immune inflammation.

Although, the GM-CSF domain was critical for antigenic targeting, tolerance, and Treg induction, a central finding here was that the NAg domain was also critical in directing the vaccine outcome which was dependent on the efficiency of NAg recognition by TCR. These studies showed that low-efficiency antigen recognition elicited tolerogenic responses while high-efficiency antigen recognition elicited immunogenic outcomes when paired with GM-CSF. Thus, GMCSF-NAg vaccines which interacted with the same 2D2 TCR and contained the low-efficiency antigen MOG^{35-55} or the high-efficiency antigen NFM^{13-37} peptide elicited or precluded Treg responses in 2D2-FIG mice respectively (Figure 3.7). Likewise, the GMCSF-OVA vaccine which contained $OVA^{323-339}$ that interacted with the OTII TCR with high-efficiency lacked Treg inductive activity (Figure 3.6). The GMCSF-NFM vaccine not only precluded Treg induction but led to robust memory Tcon responses because splenocytes from GMCSF-NFM vaccinated 2D2-FIG mice exhibited vigorous proliferation ex vivo in response to both NFM^{13-37} and MOG^{35-55} (Figure 4.2).

Because low and high-efficiency antigen recognition events elicited Treg and Tcon responses, respectively, we investigated the role of antigen-inducible CD40L/CD40 cross talk between T cells and APC. It has been shown that increased levels of TCR stimulation leads to amplified activation of the CD40L/CD40 pathway which, in turn, drives numerous immunogenic processes including antibody class switching, APC licensing, and differentiation of TH17 cells (259-262). However, little is known about the effects of antigen-activated CD40L expression on Treg populations. Here we provide evidence that high-efficiency antigen recognition promotes the activation of CD40L/CD40 pathway which directs T cell into the Tcon lineage while reduced

levels of CD40L/CD40 activation favors the Treg lineage. Both of the vaccines containing high-efficiency antigens, GMCSF-NFM and NFM^{13-37}, induced CD40L expression in 2D2-FIG splenocytes *in vitro*. In contrast, the vaccines with low-efficiency antigens, GMCSF-MOG and MOG^{35-55}, lacked sufficient TCR stimulation to drive CD40L expression (Figure 4.1). Furthermore, the activation of the CD40L/CD40 pathway prohibited Treg induction with the low-efficiency GMCSF-MOG vaccine *in vivo*. Pretreatment of 2D2-FIG mice with an agonist anti-CD40 antibody which led to the activation of CD40L/CD40 pathway decimated Treg induction with the low-efficiency GMCSF-MOG vaccine (Figure 4.3). These findings suggest that the efficiency of antigen recognition is integrated, at least in part, through the CD40L/CD40 pathway to determine which T cell population will dominate the response. These studies show that reduced levels of CD40L activation allow dominant Treg responses. Therefore, therapies which preclude CD40L/CD40 activation may be effective methods for inducing Tregs and tolerance. In contrast, activation of the CD40L/CD40 pathway with agonistic anti-CD40 may prove to be an effective modality for overcoming detrimental Treg responses that prevent the successful clearance of cancers.

T cell clones specific for self-antigens are typically limited to low-efficiency interactions because high-efficiency auto-reactive T cell clones are deleted during negative thymic selection (3, 4). Therefore, we would suggest that a majority of auto-antigens will elicit low-efficiency responses leading to Tregs and tolerance when fused with GM-CSF. In support of these conclusions fusion proteins comprised of GM-CSF and MBP^{73-87}, $PLP^{139-151}$, or MOG^{35-55} induced tolerance and prevented EAE (185, 187, 190). The high-efficiency interaction of the self-antigen NFM^{13-37} and the 2D2 TCR most likely represents an aberrant T cell response. Evidence suggests that NFM^{13-37} fails to elicit central tolerance in C57BL/6 mice (236-238).

Overall, the NFM-reactive T cell repertoire may be restrained via immune ignorance or by mechanisms of peripheral tolerance. Either way, self-tolerance to NFM^{13-37} is maintained because NFM^{13-37} lacks encephalitogenic activity in C57BL/6 mice (237). The GMCSF-OVA vaccine, which contains a high-efficiency antigen, also failed to induce Tregs in OTII-FIG mice which provides evidence that pairing GM-CSF with foreign-antigens favored immunogenic responses (Figure 3.6). Consistent with this idea, vaccines comprised of GM-CSF and foreign viral and bacterial antigens have been shown to enhance immunogenic pathogen-specific T cell responses (210, 263-265).

The low-efficiency GMCSF-NAg vaccines not only induced Tregs within the confounds of an inflammatory environment of CFA, but also in the presence of high-efficiency antigen recognition. Vaccination of 2D2-FIG mice with both the low-efficiency GMCSF-MOG and high-efficiency GMCSF-NFM vaccine in saline elicited significant Treg induction and decreased the Vβ11 TCR expression on a per cell basis as compared to the GMCSF-NFM vaccine alone (Figure 4.4). Therefore, low-efficiency antigen recognition events which favor Tregs were partially dominant over concurrent high-efficiency antigen recognition events that favor Tcons. One possibility is that low-efficiency antigen recognition may act as a partial TCR antagonist that disrupts efficient TCR signal transduction during high-efficiency TCR ligation. The impaired TCR-MHC synapse formation my also prevent robust CD40L/CD40 signaling due to decreased T cell- APC interactions. Another non-exclusive possibility is that high-efficiency antigens are more rapidly cleared from the APC surface and therefore act only during the initial responses (266). In contrast, low-efficiency antigens may persist on APC for longer periods of time and may drive tolerogenic responses after the clearance of the high-efficiency antigens. The fact that low-efficiency Treg responses prevail in the context of high-efficiency antigen

recognition provides evidence that myeloid APC maintain Treg populations during the clearance of cross-reactive foreign-antigens.

5.5 GM-CSF amplifies both tolerogenic and immunogenic responses.

GM-CSF is a cytokine that supports myeloid cell differentiation, survival, and function (267). GM-CSF binds and signals through the GM-CSF-specific α chain (CD116) and the shared common β chain (CD131) which combine to form a dodecamer signaling complex consisting of 4 GM-CSF molecules, 4 CD116, and 4 CD131 (268). Following the formation of the dodecamer complex, GM-CSF signals through the JAK2-STAT5 and PI3-Akt pathways to control the expression of over ~3000 genes (269). There are multiple cellular sources of GM-CSF including epithelial cells, fibroblasts, stromal cells, T cells, and hematopoietic cells. A substantial literature supports the concept that GM-CSF has a pro-inflammatory role in EAE. For example, $Csf2^{-/-}$ (GM-CSF knockout) mice are resistant to the development of EAE, and neutralizing mAb against GM-CSF have been shown to ameliorate EAE. Furthermore, administration of recombinant GM-CSF restored susceptibility to EAE in $Csf2^{-/-}$ mice (194). However, it was later shown that GM-CSF was not absolutely required for the development of EAE in $Csf2^{-/-}$ mice because depletion of Tregs with the anti-CD25 antibody PC61 restored disease susceptibility. The study showed that $Csf2^{-/-}$ mice had deficiencies in T cell priming which was unable to overcome the natural immunosuppressive Treg barrier in order to drive disease (240). In agreement with these findings, another study showed that the impaired T cell priming in $Csf2^{-/-}$ mice could be overcome by adoptively transferring ex-vivo stimulated $Csf2^{-/-}$ TH17 polarized T cells to elicit EAE (270). Therefore, GM-CSF is not a dedicated pathogenic cytokine in EAE, but instead supports APC function and T cell priming. Our data support this idea because fusing GM-CSF to the antigen had a significant effect on T cell priming toward that antigen. While this

is, in part, due to antigen targeting, it also is likely mediated by GM-CSF signaling in the responder APC.

In contrast to the proinflammatory roles of GM-CSF in EAE, there is mounting evidence that GM-CSF also has profound anti-inflammatory properties. For example, administration of exogenous GM-CSF can reduce disease in numerous animal models of autoimmunity including myasthenia gravis, thyroiditis, type 1 diabetes, and graph versus host disease (201, 208, 217, 220, 221). A consistent theme among these studies was that GM-CSF expanded DC populations which, in turn, induced Tregs to reduce the disease course. These studies administered recombinant GM-CSF alone and did not include auto-antigens. Therefore the effects of GM-CSF were antigen independent or dependent on endogenous auto-antigen presentation. The studies described here were novel and showed that GM-CSF fused to exogenous auto-antigens elicited antigen-specific Tregs and tolerance (Figure 3.1, 3.2, and 4.6). These findings suggest that GM-CSF signaling permits or even supports Treg responses during antigen stimulation. Our studies also showed that GM-CSF supported immunogenic responses depending on the quality of antigen recognition (Figure 4.2).

Because GM-CSF appears to support both inflammatory and anti-inflammatory processes we would suggest that GM-CSF simply amplifies the immune response by supporting myeloid APC differentiation, function, and survival. We suggest that the total immune response is directed by either the quality of antigen recognition by $CD4^+$ T cells as seen in these studies or by the presence of other directing stimuli. Redefining GM-CSF as a hematopoietic growth factor that supports APC populations unifies the complex and diverse functions of GM-CSF in tolerance and inflammation.

5.6 GMCSF-NAg expands pre-existing Tregs to induce tolerance.

Tolerogenic vaccines that elicit Treg responses can expand pre-existing Tregs and/ or induce naïve T cells to differentiate into Tregs. Therefore, tolerogenic vaccines can be separated into the three categories, Treg-inductive vaccines, Treg-expansive vaccines, or vaccines that expand and induce Tregs. Mounting evidence suggests that GMCSF-NAg are Treg-expansive vaccines. First, the quantity of pre-existing Tregs significantly affected the timing of GMCSF-MOG-induced Treg expansion. GMCSF-MOG-induced Tregs were delayed by ~1 week in 2D2-FIG-*Rag1*$^{-/-}$ mice which had limited pre-existing Treg populations as compared to 2D2-FIG mice which had pre-existing Treg populations (Figure 3.10). These experiments showed that GMCSF-NAg vaccines required pre-existing Treg populations for the rapid emergence of vaccine-induced Tregs. It remains a possibility that pre-existing Tregs are required for the differentiation of naïve T cells into Tregs. Second, GMCSF-MOG vaccines specifically expanded memory Tregs 3 days post-vaccination from a mixed memory CD45.1-2D2-FIG Treg and Tcon pool that was adoptively transferred into 2D2-FIG-*Rag1*$^{-/-}$ mice (Figure 4.7). These experiments showed that GMCSF-MOG vaccines expanded pre-existing memory Treg instead of Tcon populations and provided evidence that 2D2-FIG-*Rag1*$^{-/-}$ mice had normal antigen presentation capabilities. Additionally, these data suggest that pre-existing Tregs are not sufficient for vaccine-mediated Treg induction because the presence of adoptively transferred memory Tregs did not provoke Treg induction in the 2D2-FIG-*Rag1*$^{-/-}$ T cell population by day 3 (data not shown). Third, GMCSF-NAg required pre-existing Tregs for the induction of tolerance because GMCSF-MOG induced EAE in 2D2-FIG-*Rag1*$^{-/-}$ but not in 2D2-FIG mice (Figure 4.6). These experiments showed that GMCSF-NAg led to encephalitogenic priming instead of Treg and tolerogenic responses when pre-existing Tregs were absent. Fourth, GMCSF-NAg-induced Tregs had a

phenotype that was similar to pre-existing Tregs in which there was an equal ratio of Tregs positive and negative for the markers CD25, LAP, and $CD44^{high}$ $CD62L^{low}$ (Figure 3.5). Together these data suggest that GMCSF-NAg expand pre-existing Tregs to elicit NAg-specific tolerance.

A Treg-expansive vaccine may have advantages over Treg-inductive vaccines. For example, a number of studies have shown that peripherally induced Tregs are unstable and less immunosuppressive compared to the expansion of thymically-derived Tregs (271-274). These functional differences have been attributed to the methylation status of the Treg-specific demethylated region (TSDR). Increasing levels of TSDR demethylation increases FOXP3 expression in Tregs and therefore increases Treg function and stability. Studies have shown that naturally occurring Tregs have higher levels of TSDR demethylation as compared to peripherally induced Tregs (275, 276). Therefore vaccines, such as GMCSF-NAg, that expand pre-existing Tregs may be advantageous and elicit Tregs with increased stability and immunosuppressive properties.

5.7 GMCSF-NAg vaccines induce Tregs regardless the route of administration.

The manner in which tolerogenic vaccines are administered, including the route and inclusion of adjuvants, can have profound effects on outcome. Typically immunogenic vaccines are administered IM or in adjuvants in order to create an antigen depot to enhance local inflammation. Conversely, tolerogenic vaccines are typically given in saline to elicit diffuse less immunogenic responses. Therefore many tolerogenic vaccines would likely be immunogenic if emulsified in pro-inflammatory adjuvants like CFA or alum. However, GMCSF-NAg elicited Tregs when administered in saline and in both the inflammatory adjuvants CFA and alum which promote TH1 and TH2 responses respectively (Figure 3.8). In addition, GMCSF-NAg vaccines were equally effective at inducing Tregs when administered SC and IV (Figure 3.9). It is

assumed that SC administration of GMCSF-NAg vaccine introduces the vaccine into skin resident APC or draining lymphatics to elicit the tolerogenic response. However, both skin resident APC and draining lymphatics were dispensable because GMCSF-MOG was equally effective when administered IV, which indicated either the blood, spleen or liver were also sufficient to drive the observed Treg responses. In contrast, many other vaccine platforms are contingent upon the route of immunization. These observations indicate that the GM-CSF domain targets the NAg domain into a tolerogenic APC niche regardless of the manner of administration.

5.8 GMCSF-MOG vaccines elicit enhanced CD44^{high} responses in 2D2-FIG mice.

CD44 is an adhesion receptor that is upregulated following antigen recognition events and is maintained on memory T cell populations. CD44 is involved in diverse biological processes including inflammation and tolerance. The studies here showed that CD44 was differentially regulated by the strength of the antigen-TCR interaction because the low-efficiency antigen GMCSF-MOG induced higher percentages of CD44^{high} Tregs and Tcons as compared to the high-efficiency GMCSF-NFM vaccine in 2D2-FIG mice (Figure 4.5). There are two mechanisms that may account for the differential regulation of CD44. First, low-efficiency antigens are maintained for longer periods of time in MHCII complexes on APC as compared to high-efficiency antigens (266). Therefore low-efficiency antigens may persist longer leading to the prolonged activation of T cells and increasing the CD44 expression. Second, CD44 has been shown to potentiate TCR signaling events and may represent a mechanism by which T cells tune antigen recognition to increase the efficiency of low-efficiency recognition events (277). These findings are interesting because CD44 expression is linked to Treg function and persistence as well as the induction of apoptosis in effector cells. For example, levels of CD44 expression are

positively correlated with FOXP3 expression and the suppressive function of Tregs (278, 279). Additionally, CD44 is involved in activation of the FasL/Fas signaling pathway which is pivotal for the deletion of autoreactive T cells and the maintenance of tolerance (280). In conclusion low-efficiency GMCSF-NAg vaccines increase CD44 expression which may represent an ideal tolerogenic outcome that favors Treg function and persistence while leading to the decrement of Tcons through activation-induced cell death.

5.9 Conclusions

GMCSF-NAg fusion proteins are a tolerogenic vaccine platform that elicited robust NAg-specific tolerance. The emerging model (Figure 5.1) is that the GM-CSF domain binds to the GM-CSF receptor (CD116, CD131) on myeloid APC which, in turn, elicits receptor-mediated endocytosis effectively targeting the NAg domain into the antigen processing pathway of myeloid APC. We suggest that GM-CSF signaling through the GM-CSF receptor enhances myeloid APC survival and function leaving the APC poised to stimulate either tolerogenic or immunogenic responses. Presentation of self-antigens including the NAg domain to $CD4^+$ T cells results in low-efficiency antigen recognition events which fall below the CD40L/CD40 stimulatory threshold inducing the expansion of pre-existing NAg-specific $FOXP3^+$ Tregs. In contrast, presentation of non-self-antigens to $CD4^+$ T cells will result in high-efficiency antigen recognition events that activate the CD40L/CD40 pathway resulting in the induction of memory Tcon responses. Low-efficiency $CD4^+$ T cell responses targeted to the NAg domain mediate dominant tolerance in the contexts of inflammatory environments and in opposition to high-efficiency TCR ligation events. The low-efficiency NAg recognition leads to the desensitization of the NAg-specific T cell repertoire through the loss of $CD3^+$ Tcons and down regulation of the TCR. The tolerogenic outcome of the GMCSF-NAg vaccine is dependent on pre-existing NAg-

specific Tregs. This tolerogenic vaccine platform provides mechanistic insight into Treg biology while advancing antigen-specific therapies to fulfill an unmet clinical need in the treatment of MS.

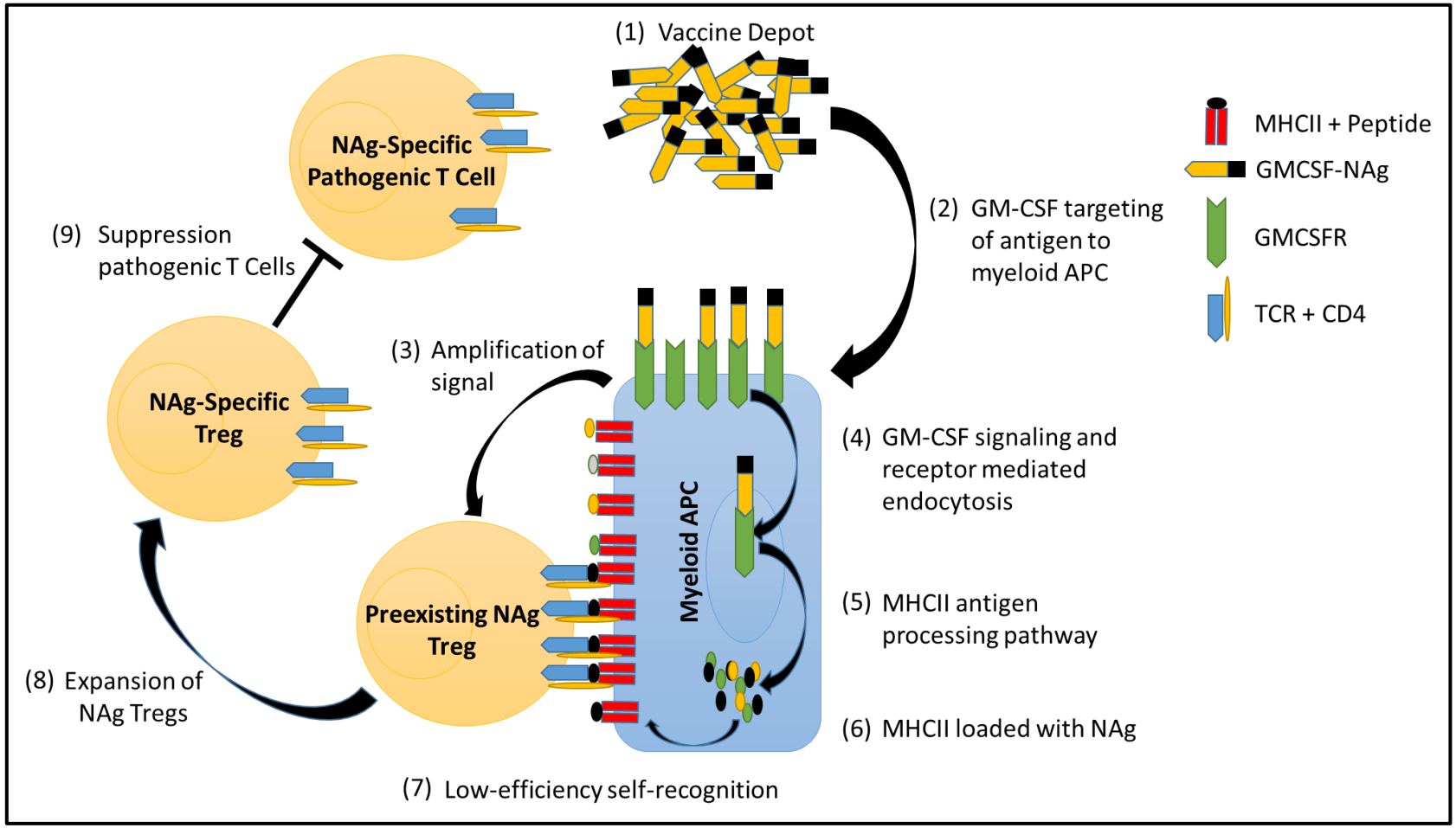
(1) Vaccine Depot
NAg-Specific Pathogenic T Cell
(9) Suppression pathogenic T Cells
NAg-Specific Treg
(3) Amplification of signal
Preexisting NAg Treg
Myeloid APC
(2) GM-CSF targeting of antigen to myeloid APC
(4) GM-CSF signaling and receptor mediated endocytosis
(5) MHCII antigen processing pathway
(6) MHCII loaded with NAg
(7) Low-efficiency self-recognition
(8) Expansion of NAg Tregs
MHCII + Peptide
GMCSF-NAg
GMCSFR
TCR + CD4

Figure 5.1: Model of GMCSF-NAg vaccine tolerogenic activity. (1) Vaccination with GMCSF-NAg results in a local vaccine depot. **(2)** The GM-CSF domain targets the tethered antigen to the GM-CSF receptor (GMCSFR) (CD116 and CD131) on myeloid APC. **(3)** GM-CSF stimulates the myeloid APC promoting viability and increased functional activity, priming the myeloid APC for effector functions. **(4)** Binding of the GM-CSF domain stimulates receptor-mediated endocytosis. **(5)** The GMCSF-NAg vaccine enters the MHCII antigen processing pathway. **(6)** The immunodominant NAg is loaded into MHCII molecules which are then presented on the surface of the myeloid APC. **(7)** Pre-existing NAg-specific Tregs recognize the NAg/MHCII complexes on myeloid APC resulting in low-efficiency antigen recognition. **(8)** The NAg-specific pre-existing Treg population is expanded via NAg recognition on the GM-CSF stimulated myeloid APC. **(9)** The expanded NAg-specific Tregs prevent NAg-specific Tcon responses resulting in tolerance.

CHAPTER 6

REFERENCES

1. Sakaguchi, S., T. Yamaguchi, T. Nomura, and M. Ono. 2008. Regulatory T cells and immune tolerance. *Cell* 133: 775-787.

2. Nemazee, D. 2000. Receptor selection in B and T lymphocytes. *Annu Rev Immunol* 18: 19-51.

3. Hogquist, K. A., T. A. Baldwin, and S. C. Jameson. 2005. Central tolerance: learning self-control in the thymus. *Nat Rev Immunol* 5: 772-782.

4. Pelanda, R., and R. M. Torres. 2012. Central B-cell tolerance: where selection begins. *Cold Spring Harb Perspect Biol* 4: a007146.

5. Burger, M. L., K. K. Leung, M. J. Bennett, and A. Winoto. 2014. T cell-specific inhibition of multiple apoptotic pathways blocks negative selection and causes autoimmunity. *Elife* 3.

6. Tsubata, T. 2017. B-cell tolerance and autoimmunity. *F1000Res* 6: 391.

7. Yan, J., and M. J. Mamula. 2002. Autoreactive T cells revealed in the normal repertoire: escape from negative selection and peripheral tolerance. *J Immunol* 168: 3188-3194.

8. Xing, Y., and K. A. Hogquist. 2012. T-cell tolerance: central and peripheral. *Cold Spring Harb Perspect Biol* 4.

9. Sakaguchi, S., K. Wing, and T. Yamaguchi. 2009. Dynamics of peripheral tolerance and immune regulation mediated by Treg. *Eur J Immunol* 39: 2331-2336.

10. van der Vliet, H. J., and E. E. Nieuwenhuis. 2007. IPEX as a result of mutations in FOXP3. *Clin Dev Immunol* 2007: 89017.

11. Ramsdell, F., and S. F. Ziegler. 2014. FOXP3 and scurfy: how it all began. *Nat Rev Immunol* 14: 343-349.

12. Kim, J. M., J. P. Rasmussen, and A. Y. Rudensky. 2007. Regulatory T cells prevent catastrophic autoimmunity throughout the lifespan of mice. *Nat Immunol* 8: 191-197.

13. Lee, H. M., J. L. Bautista, and C. S. Hsieh. 2011. Thymic and peripheral differentiation of regulatory T cells. *Adv Immunol* 112: 25-71.

14. Sharma, A., and D. Rudra. 2018. Emerging Functions of Regulatory T Cells in Tissue Homeostasis. *Front Immunol* 9: 883.

15. Commins, S. P. 2015. Mechanisms of Oral Tolerance. *Pediatric clinics of North America* 62: 1523-1529.

16. Duan, W., and M. Croft. 2014. Control of regulatory T cells and airway tolerance by lung macrophages and dendritic cells. *Ann Am Thorac Soc* 11 Suppl 5: S306-313.

17. Hasegawa, H., and T. Matsumoto. 2018. Mechanisms of Tolerance Induction by Dendritic Cells In Vivo. *Front Immunol* 9: 350.

18. Sawant, D. V., and D. A. Vignali. 2014. Once a Treg, always a Treg? *Immunol Rev* 259: 173-191.

19. Smigiel, K. S., S. Srivastava, J. M. Stolley, and D. J. Campbell. 2014. Regulatory T-cell homeostasis: steady-state maintenance and modulation during inflammation. *Immunol Rev* 259: 40-59.

20. Nelson, B. H. 2004. IL-2, regulatory T cells, and tolerance. *J Immunol* 172: 3983-3988.

21. Zhao, H., X. Liao, and Y. Kang. 2017. Tregs: Where We Are and What Comes Next? *Front Immunol* 8: 1578.

22. Chougnet, C., and D. Hildeman. 2016. Helios-controller of Treg stability and function. *Transl Cancer Res* 5: S338-S341.

23. Corthay, A. 2009. How do regulatory T cells work? *Scand J Immunol* 70: 326-336.

24. Arce-Sillas, A., D. D. Alvarez-Luquin, B. Tamaya-Dominguez, S. Gomez-Fuentes, A. Trejo-Garcia, M. Melo-Salas, G. Cardenas, J. Rodriguez-Ramirez, and L. Adalid-Peralta. 2016. Regulatory T Cells: Molecular Actions on Effector Cells in Immune Regulation. *J Immunol Res* 2016: 1720827.

25. Rosser, E. C., and C. Mauri. 2015. Regulatory B cells: origin, phenotype, and function. *Immunity* 42: 607-612.

26. Zeng, H., R. Zhang, B. Jin, and L. Chen. 2015. Type 1 regulatory T cells: a new mechanism of peripheral immune tolerance. *Cell Mol Immunol* 12: 566-571.

27. Domogalla, M. P., P. V. Rostan, V. K. Raker, and K. Steinbrink. 2017. Tolerance through Education: How Tolerogenic Dendritic Cells Shape Immunity. *Frontiers in Immunology* 8.

28. Gravano, D. M., and D. A. Vignali. 2012. The battle against immunopathology: infectious tolerance mediated by regulatory T cells. *Cell Mol Life Sci* 69: 1997-2008.

29. Tran, D. Q. 2012. TGF-beta: the sword, the wand, and the shield of FOXP3(+) regulatory T cells. *J Mol Cell Biol* 4: 29-37.

30. Vanderlugt, C. L., and S. D. Miller. 2002. Epitope spreading in immune-mediated diseases: implications for immunotherapy. *Nat Rev Immunol* 2: 85-95.

31. Rosenblum, M. D., I. K. Gratz, J. S. Paw, and A. K. Abbas. 2012. Treating human autoimmunity: current practice and future prospects. *Sci Transl Med* 4: 125sr121.

32. Dobson, R., and G. Giovannoni. 2019. Multiple sclerosis - a review. *Eur J Neurol* 26: 27-40.

33. Hunter, S. F. 2016. Overview and diagnosis of multiple sclerosis. *Am J Manag Care* 22: s141-150.

34. Wallin, M. T., W. J. Culpepper, J. D. Campbell, L. M. Nelson, A. Langer-Gould, R. A. Marrie, G. R. Cutter, W. E. Kaye, L. Wagner, H. Tremlett, S. L. Buka, P. Dilokthornsakul, B. Topol, L. H. Chen, N. G. LaRocca, and U. S. M. S. P. Workgroup. 2019. The prevalence of MS in the United States: A population-based estimate using health claims data. *Neurology* 92: e1029-e1040.

35. Collaborators, G. B. D. M. S. 2019. Global, regional, and national burden of multiple sclerosis 1990-2016: a systematic analysis for the Global Burden of Disease Study 2016. *Lancet Neurol* 18: 269-285.

36. Svendsen, B., N. Grytten, L. Bo, H. Aarseth, T. Smedal, and K. M. Myhr. 2018. The economic impact of multiple sclerosis to the patients and their families in Norway. *Eur J Health Econ* 19: 1243-1257.

37. Hakim, E. A., A. M. Bakheit, T. N. Bryant, M. W. Roberts, S. A. McIntosh-Michaelis, A. J. Spackman, J. P. Martin, and D. L. McLellan. 2000. The social impact of multiple sclerosis--a study of 305 patients and their relatives. *Disabil Rehabil* 22: 288-293.

38. Efendi, H. 2015. Clinically Isolated Syndromes: Clinical Characteristics, Differential Diagnosis, and Management. *Noro Psikiyatr Ars* 52: S1-S11.

39. Trojano, M., D. Paolicelli, A. Bellacosa, and S. Cataldo. 2003. The transition from relapsing-remitting MS to irreversible disability: clinical evaluation. *Neurol Sci* 24 Suppl 5: S268-270.

40. Garg, N., and T. W. Smith. 2015. An update on immunopathogenesis, diagnosis, and treatment of multiple sclerosis. *Brain Behav* 5: e00362.

41. Lassmann, H. 2017. Targets of therapy in progressive MS. *Mult Scler* 23: 1593-1599.

42. O'Gorman, C., R. Lin, J. Stankovich, and S. A. Broadley. 2013. Modelling genetic susceptibility to multiple sclerosis with family data. *Neuroepidemiology* 40: 1-12.

43. Ebers, G. C., A. D. Sadovnick, and N. J. Risch. 1995. A genetic basis for familial aggregation in multiple sclerosis. Canadian Collaborative Study Group. *Nature* 377: 150-151.

44. Flores, J., S. Gonzalez, X. Morales, P. Yescas, A. Ochoa, and T. Corona. 2012. Absence of Multiple Sclerosis and Demyelinating Diseases among Lacandonians, a Pure Amerindian Ethnic Group in Mexico. *Mult Scler Int* 2012: 292631.

45. Rosati, G. 2001. The prevalence of multiple sclerosis in the world: an update. *Neurol Sci* 22: 117-139.

46. Cotsapas, C., and M. Mitrovic. 2018. Genome-wide association studies of multiple sclerosis. *Clin Transl Immunology* 7: e1018.

47. Kular, L., Y. Liu, S. Ruhrmann, G. Zheleznyakova, F. Marabita, D. Gomez-Cabrero, T. James, E. Ewing, M. Linden, B. Gornikiewicz, S. Aeinehband, P. Stridh, J. Link, T. F. M. Andlauer, C. Gasperi, H. Wiendl, F. Zipp, R. Gold, B. Tackenberg, F. Weber, B. Hemmer, K. Strauch, S. Heilmann-Heimbach, R. Rawal, U. Schminke, C. O. Schmidt, T. Kacprowski, A. Franke, M. Laudes, A. T. Dilthey, E. G. Celius, H. B. Sondergaard, J. Tegner, H. F. Harbo, A. B. Oturai, S. Olafsson, H. P. Eggertsson, B. V. Halldorsson, H. Hjaltason, E. Olafsson, I. Jonsdottir, K. Stefansson, T. Olsson, F. Piehl, T. J. Ekstrom, I. Kockum, A. P. Feinberg, and M. Jagodic. 2018. DNA methylation as a mediator of HLA-DRB1*15:01 and a protective variant in multiple sclerosis. *Nat Commun* 9: 2397.

48. D'Alfonso, S., E. Bolognesi, F. R. Guerini, N. Barizzone, S. Bocca, D. Ferrante, L. Castelli, L. Bergamaschi, C. Agliardi, P. Ferrante, P. Naldi, M. Leone, D. Caputo, C. Ballerini, M. Salvetti, D. Galimberti, L. Massacesi, M. Trojano, and P. Momigliano-Richiardi. 2007. A sequence variation in the MOG gene is involved in multiple sclerosis susceptibility in Italy. *Genes And Immunity* 9: 7.

49. Zuvich, R. L., J. L. McCauley, J. R. Oksenberg, S. J. Sawcer, P. L. De Jager, C. International Multiple Sclerosis Genetics, C. Aubin, A. H. Cross, L. Piccio, N. T. Aggarwal, D. Evans, D. A. Hafler, A. Compston, S. L. Hauser, M. A. Pericak-Vance, and J. L. Haines. 2010. Genetic variation in the IL7RA/IL7 pathway increases multiple sclerosis susceptibility. *Hum Genet* 127: 525-535.

50. Alcina, A., M. Fedetz, D. Ndagire, O. Fernandez, L. Leyva, M. Guerrero, M. M. Abad-Grau, C. Arnal, C. Delgado, M. Lucas, G. Izquierdo, and F. Matesanz. 2009. IL2RA/CD25 gene polymorphisms: uneven association with multiple sclerosis (MS) and type 1 diabetes (T1D). *PLoS One* 4: e4137.

51. Didonna, A., and J. R. Oksenberg. 2015. Genetic determinants of risk and progression in multiple sclerosis. *Clin Chim Acta* 449: 16-22.

52. Dendrou, C. A., L. Fugger, and M. A. Friese. 2015. Immunopathology of multiple sclerosis. *Nat Rev Immunol* 15: 545-558.

53. Alfredsson, L., and T. Olsson. 2019. Lifestyle and Environmental Factors in Multiple Sclerosis. *Cold Spring Harb Perspect Med* 9.

54. Dankers, W., E. M. Colin, J. P. van Hamburg, and E. Lubberts. 2016. Vitamin D in Autoimmunity: Molecular Mechanisms and Therapeutic Potential. *Front Immunol* 7: 697.

55. Huh, J. Y., Y. J. Park, M. Ham, and J. B. Kim. 2014. Crosstalk between adipocytes and immune cells in adipose tissue inflammation and metabolic dysregulation in obesity. *Mol Cells* 37: 365-371.

56. Garcia-Hernandez, M. H., E. Rodriguez-Varela, R. E. Garcia-Jacobo, M. Hernandez-De la Torre, E. E. Uresti-Rivera, R. Gonzalez-Amaro, and D. P. Portales-Perez. 2018. Frequency of regulatory B cells in adipose tissue and peripheral blood from individuals with overweight, obesity and normal-weight. *Obes Res Clin Pract* 12: 513-519.

57. Hedström, A. K., T. Olsson, and L. Alfredsson. 2012. High body mass index before age 20 is associated with increased risk for multiple sclerosis in both men and women. *Multiple Sclerosis Journal* 18: 1334-1336.

58. Wingerchuk, D. M. 2012. Smoking: effects on multiple sclerosis susceptibility and disease progression. *Ther Adv Neurol Disord* 5: 13-22.

59. Riccio, P., and R. Rossano. 2018. Diet, Gut Microbiota, and Vitamins D + A in Multiple Sclerosis. *Neurotherapeutics* 15: 75-91.

60. Hedstrom, A. K., O. Hossjer, M. Katsoulis, I. Kockum, T. Olsson, and L. Alfredsson. 2018. Organic solvents and MS susceptibility: Interaction with MS risk HLA genes. *Neurology* 91: e455-e462.

61. Reza Dorosty-Motlagh, A., N. Mohammadzadeh Honarvar, M. Sedighiyan, and M. Abdolahi. 2016. The Molecular Mechanisms of Vitamin A Deficiency in Multiple Sclerosis. *J Mol Neurosci* 60: 82-90.

62. Virtanen, J. O., and S. Jacobson. 2012. Viruses and multiple sclerosis. *CNS Neurol Disord Drug Targets* 11: 528-544.

63. Root-Bernstein, R., and D. Fairweather. 2014. Complexities in the relationship between infection and autoimmunity. *Curr Allergy Asthma Rep* 14: 407.

64. Fujinami, R. S., M. G. von Herrath, U. Christen, and J. L. Whitton. 2006. Molecular mimicry, bystander activation, or viral persistence: infections and autoimmune disease. *Clin Microbiol Rev* 19: 80-94.

65. Pawate, S., and S. Sriram. 2010. The role of infections in the pathogenesis and course of multiple sclerosis. *Ann Indian Acad Neurol* 13: 80-86.

66. Cossu, D., K. Yokoyama, and N. Hattori. 2018. Bacteria-Host Interactions in Multiple Sclerosis. *Front Microbiol* 9: 2966.

67. Kakalacheva, K., C. Munz, and J. D. Lunemann. 2011. Viral triggers of multiple sclerosis. *Biochim Biophys Acta* 1812: 132-140.

68. Ascherio, A., and K. L. Munger. 2010. Epstein-barr virus infection and multiple sclerosis: a review. *J Neuroimmune Pharmacol* 5: 271-277.

69. Chitnis, T. 2007. The role of CD4 T cells in the pathogenesis of multiple sclerosis. *Int Rev Neurobiol* 79: 43-72.

70. Hoglund, R. A., and A. A. Maghazachi. 2014. Multiple sclerosis and the role of immune cells. *World J Exp Med* 4: 27-37.

71. Fletcher, J. M., S. J. Lalor, C. M. Sweeney, N. Tubridy, and K. H. Mills. 2010. T cells in multiple sclerosis and experimental autoimmune encephalomyelitis. *Clin Exp Immunol* 162: 1-11.

72. Fernando, V., S. Omura, F. Sato, E. Kawai, N. E. Martinez, S. F. Elliott, K. Yoh, S. Takahashi, and I. Tsunoda. 2014. Regulation of an autoimmune model for multiple sclerosis in Th2-biased GATA3 transgenic mice. *Int J Mol Sci* 15: 1700-1718.

73. Duda, P. W., M. C. Schmied, S. L. Cook, J. I. Krieger, and D. A. Hafler. 2000. Glatiramer acetate (Copaxone) induces degenerate, Th2-polarized immune responses in patients with multiple sclerosis. *J Clin Invest* 105: 967-976.

74. Huseby, E. S., P. G. Huseby, S. Shah, R. Smith, and B. D. Stadinski. 2012. Pathogenic CD8 T cells in multiple sclerosis and its experimental models. *Front Immunol* 3: 64.

75. Ortega, S. B., V. P. Kashi, A. F. Tyler, K. Cunnusamy, J. P. Mendoza, and N. J. Karandikar. 2013. The disease-ameliorating function of autoregulatory CD8 T cells is mediated by targeting of encephalitogenic CD4 T cells in experimental autoimmune encephalomyelitis. *J Immunol* 191: 117-126.

76. Disanto, G., J. M. Morahan, M. H. Barnett, G. Giovannoni, and S. V. Ramagopalan. 2012. The evidence for a role of B cells in multiple sclerosis. *Neurology* 78: 823-832.

77. Li, R., K. R. Patterson, and A. Bar-Or. 2018. Reassessing B cell contributions in multiple sclerosis. *Nat Immunol* 19: 696-707.

78. Krumbholz, M., T. Derfuss, R. Hohlfeld, and E. Meinl. 2012. B cells and antibodies in multiple sclerosis pathogenesis and therapy. *Nat Rev Neurol* 8: 613-623.

79. Mishra, M. K., and V. W. Yong. 2016. Myeloid cells - targets of medication in multiple sclerosis. *Nat Rev Neurol* 12: 539-551.

80. Chuluundorj, D., S. A. Harding, D. Abernethy, and A. C. La Flamme. 2014. Expansion and preferential activation of the CD14(+)CD16(+) monocyte subset during multiple sclerosis. *Immunol Cell Biol* 92: 509-517.

81. Kouwenhoven, M., V. Ozenci, A. Gomes, D. Yarilin, V. Giedraitis, R. Press, and H. Link. 2001. Multiple sclerosis: elevated expression of matrix metalloproteinases in blood monocytes. *J Autoimmun* 16: 463-470.

82. Ohl, K., K. Tenbrock, and M. Kipp. 2016. Oxidative stress in multiple sclerosis: Central and peripheral mode of action. *Exp Neurol* 277: 58-67.

83. Marta, C. B., R. Bansal, and S. E. Pfeiffer. 2008. Microglial Fc receptors mediate physiological changes resulting from antibody cross-linking of myelin oligodendrocyte glycoprotein. *J Neuroimmunol* 196: 35-40.

84. Jiang, Z., J. X. Jiang, and G. X. Zhang. 2014. Macrophages: a double-edged sword in experimental autoimmune encephalomyelitis. *Immunol Lett* 160: 17-22.

85. Danikowski, K. M., S. Jayaraman, and B. S. Prabhakar. 2017. Regulatory T cells in multiple sclerosis and myasthenia gravis. *J Neuroinflammation* 14: 117.

86. Haas, J., A. Hug, A. Viehover, B. Fritzsching, C. S. Falk, A. Filser, T. Vetter, L. Milkova, M. Korporal, B. Fritz, B. Storch-Hagenlocher, P. H. Krammer, E. Suri-Payer, and B. Wildemann. 2005. Reduced suppressive effect of CD4+CD25high regulatory T cells on the T cell immune response against myelin oligodendrocyte glycoprotein in patients with multiple sclerosis. *Eur J Immunol* 35: 3343-3352.

87. Venken, K., N. Hellings, M. Thewissen, V. Somers, K. Hensen, J.-L. Rummens, R. Medaer, R. Hupperts, and P. Stinissen. 2008. Compromised CD4+ CD25(high) regulatory T-cell function in patients with relapsing-remitting multiple sclerosis is correlated with a reduced frequency of FOXP3-positive cells and reduced FOXP3 expression at the single-cell level. *Immunology* 123: 79-89.

88. Schwarz, A., M. Schumacher, D. Pfaff, K. Schumacher, S. Jarius, B. Balint, H. Wiendl, J. Haas, and B. Wildemann. 2013. Fine-tuning of regulatory T cell function: the role of calcium signals and naive regulatory T cells for regulatory T cell deficiency in multiple sclerosis. *J Immunol* 190: 4965-4970.

89. Fletcher, J. M., R. Lonergan, L. Costelloe, K. Kinsella, B. Moran, C. O'Farrelly, N. Tubridy, and K. H. Mills. 2009. CD39+Foxp3+ regulatory T Cells suppress pathogenic Th17 cells and are impaired in multiple sclerosis. *J Immunol* 183: 7602-7610.

90. Schneider-Hohendorf, T., M. P. Stenner, C. Weidenfeller, A. L. Zozulya, O. J. Simon, N. Schwab, and H. Wiendl. 2010. Regulatory T cells exhibit enhanced migratory characteristics, a feature impaired in patients with multiple sclerosis. *Eur J Immunol* 40: 3581-3590.

91. Vasileiadis, G. K., E. Dardiotis, A. Mavropoulos, Z. Tsouris, V. Tsimourtou, D. P. Bogdanos, L. I. Sakkas, and G. M. Hadjigeorgiou. 2018. Regulatory B and T lymphocytes in multiple sclerosis: friends or foes? *Auto Immun Highlights* 9: 9.

92. Astier, A. L., and D. A. Hafler. 2007. Abnormal Tr1 differentiation in multiple sclerosis. *J Neuroimmunol* 191: 70-78.

93. Constantinescu, C. S., N. Farooqi, K. O'Brien, and B. Gran. 2011. Experimental autoimmune encephalomyelitis (EAE) as a model for multiple sclerosis (MS). *Br J Pharmacol* 164: 1079-1106.

94. Nathoo, N., V. W. Yong, and J. F. Dunn. 2014. Understanding disease processes in multiple sclerosis through magnetic resonance imaging studies in animal models. *Neuroimage Clin* 4: 743-756.

95. Croxford, A. L., F. C. Kurschus, and A. Waisman. 2011. Mouse models for multiple sclerosis: historical facts and future implications. *Biochim Biophys Acta* 1812: 177-183.

96. Simmons, S. B., E. R. Pierson, S. Y. Lee, and J. M. Goverman. 2013. Modeling the heterogeneity of multiple sclerosis in animals. *Trends Immunol* 34: 410-422.

97. Glatigny, S., and E. Bettelli. 2018. Experimental Autoimmune Encephalomyelitis (EAE) as Animal Models of Multiple Sclerosis (MS). *Cold Spring Harb Perspect Med* 8.

98. Pierson, E., S. B. Simmons, L. Castelli, and J. M. Goverman. 2012. Mechanisms regulating regional localization of inflammation during CNS autoimmunity. *Immunol Rev* 248: 205-215.

99. Murta, V., and C. C. Ferrari. 2013. Influence of Peripheral inflammation on the progression of multiple sclerosis: evidence from the clinic and experimental animal models. *Mol Cell Neurosci* 53: 6-13.

100. McRae, B. L., C. L. Vanderlugt, M. C. Dal Canto, and S. D. Miller. 1995. Functional evidence for epitope spreading in the relapsing pathology of experimental autoimmune encephalomyelitis. *The Journal of experimental medicine* 182: 75-85.

101. Lees, J. R., P. T. Golumbek, J. Sim, D. Dorsey, and J. H. Russell. 2008. Regional CNS responses to IFN-gamma determine lesion localization patterns during EAE pathogenesis. *The Journal of experimental medicine* 205: 2633-2642.

102. Miller, N. M., J. Wang, Y. Tan, and B. N. Dittel. 2015. Anti-inflammatory mechanisms of IFN-gamma studied in experimental autoimmune encephalomyelitis reveal neutrophils as a potential target in multiple sclerosis. *Frontiers in neuroscience* 9: 287.

103. McCarthy, D. P., M. H. Richards, and S. D. Miller. 2012. Mouse models of multiple sclerosis: experimental autoimmune encephalomyelitis and Theiler's virus-induced demyelinating disease. *Methods Mol Biol* 900: 381-401.

104. Torkildsen, O., L. A. Brunborg, K. M. Myhr, and L. Bo. 2008. The cuprizone model for demyelination. *Acta Neurol Scand Suppl* 188: 72-76.

105. Ciotti, J. R., and A. H. Cross. 2018. Disease-Modifying Treatment in Progressive Multiple Sclerosis. *Curr Treat Options Neurol* 20: 12.

106. Smets, I., L. Van Deun, C. Bohyn, V. van Pesch, L. Vanopdenbosch, D. Dive, V. Bissay, B. Dubois, and S. Belgian Study Group for Multiple. 2017. Corticosteroids in the management of acute multiple sclerosis exacerbations. *Acta Neurol Belg* 117: 623-633.

107. Reder, A. T., and X. Feng. 2014. How type I interferons work in multiple sclerosis and other diseases: some unexpected mechanisms. *J Interferon Cytokine Res* 34: 589-599.

108. Kieseier, B. C. 2011. The mechanism of action of interferon-beta in relapsing multiple sclerosis. *CNS Drugs* 25: 491-502.

109. Chen, M., G. Chen, S. Deng, X. Liu, G. J. Hutton, and J. Hong. 2012. IFN-beta induces the proliferation of CD4+CD25+Foxp3+ regulatory T cells through upregulation of GITRL on dendritic cells in the treatment of multiple sclerosis. *J Neuroimmunol* 242: 39-46.

110. Plosker, G. L. 2011. Interferon-beta-1b: a review of its use in multiple sclerosis. *CNS Drugs* 25: 67-88.

111. Sominanda, A., M. Lundkvist, A. Fogdell-Hahn, B. Hemmer, H. P. Hartung, J. Hillert, T. Menge, and B. C. Kieseier. 2010. Inhibition of endogenous interferon beta by neutralizing antibodies against recombinant interferon beta. *Arch Neurol* 67: 1095-1101.

112. Comi, G., M. P. Amato, A. Bertolotto, D. Centonze, N. De Stefano, C. Farina, P. Gallo, A. Ghezzi, L. M. Grimaldi, G. Mancardi, M. G. Marrosu, E. Montanari, F. Patti, C. Pozzilli, L. Provinciali, M. Salvetti, G. Tedeschi, and M. Trojano. 2016. The heritage of glatiramer acetate and its use in multiple sclerosis. *Multiple Sclerosis and Demyelinating Disorders* 1: 6.

113. Rommer, P. S., R. Milo, M. H. Han, S. Satyanarayan, J. Sellner, L. Hauer, Z. Illes, C. Warnke, S. Laurent, M. S. Weber, Y. Zhang, and O. Stuve. 2019. Immunological Aspects of Approved MS Therapeutics. *Frontiers in Immunology* 10.

114. Voge, N. V., and E. Alvarez. 2019. Monoclonal Antibodies in Multiple Sclerosis: Present and Future. *Biomedicines* 7.

115. Behrangi, N., F. Fischbach, and M. Kipp. 2019. Mechanism of Siponimod: Anti-Inflammatory and Neuroprotective Mode of Action. *Cells* 8.

116. Epstein, D. J., J. Dunn, and S. Deresinski. 2018. Infectious Complications of Multiple Sclerosis Therapies: Implications for Screening, Prophylaxis, and Management. *Open Forum Infect Dis* 5: ofy174.

117. The, L. 2018. End of the road for daclizumab in multiple sclerosis. *Lancet* 391: 1000.

118. Sorensen, P. S., and F. Sellebjerg. 2019. Pulsed immune reconstitution therapy in multiple sclerosis. *Ther Adv Neurol Disord* 12: 1756286419836913.

119. Alamo, A., R. A. Condorelli, S. La Vignera, and A. E. Calogero. 2019. Autoimmune thyroid disease following treatment with alemtuzumab for multiple sclerosis. *Int J Immunopathol Pharmacol* 33: 2058738419843690.

120. Mills, E. A., M. A. Ogrodnik, A. Plave, and Y. Mao-Draayer. 2018. Emerging Understanding of the Mechanism of Action for Dimethyl Fumarate in the Treatment of Multiple Sclerosis. *Front Neurol* 9: 5.

121. Cohen, J. A., L. E. Baldassari, H. L. Atkins, J. D. Bowen, C. Bredeson, P. A. Carpenter, J. R. Corboy, M. S. Freedman, L. M. Griffith, R. Lowsky, N. S. Majhail, P. A. Muraro, R. A. Nash, M. C. Pasquini, S. Sarantopoulos, B. N. Savani, J. Storek, K. M. Sullivan, and G. E. Georges. 2019. Autologous Hematopoietic Cell Transplantation for Treatment-Refractory Relapsing Multiple Sclerosis: Position Statement from the American Society for Blood and Marrow Transplantation. *Biol Blood Marrow Transplant* 25: 845-854.

122. Weber, M. S., B. Hemmer, and S. Cepok. 2011. The role of antibodies in multiple sclerosis. *Biochim Biophys Acta* 1812: 239-245.

123. Wong, B., J. Cahill, and S. Rizvi. 2018. Moving Towards a Cure for MS: Increased Immunosuppression and Striving for No Evidence of Disease Activity (NEDA). *R I Med J (2013)* 101: 26-29.

124. Ragonese, P., P. Aridon, G. Vazzoler, M. A. Mazzola, V. Lo Re, M. Lo Re, S. Realmuto, S. Alessi, M. D'Amelio, G. Savettieri, and G. Salemi. 2017. Association between multiple sclerosis, cancer risk, and immunosuppressant treatment: a cohort study. *BMC Neurol* 17: 155.

125. Williamson, E. M., and J. R. Berger. 2015. Infection risk in patients on multiple sclerosis therapeutics. *CNS Drugs* 29: 229-244.

126. Claflin, S. B., S. Broadley, and B. V. Taylor. 2018. The Effect of Disease Modifying Therapies on Disability Progression in Multiple Sclerosis: A Systematic Overview of Meta-Analyses. *Front Neurol* 9: 1150.

127. Ontaneda, D., R. J. Fox, and J. Chataway. 2015. Clinical trials in progressive multiple sclerosis: lessons learned and future perspectives. *Lancet Neurol* 14: 208-223.

128. Hartung, D. M., D. N. Bourdette, S. M. Ahmed, and R. H. Whitham. 2015. The cost of multiple sclerosis drugs in the US and the pharmaceutical industry: Too big to fail? *Neurology* 84: 2185-2192.

129. Serra, P., and P. Santamaria. 2019. Antigen-specific therapeutic approaches for autoimmunity. *Nat Biotechnol* 37: 238-251.

130. Mannie, M. D., and A. D. Curtis, 2nd. 2013. Tolerogenic vaccines for Multiple sclerosis. *Hum Vaccin Immunother* 9: 1032-1038.

131. Willekens, B., and N. Cools. 2018. Beyond the Magic Bullet: Current Progress of Therapeutic Vaccination in Multiple Sclerosis. *CNS Drugs* 32: 401-410.

132. Bielekova, B., B. Goodwin, N. Richert, I. Cortese, T. Kondo, G. Afshar, B. Gran, J. Eaton, J. Antel, J. A. Frank, H. F. McFarland, and R. Martin. 2000. Encephalitogenic potential of the myelin basic protein peptide (amino acids 83-99) in multiple sclerosis: results of a phase II clinical trial with an altered peptide ligand. *Nat Med* 6: 1167-1175.

133. Steinman, L. 2015. The re-emergence of antigen-specific tolerance as a potential therapy for MS. *Mult Scler* 21: 1223-1238.

134. Mirshafiey, A., and M. Kianiaslani. 2013. Autoantigens and autoantibodies in multiple sclerosis. *Iran J Allergy Asthma Immunol* 12: 292-303.

135. Riedhammer, C., and R. Weissert. 2015. Antigen Presentation, Autoantigens, and Immune Regulation in Multiple Sclerosis and Other Autoimmune Diseases. *Front Immunol* 6: 322.

136. Hohlfeld, R., K. Dornmair, E. Meinl, and H. Wekerle. 2016. The search for the target antigens of multiple sclerosis, part 1: autoreactive CD4+ T lymphocytes as pathogenic effectors and therapeutic targets. *Lancet Neurol* 15: 198-209.

137. Mekala, D. J., R. S. Alli, and T. L. Geiger. 2005. IL-10-dependent infectious tolerance after the treatment of experimental allergic encephalomyelitis with redirected CD4+CD25+ T lymphocytes. *Proc Natl Acad Sci U S A* 102: 11817-11822.

138. Flórez-Grau, G., I. Zubizarreta, R. Cabezón, P. Villoslada, and D. Benitez-Ribas. 2018. Tolerogenic Dendritic Cells as a Promising Antigen-Specific Therapy in the Treatment of Multiple Sclerosis and Neuromyelitis Optica From Preclinical to Clinical Trials. *Frontiers in Immunology* 9.

139. Xie, Z. X., H. L. Zhang, X. J. Wu, J. Zhu, D. H. Ma, and T. Jin. 2015. Role of the immunogenic and tolerogenic subsets of dendritic cells in multiple sclerosis. *Mediators Inflamm* 2015: 513295.

140. Larsen, J. N., L. Broge, and H. Jacobi. 2016. Allergy immunotherapy: the future of allergy treatment. *Drug Discov Today* 21: 26-37.

141. Szczepanik, M. 2014. Skin-induced tolerance as a new needle free therapeutic strategy. *Pharmacol Rep* 66: 192-197.

142. Yu, W., D. M. H. Freeland, and K. C. Nadeau. 2016. Food allergy: immune mechanisms, diagnosis and immunotherapy. *Nat Rev Immunol* 16: 751-765.

143. Chinthrajah, R. S., J. D. Hernandez, S. D. Boyd, S. J. Galli, and K. C. Nadeau. 2016. Molecular and cellular mechanisms of food allergy and food tolerance. *J Allergy Clin Immunol* 137: 984-997.

144. Wang, X., A. Sherman, G. Liao, K. W. Leong, H. Daniell, C. Terhorst, and R. W. Herzog. 2013. Mechanism of oral tolerance induction to therapeutic proteins. *Adv Drug Deliv Rev* 65: 759-773.

145. Akdis, C. A., and M. Akdis. 2015. Mechanisms of allergen-specific immunotherapy and immune tolerance to allergens. *World Allergy Organ J* 8: 17.

146. Badawi, A. H., and T. J. Siahaan. 2012. Immune modulating peptides for the treatment and suppression of multiple sclerosis. *Clin Immunol* 144: 127-138.

147. Chen, Y. H., and H. L. Weiner. 1996. Dose-dependent activation and deletion of antigen-specific T cells following oral tolerance. *Ann N Y Acad Sci* 778: 111-121.

148. Beverly, B., S. M. Kang, M. J. Lenardo, and R. H. Schwartz. 1992. Reversal of in vitro T cell clonal anergy by IL-2 stimulation. *Int Immunol* 4: 661-671.

149. Bercovici, N., J. Delon, C. Cambouris, N. Escriou, P. Debre, and R. S. Liblau. 1999. Chronic intravenous injections of antigen induce and maintain tolerance in T cell receptor-transgenic mice. *Eur J Immunol* 29: 345-354.

150. Lechler, R. I., O. A. Garden, and L. A. Turka. 2003. The complementary roles of deletion and regulation in transplantation tolerance. *Nat Rev Immunol* 3: 147-158.

151. Walsh, P. T., D. K. Taylor, and L. A. Turka. 2004. Tregs and transplantation tolerance. *J Clin Invest* 114: 1398-1403.

152. Weiner, H. L., G. A. Mackin, M. Matsui, E. J. Orav, S. J. Khoury, D. M. Dawson, and D. A. Hafler. 1993. Double-blind pilot trial of oral tolerization with myelin antigens in multiple sclerosis. *Science* 259: 1321-1324.

153. Marusic, S., and S. Tonegawa. 1997. Tolerance induction and autoimmune encephalomyelitis amelioration after administration of myelin basic protein-derived peptide. *The Journal of experimental medicine* 186: 507-515.

154. Khoury, S. J., M. H. Sayegh, W. W. Hancock, L. Gallon, C. B. Carpenter, and H. L. Weiner. 1993. Acquired tolerance to experimental autoimmune encephalomyelitis by intrathymic injection of myelin basic protein or its major encephalitogenic peptide. *The Journal of experimental medicine* 178: 559-566.

155. al-Sabbagh, A., P. A. Nelson, Y. Akselband, R. A. Sobel, and H. L. Weiner. 1996. Antigen-driven peripheral immune tolerance: suppression of experimental autoimmmune encephalomyelitis and collagen-induced arthritis by aerosol administration of myelin basic protein or type II collagen. *Cell Immunol* 171: 111-119.

156. Thati, S., C. Kuehl, B. Hartwell, J. Sestak, T. Siahaan, M. L. Forrest, and C. Berkland. 2015. Routes of administration and dose optimization of soluble antigen arrays in mice with experimental autoimmune encephalomyelitis. *J Pharm Sci* 104: 714-721.

157. Keijzer, C., R. van der Zee, W. van Eden, and F. Broere. 2013. Treg inducing adjuvants for therapeutic vaccination against chronic inflammatory diseases. *Front Immunol* 4: 245.

158. Ben-Akiva, E., S. Est Witte, R. A. Meyer, K. R. Rhodes, and J. J. Green. 2018. Polymeric micro- and nanoparticles for immune modulation. *Biomater Sci* 7: 14-30.

159. Capurso, N. A., M. Look, L. Jeanbart, H. Nowyhed, C. Abraham, J. Craft, and T. M. Fahmy. 2010. Development of a nanoparticulate formulation of retinoic acid that suppresses Th17 cells and upregulates regulatory T cells. *Self Nonself* 1: 335-340.

160. Yeste, A., M. Nadeau, E. J. Burns, H. L. Weiner, and F. J. Quintana. 2012. Nanoparticle-mediated codelivery of myelin antigen and a tolerogenic small molecule suppresses experimental autoimmune encephalomyelitis. *Proc Natl Acad Sci U S A* 109: 11270-11275.

161. Tostanoski, L. H., Y. C. Chiu, J. M. Gammon, T. Simon, J. I. Andorko, J. S. Bromberg, and C. M. Jewell. 2016. Reprogramming the Local Lymph Node Microenvironment Promotes Tolerance that Is Systemic and Antigen Specific. *Cell Rep* 16: 2940-2952.

162. Apostolopoulos, V., T. Thalhammer, A. G. Tzakos, and L. Stojanovska. 2013. Targeting antigens to dendritic cell receptors for vaccine development. *J Drug Deliv* 2013: 869718.

163. Chappell, C. P., N. V. Giltiay, C. Dresch, and E. A. Clark. 2014. Controlling immune responses by targeting antigens to dendritic cell subsets and B cells. *Int Immunol* 26: 3-11.

164. Mannie, M. D., J. L. Blanchfield, S. M. Islam, and D. J. Abbott. 2012. Cytokine-neuroantigen fusion proteins as a new class of tolerogenic, therapeutic vaccines for treatment of inflammatory demyelinating disease in rodent models of multiple sclerosis. *Front Immunol* 3: 255.

165. Legge, K. L., R. K. Gregg, R. Maldonado-Lopez, L. Li, J. C. Caprio, M. Moser, and H. Zaghouani. 2002. On the role of dendritic cells in peripheral T cell tolerance and modulation of autoimmunity. *The Journal of experimental medicine* 196: 217-227.

166. Ring, S., M. Maas, D. M. Nettelbeck, A. H. Enk, and K. Mahnke. 2013. Targeting of autoantigens to DEC205(+) dendritic cells in vivo suppresses experimental allergic encephalomyelitis in mice. *J Immunol* 191: 2938-2947.

167. Fissolo, N., X. Montalban, and M. Comabella. 2012. DNA-based vaccines for multiple sclerosis: current status and future directions. *Clin Immunol* 142: 76-83.

168. Ramshaw, I. A., S. A. Fordham, C. C. Bernard, D. Maguire, W. B. Cowden, and D. O. Willenborg. 1997. DNA vaccines for the treatment of autoimmune disease. *Immunol Cell Biol* 75: 409-413.

169. Castor, T., N. Yogev, T. Blank, C. Barwig, M. Prinz, A. Waisman, M. Bros, and A. B. Reske-Kunz. 2018. Inhibition of experimental autoimmune encephalomyelitis by tolerance-promoting DNA vaccination focused to dendritic cells. *PLoS One* 13: e0191927.

170. Keeler, G. D., S. Kumar, B. Palaschak, E. L. Silverberg, D. M. Markusic, N. T. Jones, and B. E. Hoffman. 2018. Gene Therapy-Induced Antigen-Specific Tregs Inhibit Neuro-inflammation and Reverse Disease in a Mouse Model of Multiple Sclerosis. *Mol Ther* 26: 173-183.

171. Gliwinski, M., D. Iwaszkiewicz-Grzes, and P. Trzonkowski. 2017. Cell-Based Therapies with T Regulatory Cells. *BioDrugs* 31: 335-347.

172. Huang, X., H. Wu, and Q. Lu. 2014. The mechanisms and applications of T cell vaccination for autoimmune diseases: a comprehensive review. *Clin Rev Allergy Immunol* 47: 219-233.

173. Verhagen, J., L. Gabryšová, E. R. Shepard, and D. C. Wraith. 2014. Ctla-4 modulates the differentiation of inducible Foxp3+ Treg cells but IL-10 mediates their function in experimental autoimmune encephalomyelitis. *PloS one* 9: e108023-e108023.

174. Kieback, E., E. Hilgenberg, U. Stervbo, V. Lampropoulou, P. Shen, M. Bunse, Y. Jaimes, P. Boudinot, A. Radbruch, U. Klemm, Anja A. Kühl, R. Liblau, N. Hoevelmeyer, Stephen M. Anderton, W. Uckert, and S. Fillatreau. 2016. Thymus-Derived Regulatory T Cells Are Positively Selected on Natural Self-Antigen through Cognate Interactions of High Functional Avidity. *Immunity* 44: 1114-1126.

175. Adair, P. R., Y. C. Kim, A. H. Zhang, J. Yoon, and D. W. Scott. 2017. Human Tregs Made Antigen Specific by Gene Modification: The Power to Treat Autoimmunity and Antidrug Antibodies with Precision. *Front Immunol* 8: 1117.

176. Ferreira, L. M. R., Y. D. Muller, J. A. Bluestone, and Q. Tang. 2019. Next-generation regulatory T cell therapy. *Nat Rev Drug Discov* 18: 749-769.

177. Smith, C. E., and S. D. Miller. 2006. Multi-peptide coupled-cell tolerance ameliorates ongoing relapsing EAE associated with multiple pathogenic autoreactivities. *J Autoimmun* 27: 218-231.

178. Smith, C. E., T. N. Eagar, J. L. Strominger, and S. D. Miller. 2005. Differential induction of IgE-mediated anaphylaxis after soluble vs. cell-bound tolerogenic peptide therapy of autoimmune encephalomyelitis. *Proc Natl Acad Sci U S A* 102: 9595-9600.

179. Getts, D. R., D. M. Turley, C. E. Smith, C. T. Harp, D. McCarthy, E. M. Feeney, M. T. Getts, A. J. Martin, X. Luo, R. L. Terry, N. J. King, and S. D. Miller. 2011. Tolerance induced by apoptotic antigen-coupled leukocytes is induced by PD-L1+ and IL-10-producing splenic macrophages and maintained by T regulatory cells. *J Immunol* 187: 2405-2417.

180. Lutterotti, A., S. Yousef, A. Sputtek, K. H. Sturner, J. P. Stellmann, P. Breiden, S. Reinhardt, C. Schulze, M. Bester, C. Heesen, S. Schippling, S. D. Miller, M. Sospedra, and R. Martin. 2013. Antigen-specific tolerance by autologous myelin peptide-coupled cells: a phase 1 trial in multiple sclerosis. *Sci Transl Med* 5: 188ra175.

181. Jones, A., and D. Hawiger. 2017. Peripherally Induced Regulatory T Cells: Recruited Protectors of the Central Nervous System against Autoimmune Neuroinflammation. *Front Immunol* 8: 532.

182. Mannie, M. D., J. L. Devine, B. A. Clayson, L. T. Lewis, and D. J. Abbott. 2007. Cytokine-neuroantigen fusion proteins: new tools for modulation of myelin basic protein (MBP)-specific T cell responses in experimental autoimmune encephalomyelitis. *J Immunol Methods* 319: 118-132.

183. Mannie, M. D., and D. J. Abbott. 2007. A fusion protein consisting of IL-16 and the encephalitogenic peptide of myelin basic protein constitutes an antigen-specific tolerogenic vaccine that inhibits experimental autoimmune encephalomyelitis. *J Immunol* 179: 1458-1465.

184. Mannie, M. D., B. A. Clayson, E. J. Buskirk, J. L. DeVine, J. J. Hernandez, and D. J. Abbott. 2007. IL-2/neuroantigen fusion proteins as antigen-specific tolerogens in experimental autoimmune encephalomyelitis (EAE): correlation of T cell-mediated antigen presentation and tolerance induction. *J Immunol* 178: 2835-2843.

185. Blanchfield, J. L., and M. D. Mannie. 2010. A GMCSF-neuroantigen fusion protein is a potent tolerogen in experimental autoimmune encephalomyelitis (EAE) that is associated with efficient targeting of neuroantigen to APC. *J Leukoc Biol* 87: 509-521.

186. Moorman, C. D., A. D. Curtis, 2nd, A. G. Bastian, S. E. Elliott, and M. D. Mannie. 2018. A GMCSF-Neuroantigen Tolerogenic Vaccine Elicits Systemic Lymphocytosis of CD4(+) CD25(high) FOXP3(+) Regulatory T Cells in Myelin-Specific TCR Transgenic Mice Contingent Upon Low-Efficiency T Cell Antigen Receptor Recognition. *Front Immunol* 9: 3119.

187. Islam, S. M., A. D. Curtis, 2nd, N. Taslim, D. S. Wilkinson, and M. D. Mannie. 2014. GM-CSF-neuroantigen fusion proteins reverse experimental autoimmune encephalomyelitis and mediate tolerogenic activity in adjuvant-primed environments: association with inflammation-dependent, inhibitory antigen presentation. *J Immunol* 193: 2317-2329.

188. Mannie, M. D., D. J. Abbott, and J. L. Blanchfield. 2009. Experimental autoimmune encephalomyelitis in Lewis rats: IFN-beta acts as a tolerogenic adjuvant for induction of neuroantigen-dependent tolerance. *J Immunol* 182: 5331-5341.

189. Wang, D., D. Ghosh, S. M. Islam, C. D. Moorman, A. E. Thomason, D. S. Wilkinson, and M. D. Mannie. 2016. IFN-beta Facilitates Neuroantigen-Dependent Induction of

CD25+ FOXP3+ Regulatory T Cells That Suppress Experimental Autoimmune Encephalomyelitis. *J Immunol* 197: 2992-3007.

190. Abbott, D. J., J. L. Blanchfield, D. A. Martinson, S. C. Russell, N. Taslim, A. D. Curtis, and M. D. Mannie. 2011. Neuroantigen-specific, tolerogenic vaccines: GM-CSF is a fusion partner that facilitates tolerance rather than immunity to dominant self-epitopes of myelin in murine models of experimental autoimmune encephalomyelitis (EAE). *BMC Immunol* 12: 72.

191. Abbas, A. K., E. Trotta, R. S. D, A. Marson, and J. A. Bluestone. 2018. Revisiting IL-2: Biology and therapeutic prospects. *Sci Immunol* 3.

192. Yang, J. Z., J. Q. Zhang, and L. X. Sun. 2016. Mechanisms for T cell tolerance induced with granulocyte colony-stimulating factor. *Mol Immunol* 70: 56-62.

193. Bhattacharya, P., M. Thiruppathi, H. A. Elshabrawy, K. Alharshawi, P. Kumar, and B. S. Prabhakar. 2015. GM-CSF: An immune modulatory cytokine that can suppress autoimmunity. *Cytokine* 75: 261-271.

194. McQualter, J. L., R. Darwiche, C. Ewing, M. Onuki, T. W. Kay, J. A. Hamilton, H. H. Reid, and C. C. Bernard. 2001. Granulocyte macrophage colony-stimulating factor: a new putative therapeutic target in multiple sclerosis. *The Journal of experimental medicine* 194: 873-882.

195. Sonderegger, I., G. Iezzi, R. Maier, N. Schmitz, M. Kurrer, and M. Kopf. 2008. GM-CSF mediates autoimmunity by enhancing IL-6-dependent Th17 cell development and survival. *The Journal of experimental medicine* 205: 2281-2294.

196. Campbell, I. K., M. J. Rich, R. J. Bischof, A. R. Dunn, D. Grail, and J. A. Hamilton. 1998. Protection from collagen-induced arthritis in granulocyte-macrophage colony-stimulating factor-deficient mice. *J Immunol* 161: 3639-3644.

197. Cook, A. D., E. L. Braine, I. K. Campbell, M. J. Rich, and J. A. Hamilton. 2001. Blockade of collagen-induced arthritis post-onset by antibody to granulocyte-macrophage colony-stimulating factor (GM-CSF): requirement for GM-CSF in the effector phase of disease. *Arthritis Res* 3: 293-298.

198. Scholz, T., A. Weigert, B. Brune, C. D. Sadik, B. Bohm, and H. Burkhardt. 2017. GM-CSF in murine psoriasiform dermatitis: Redundant and pathogenic roles uncovered by antibody-induced neutralization and genetic deficiency. *PLoS One* 12: e0182646.

199. Yamashita, N., H. Tashimo, H. Ishida, F. Kaneko, J. Nakano, H. Kato, K. Hirai, T. Horiuchi, and K. Ohta. 2002. Attenuation of airway hyperresponsiveness in a murine asthma model by neutralization of granulocyte–macrophage colony-stimulating factor (GM-CSF). *Cellular Immunology* 219: 92-97.

200. Kitching, A. R., X. Ru Huang, A. L. Turner, P. G. Tipping, A. R. Dunn, and S. R. Holdsworth. 2002. The requirement for granulocyte-macrophage colony-stimulating factor and granulocyte colony-stimulating factor in leukocyte-mediated immune glomerular injury. *J Am Soc Nephrol* 13: 350-358.

201. Park, M.-Y., B.-G. Lim, S.-Y. Kim, H.-J. Sohn, S. Kim, and T.-G. Kim. 2019. GM-CSF Promotes the Expansion and Differentiation of Cord Blood Myeloid-Derived Suppressor Cells, Which Attenuate Xenogeneic Graft-vs.-Host Disease. *Frontiers in Immunology* 10.

202. Campbell, I. K., A. Bendele, D. A. Smith, and J. A. Hamilton. 1997. Granulocyte-macrophage colony stimulating factor exacerbates collagen induced arthritis in mice. *Ann Rheum Dis* 56: 364-368.

203. Rasouli, J., B. Ciric, J. Imitola, P. Gonnella, D. Hwang, K. Mahajan, E. R. Mari, F. Safavi, T. P. Leist, G.-X. Zhang, and A. Rostami. 2015. Expression of GM-CSF in T Cells Is Increased in Multiple Sclerosis and Suppressed by IFN-β Therapy. *The Journal of Immunology* 194: 5085-5093.

204. Reynolds, G., J. R. Gibbon, A. G. Pratt, M. J. Wood, D. Coady, G. Raftery, A. R. Lorenzi, A. Gray, A. Filer, C. D. Buckley, M. A. Haniffa, J. D. Isaacs, and C. M. Hilkens. 2016. Synovial CD4+ T-cell-derived GM-CSF supports the differentiation of an inflammatory dendritic cell population in rheumatoid arthritis. *Ann Rheum Dis* 75: 899-907.

205. Small, E. J., P. Fratesi, D. M. Reese, G. Strang, R. Laus, M. V. Peshwa, and F. H. Valone. 2000. Immunotherapy of hormone-refractory prostate cancer with antigen-loaded dendritic cells. *J Clin Oncol* 18: 3894-3903.

206. Shiomi, A., and T. Usui. 2015. Pivotal roles of GM-CSF in autoimmunity and inflammation. *Mediators Inflamm* 2015: 568543.

207. Ushach, I., and A. Zlotnik. 2016. Biological role of granulocyte macrophage colony-stimulating factor (GM-CSF) and macrophage colony-stimulating factor (M-CSF) on cells of the myeloid lineage. *J Leukoc Biol* 100: 481-489.

208. Ganesh, B. B., D. M. Cheatem, J. R. Sheng, C. Vasu, and B. S. Prabhakar. 2009. GM-CSF-induced CD11c+CD8a—dendritic cells facilitate Foxp3+ and IL-10+ regulatory T cell expansion resulting in suppression of autoimmune thyroiditis. *International Immunology* 21: 269-282.

209. Borrello, I., and D. Pardoll. 2002. GM-CSF-based cellular vaccines: a review of the clinical experience. *Cytokine Growth Factor Rev* 13: 185-193.

210. Somasundraam, r. 2015. Recent Advances and Current Status of GM-CSF as an Adjuvant in DNA Vaccines for Viral Diseases. *Journal of Investigative Genomics* 2: 54-56.

211. Chang, D. Z., W. Lomazow, C. Joy Somberg, R. Stan, and M. A. Perales. 2004. Granulocyte-macrophage colony stimulating factor: an adjuvant for cancer vaccines. *Hematology* 9: 207-215.

212. Jones, T., A. Stern, and R. Lin. 1994. Potential role of granulocyte-macrophage colony-stimulating factor as vaccine adjuvant. *Eur J Clin Microbiol Infect Dis* 13 Suppl 2: S47-53.

213. Cheever, M. A., and C. S. Higano. 2011. PROVENGE (Sipuleucel-T) in prostate cancer: the first FDA-approved therapeutic cancer vaccine. *Clin Cancer Res* 17: 3520-3526.

214. Parmiani, G., C. Castelli, L. Pilla, M. Santinami, M. Colombo, and L. Rivoltini. 2006. Opposite immune functions of GM-CSF administered as vaccine adjuvant in cancer patients. *Annals of Oncology* 18: 226-232.

215. Rosenberg, S. A., J. C. Yang, D. J. Schwartzentruber, P. Hwu, F. M. Marincola, S. L. Topalian, N. P. Restifo, M. Sznol, S. L. Schwarz, P. J. Spiess, J. R. Wunderlich, C. A. Seipp, J. H. Einhorn, L. Rogers-Freezer, and D. E. White. 1999. Impact of cytokine administration on the generation of antitumor reactivity in patients with metastatic melanoma receiving a peptide vaccine. *J Immunol* 163: 1690-1695.

216. von Mehren, M., P. Arlen, J. Gulley, A. Rogatko, H. S. Cooper, N. J. Meropol, R. K. Alpaugh, M. Davey, S. McLaughlin, M. T. Beard, K. Y. Tsang, J. Schlom, and L. M. Weiner. 2001. The influence of granulocyte macrophage colony-stimulating factor and prior chemotherapy on the immunological response to a vaccine (ALVAC-CEA B7.1) in patients with metastatic carcinoma. *Clin Cancer Res* 7: 1181-1191.

217. Hotta, M., H. Yoshimura, A. Satake, Y. Tsubokura, T. Ito, and S. Nomura. 2019. GM-CSF therapy inhibits chronic graft-versus-host disease via expansion of regulatory T cells. *Eur J Immunol* 49: 179-191.

218. Sheng, J. R., L. C. Li, B. B. Ganesh, B. S. Prabhakar, and M. N. Meriggioli. 2008. Regulatory T cells induced by GM-CSF suppress ongoing experimental myasthenia gravis. *Clin Immunol* 128: 172-180.

219. Gangi, E., C. Vasu, D. Cheatem, and B. S. Prabhakar. 2005. IL-10-producing CD4+CD25+ regulatory T cells play a critical role in granulocyte-macrophage colony-stimulating factor-induced suppression of experimental autoimmune thyroiditis. *J Immunol* 174: 7006-7013.

220. Cheatem, D., B. B. Ganesh, E. Gangi, C. Vasu, and B. S. Prabhakar. 2009. Modulation of dendritic cells using granulocyte-macrophage colony-stimulating factor (GM-CSF) delays type 1 diabetes by enhancing CD4+CD25+ regulatory T cell function. *Clinical Immunology* 131: 260-270.

221. Sheng, J. R., L. Li, B. B. Ganesh, C. Vasu, B. S. Prabhakar, and M. N. Meriggioli. 2006. Suppression of experimental autoimmune myasthenia gravis by granulocyte-macrophage

colony-stimulating factor is associated with an expansion of FoxP3+ regulatory T cells. *J Immunol* 177: 5296-5306.

222. Enzler, T., S. Gillessen, M. Dougan, J. P. Allison, D. Neuberg, D. A. Oble, M. Mihm, and G. Dranoff. 2007. Functional deficiencies of granulocyte-macrophage colony stimulating factor and interleukin-3 contribute to insulitis and destruction of beta cells. *Blood* 110: 954-961.

223. Enzler, T., S. Gillessen, J. P. Manis, D. Ferguson, J. Fleming, F. W. Alt, M. Mihm, and G. Dranoff. 2003. Deficiencies of GM-CSF and interferon gamma link inflammation and cancer. *The Journal of experimental medicine* 197: 1213-1219.

224. Nakamura, T., and H. Ushigome. 2018. Myeloid-Derived Suppressor Cells as a Regulator of Immunity in Organ Transplantation. *International journal of molecular sciences* 19: 2357.

225. Gottschalk, R. A., E. Corse, and J. P. Allison. 2010. TCR ligand density and affinity determine peripheral induction of Foxp3 in vivo. *The Journal of experimental medicine* 207: 1701-1711.

226. Kretschmer, K., I. Apostolou, D. Hawiger, K. Khazaie, M. C. Nussenzweig, and H. von Boehmer. 2005. Inducing and expanding regulatory T cell populations by foreign antigen. *Nat Immunol* 6: 1219-1227.

227. Corse, E., R. A. Gottschalk, and J. P. Allison. 2011. Strength of TCR-peptide/MHC interactions and in vivo T cell responses. *J Immunol* 186: 5039-5045.

228. Allison, K. A., E. Sajti, J. G. Collier, D. Gosselin, T. D. Troutman, E. L. Stone, S. M. Hedrick, and C. K. Glass. 2016. Affinity and dose of TCR engagement yield proportional enhancer and gene activity in CD4+ T cells. *Elife* 5.

229. Crowe, J. E. 2017. 122 - Host Defense Mechanisms Against Viruses. In *Fetal and Neonatal Physiology (Fifth Edition)*. R. A. Polin, S. H. Abman, D. H. Rowitch, W. E. Benitz, and W. W. Fox, eds. Elsevier. 1175-1197.e1177.

230. Mercadante, E. R., and U. M. Lorenz. 2016. Breaking Free of Control: How Conventional T Cells Overcome Regulatory T Cell Suppression. *Frontiers in immunology* 7: 193-193.

231. Barthels, C., A. Ogrinc, V. Steyer, S. Meier, F. Simon, M. Wimmer, A. Blutke, T. Straub, U. Zimber-Strobl, E. Lutgens, P. Marconi, C. Ohnmacht, D. Garzetti, B. Stecher, and T. Brocker. 2017. CD40-signalling abrogates induction of RORγt+ Treg cells by intestinal CD103+ DCs and causes fatal colitis. *Nature Communications* 8: 14715.

232. Malherbe, L., C. Hausl, L. Teyton, and M. G. McHeyzer-Williams. 2004. Clonal selection of helper T cells is determined by an affinity threshold with no further skewing of TCR binding properties. *Immunity* 21: 669-679.

233. Kim, C., D. C. Jay, and M. A. Williams. 2012. Stability and function of secondary Th1 memory cells are dependent on the nature of the secondary stimulus. *J Immunol* 189: 2348-2355.

234. Williams, M. A., E. V. Ravkov, and M. J. Bevan. 2008. Rapid culling of the CD4+ T cell repertoire in the transition from effector to memory. *Immunity* 28: 533-545.

235. Savage, P. A., J. J. Boniface, and M. M. Davis. 1999. A kinetic basis for T cell receptor repertoire selection during an immune response. *Immunity* 10: 485-492.

236. Rosenthal, K. M., L. J. Edwards, J. J. Sabatino, Jr., J. D. Hood, H. A. Wasserman, C. Zhu, and B. D. Evavold. 2012. Low 2-dimensional CD4 T cell receptor affinity for myelin sets in motion delayed response kinetics. *PLoS One* 7: e32562.

237. Blanchfield, L., J. J. Sabatino, Jr., L. Lawrence, and B. D. Evavold. 2017. NFM Cross-Reactivity to MOG Does Not Expand a Critical Threshold Level of High-Affinity T Cells Necessary for Onset of Demyelinating Disease. *Journal of immunology (Baltimore, Md. : 1950)* 199: 2680-2691.

238. Lucca, L. E., P. P. Axisa, M. Aloulou, C. Perals, A. Ramadan, P. Rufas, B. Kyewski, J. Derbinski, N. Fazilleau, L. T. Mars, and R. S. Liblau. 2016. Myelin oligodendrocyte glycoprotein induces incomplete tolerance of CD4(+) T cells specific for both a myelin and a neuronal self-antigen in mice. *Eur J Immunol* 46: 2247-2259.

239. Mannie, M. D., D. J. Fraser, and T. J. McConnell. 2003. IL-4 responsive CD4+ T cells specific for myelin basic protein: IL-2 confers a prolonged postactivation refractory phase. *Immunol Cell Biol* 81: 8-19.

240. Ghosh, D., A. D. Curtis, 2nd, D. S. Wilkinson, and M. D. Mannie. 2016. Depletion of CD4+ CD25+ regulatory T cells confers susceptibility to experimental autoimmune encephalomyelitis (EAE) in GM-CSF-deficient Csf2-/- mice. *J Leukoc Biol* 100: 747-760.

241. Wilkinson, D. S., D. Ghosh, R. A. Nickle, C. D. Moorman, and M. D. Mannie. 2017. Partial CD25 Antagonism Enables Dominance of Antigen-Inducible CD25(high) FOXP3(+) Regulatory T Cells As a Basis for a Regulatory T Cell-Based Adoptive Immunotherapy. *Front Immunol* 8: 1782.

242. Setiady, Y. Y., J. A. Coccia, and P. U. Park. 2010. In vivo depletion of CD4+FOXP3+ Treg cells by the PC61 anti-CD25 monoclonal antibody is mediated by FcgammaRIII+ phagocytes. *Eur. J. Immunol.* 40: 780-786.

243. Sheng, J. R., T. Muthusamy, B. S. Prabhakar, and M. N. Meriggioli. 2011. GM-CSF-induced regulatory T cells selectively inhibit anti-acetylcholine receptor-specific immune responses in experimental myasthenia gravis. *J. Neuroimmunol.* 240-241: 65-73.

244. Ganesh, B. B., D. M. Cheatem, J. R. Sheng, C. Vasu, and B. S. Prabhakar. 2009. GM-CSF-induced CD11c+CD8a--dendritic cells facilitate Foxp3+ and IL-10+ regulatory T cell expansion resulting in suppression of autoimmune thyroiditis. *Int. Immunol.* 21: 269-282.

245. Blanchfield, L., J. J. Sabatino, Jr., L. Lawrence, and B. D. Evavold. 2017. NFM Cross-Reactivity to MOG Does Not Expand a Critical Threshold Level of High-Affinity T Cells Necessary for Onset of Demyelinating Disease. *J. Immunol.* 199: 2680-2691.

246. Krishnamoorthy, G., A. Saxena, L. T. Mars, H. S. Domingues, R. Mentele, A. Ben-Nun, H. Lassmann, K. Dornmair, F. C. Kurschus, R. S. Liblau, and H. Wekerle. 2009. Myelin-specific T cells also recognize neuronal autoantigen in a transgenic mouse model of multiple sclerosis. *Nat. Med.* 15: 626-632.

247. Letourneau, S., C. Krieg, G. Pantaleo, and O. Boyman. 2009. IL-2- and CD25-dependent immunoregulatory mechanisms in the homeostasis of T-cell subsets. *J Allergy Clin Immunol* 123: 758-762.

248. Ye, C., D. Brand, and S. G. Zheng. 2018. Targeting IL-2: an unexpected effect in treating immunological diseases. *Signal Transduct Target Ther* 3: 2.

249. Horwitz, D. A., S. G. Zheng, J. Wang, and J. D. Gray. 2008. Critical role of IL-2 and TGF-beta in generation, function and stabilization of Foxp3+CD4+ Treg. *Eur J Immunol* 38: 912-915.

250. Kraj, P., and L. Ignatowicz. 2018. The mechanisms shaping the repertoire of CD4(+) Foxp3(+) regulatory T cells. *Immunology* 153: 290-296.

251. Darrasse-Jeze, G., S. Deroubaix, H. Mouquet, G. D. Victora, T. Eisenreich, K. H. Yao, R. F. Masilamani, M. L. Dustin, A. Rudensky, K. Liu, and M. C. Nussenzweig. 2009. Feedback control of regulatory T cell homeostasis by dendritic cells in vivo. *The Journal of experimental medicine* 206: 1853-1862.

252. Yogev, N., F. Frommer, D. Lukas, K. Kautz-Neu, K. Karram, D. Ielo, E. von Stebut, H. C. Probst, M. van den Broek, D. Riethmacher, T. Birnberg, T. Blank, B. Reizis, T. Korn, H. Wiendl, S. Jung, M. Prinz, F. C. Kurschus, and A. Waisman. 2012. Dendritic cells ameliorate autoimmunity in the CNS by controlling the homeostasis of PD-1 receptor(+) regulatory T cells. *Immunity* 37: 264-275.

253. Dudek, A. M., S. Martin, A. D. Garg, and P. Agostinis. 2013. Immature, Semi-Mature, and Fully Mature Dendritic Cells: Toward a DC-Cancer Cells Interface That Augments Anticancer Immunity. *Frontiers in immunology* 4: 438-438.

254. Kushwah, R., and J. Hu. 2011. Role of dendritic cells in the induction of regulatory T cells. *Cell Biosci* 1: 20.

255. Raker, V. K., M. P. Domogalla, and K. Steinbrink. 2015. Tolerogenic Dendritic Cells for Regulatory T Cell Induction in Man. *Front Immunol* 6: 569.

256. Pletinckx, K., A. Dohler, V. Pavlovic, and M. B. Lutz. 2011. Role of dendritic cell maturity/costimulation for generation, homeostasis, and suppressive activity of regulatory T cells. *Front Immunol* 2: 39.

257. Maldonado, R. A., and U. H. von Andrian. 2010. How tolerogenic dendritic cells induce regulatory T cells. *Advances in immunology* 108: 111-165.

258. Litjens, N. H., K. Boer, J. M. Zuijderwijk, M. Klepper, A. M. Peeters, E. P. Prens, W. Verschoor, R. Kraaijeveld, Z. Ozgur, M. C. van den Hout-van Vroonhoven, I. W. F. van, C. C. Baan, and M. G. Betjes. 2015. Allogeneic Mature Human Dendritic Cells Generate Superior Alloreactive Regulatory T Cells in the Presence of IL-15. *J Immunol* 194: 5282-5293.

259. Elgueta, R., M. J. Benson, V. C. de Vries, A. Wasiuk, Y. Guo, and R. J. Noelle. 2009. Molecular mechanism and function of CD40/CD40L engagement in the immune system. *Immunol Rev* 229: 152-172.

260. Ara, A., K. A. Ahmed, and J. Xiang. 2018. Multiple effects of CD40-CD40L axis in immunity against infection and cancer. *Immunotargets Ther* 7: 55-61.

261. Iezzi, G., I. Sonderegger, F. Ampenberger, N. Schmitz, B. J. Marsland, and M. Kopf. 2009. CD40–CD40L cross-talk integrates strong antigenic signals and microbial stimuli to induce development of IL-17-producing CD4⁺ T cells. *Proceedings of the National Academy of Sciences* 106: 876-881.

262. Sia, J. K., R. Madan-Lala, and J. Rengarajan. 2017. Th₁₇ immunity to tuberculosis requires CD40-CD40L interaction and is enhanced by CD40 engagement on Mycobacterium tuberculosis-infected dendritic cells. *The Journal of Immunology* 198: 77.77-77.77.

263. Rodriguez, D., J. R. Rodriguez, M. Llorente, I. Vazquez, P. Lucas, M. Esteban, A. C. Martinez, and G. del Real. 1999. A human immunodeficiency virus type 1 Env-granulocyte-macrophage colony-stimulating factor fusion protein enhances the cellular immune response to Env in a vaccinia virus-based vaccine. *J Gen Virol* 80 (Pt 1): 217-223.

264. Lu, H., Z. Xing, and R. C. Brunham. 2002. GM-CSF transgene-based adjuvant allows the establishment of protective mucosal immunity following vaccination with inactivated Chlamydia trachomatis. *J Immunol* 169: 6324-6331.

265. Li, N., Y. Z. Yu, W. Y. Yu, and Z. W. Sun. 2011. Enhancement of the immunogenicity of DNA replicon vaccine of Clostridium botulinum neurotoxin serotype A by GM-CSF gene adjuvant. *Immunopharmacol Immunotoxicol* 33: 211-219.

266. Mannie, M. D., J. P. Nardella, G. A. White, P. Y. Arnold, and D. K. Davidian. 1998. Class II MHC/peptide complexes on T cell antigen-presenting cells: agonistic antigen recognition inhibits subsequent antigen presentation. *Cell Immunol* 186: 111-120.

267. Becher, B., S. Tugues, and M. Greter. 2016. GM-CSF: From Growth Factor to Central Mediator of Tissue Inflammation. *Immunity* 45: 963-973.

268. Hansen, G., T. R. Hercus, B. J. McClure, F. C. Stomski, M. Dottore, J. Powell, H. Ramshaw, J. M. Woodcock, Y. Xu, M. Guthridge, W. J. McKinstry, A. F. Lopez, and M. W. Parker. 2008. The structure of the GM-CSF receptor complex reveals a distinct mode of cytokine receptor activation. *Cell* 134: 496-507.

269. Lacey, D. C., A. Achuthan, A. J. Fleetwood, H. Dinh, J. Roiniotis, G. M. Scholz, M. W. Chang, S. K. Beckman, A. D. Cook, and J. A. Hamilton. 2012. Defining GM-CSF- and macrophage-CSF-dependent macrophage responses by in vitro models. *J Immunol* 188: 5752-5765.

270. Duncker, P. C., J. S. Stoolman, A. K. Huber, and B. M. Segal. 2018. GM-CSF Promotes Chronic Disability in Experimental Autoimmune Encephalomyelitis by Altering the Composition of Central Nervous System-Infiltrating Cells, but Is Dispensable for Disease Induction. *J Immunol* 200: 966-973.

271. Koenecke, C., N. Czeloth, A. Bubke, S. Schmitz, A. Kissenpfennig, B. Malissen, J. Huehn, A. Ganser, R. Förster, and I. Prinz. 2009. Alloantigen-specific de novo-induced Foxp3+ Treg revert in vivo and do not protect from experimental GVHD. *European Journal of Immunology* 39: 3091-3096.

272. Bhela, S., S. K. Varanasi, U. Jaggi, S. S. Sloan, N. K. Rajasagi, and B. T. Rouse. 2017. The Plasticity and Stability of Regulatory T Cells during Viral-Induced Inflammatory Lesions. *J Immunol* 199: 1342-1352.

273. Inomata, T., J. Hua, A. Di Zazzo, and R. Dana. 2016. Impaired Function of Peripherally Induced Regulatory T Cells in Hosts at High Risk of Graft Rejection. *Scientific Reports* 6: 39924.

274. Yadav, M., S. Stephan, and J. A. Bluestone. 2013. Peripherally induced tregs - role in immune homeostasis and autoimmunity. *Front Immunol* 4: 232.

275. Ohkura, N., M. Hamaguchi, H. Morikawa, K. Sugimura, A. Tanaka, Y. Ito, M. Osaki, Y. Tanaka, R. Yamashita, N. Nakano, J. Huehn, H. J. Fehling, T. Sparwasser, K. Nakai, and S. Sakaguchi. 2012. T cell receptor stimulation-induced epigenetic changes and Foxp3 expression are independent and complementary events required for Treg cell development. *Immunity* 37: 785-799.

276. Someya, K., H. Nakatsukasa, M. Ito, T. Kondo, K.-i. Tateda, T. Akanuma, I. Koya, T. Sanosaka, J. Kohyama, Y.-i. Tsukada, T. Takamura-Enya, and A. Yoshimura. 2017.

Improvement of Foxp3 stability through CNS2 demethylation by TET enzyme induction and activation. *International Immunology* 29: 365-375.

277. Baaten, B. J., R. Tinoco, A. T. Chen, and L. M. Bradley. 2012. Regulation of Antigen-Experienced T Cells: Lessons from the Quintessential Memory Marker CD44. *Front Immunol* 3: 23.

278. Liu, T., L. Soong, G. Liu, R. Konig, and A. K. Chopra. 2009. CD44 expression positively correlates with Foxp3 expression and suppressive function of CD4+ Treg cells. *Biol Direct* 4: 40.

279. Bollyky, P. L., B. A. Falk, S. A. Long, A. Preisinger, K. R. Braun, R. P. Wu, S. P. Evanko, J. H. Buckner, T. N. Wight, and G. T. Nepom. 2009. CD44 costimulation promotes FoxP3+ regulatory T cell persistence and function via production of IL-2, IL-10, and TGF-beta. *J Immunol* 183: 2232-2241.

280. Nakano, K., K. Saito, S. Mine, S. Matsushita, and Y. Tanaka. 2007. Engagement of CD44 up-regulates Fas ligand expression on T cells leading to activation-induced cell death. *Apoptosis* 12: 45-54.

APPENDIX I

East Carolina University

Animal Care and
Use Commitee
212 Ed Warren Life
Sciences Building
East Carolina University
Greenville, NC 27834

252-744-2436 office
252-744-2355 fax

August 18, 2014

Mark Mannie, Ph.D.
Department of Micro/Immuno
Brody 5E-106
ECU Brody School of Medicine

Dear Dr. Mannie:

Your Animal Use Protocol entitled, "Cytokines as Adjuvants for Tolerogenic Vaccines" (AUP #K158a) was reviewed by this institution's Animal Care and Use Committee on 8/18/14. The following action was taken by the Committee:

"Approved as submitted"

Please contact Dale Aycock at 744-2997 prior to hazard use

A copy is enclosed for your laboratory files. Please be reminded that all animal procedures must be conducted as described in the approved Animal Use Protocol. Modifications of these procedures cannot be performed without prior approval of the ACUC. The Animal Welfare Act and Public Health Service Guidelines require the ACUC to suspend activities not in accordance with approved procedures and report such activities to the responsible University Official (Vice Chancellor for Health Sciences or Vice Chancellor for Academic Affairs) and appropriate federal Agencies. **Please ensure that all personnel associated with this protocol have access to this approved copy of the AUP and are familiar with its contents.**

Sincerely yours,

Susan McRae, Ph.D.
Chair, Animal Care and Use Committee

SM/jd

Enclosure

East Carolina University is a constituent institution of the University of North Carolina. An equal opportunity university.

East Carolina University

Animal Care and Use Commitee
212 Ed Warren Life Sciences Building
East Carolina University
Greenville, NC 27834

252-744-2436 office
252-744-2355 fax

August 11, 2015

Mark Mannie, Ph.D.
Department of Micro/Immuno
Brody 5E-124
ECU Brody School of Medicine

Dear Dr. Mannie:

The Amendment to your Animal Use Protocol entitled, "Cytokines as Adjuvants for Tolerogenic Vaccines" (AUP #K158a) was reviewed by this institution's Animal Care and Use Committee on August 10, 2015. The following action was taken by the Committee:

"Approved as submitted"

Note: B6.129S2-*Ifnar1*^{tm1Agt}/Mmjax mice are recommended to be housed in sterile conditions.
Note: Please check numbers to make sure you have adequate numbers to cover knockout breeding.

Please contact Dale Aycock at 744-2997 prior to hazard use

A copy is enclosed for your laboratory files. Please be reminded that all animal procedures must be conducted as described in the approved Animal Use Protocol. Modifications of these procedures cannot be performed without prior approval of the ACUC. The Animal Welfare Act and Public Health Service Guidelines require the ACUC to suspend activities not in accordance with approved procedures and report such activities to the responsible University Official (Vice Chancellor for Health Sciences or Vice Chancellor for Academic Affairs) and appropriate federal Agencies. **Please ensure that all personnel associated with this protocol have access to this approved copy of the AUP and are familiar with its contents.**

Sincerely yours,

Susan McRae, Ph.D.
Chair, Animal Care and Use Committee

SM/jd

enclosure

East Carolina University is a constituent institution of the University of North Carolina. An equal opportunity university.

East Carolina University
Tomorrow starts here.

Animal Care and
Use Committee
212 Ed Warren Life
Sciences Building
East Carolina University
Greenville, NC 27834-4354

252-744-2436 office
252-744-2355 fax

August 2, 2017

Mark Mannie, Ph.D.
Department of Micro/Immuno
Brody 5E-106
East Carolina University

Dear Dr. Mannie:

Your Animal Use Protocol entitled, "Cytokines as Adjuvants for Tolerogenic Vaccination" (AUP #K158b) was reviewed by this institution's Animal Care and Use Committee on August 2, 2017. The following action was taken by the Committee:

"Approved as submitted"

Please contact Aaron Hinkle at 744-2997 prior to hazard use

A copy is enclosed for your laboratory files. Please be reminded that all animal procedures must be conducted as described in the approved Animal Use Protocol. Modifications of these procedures cannot be performed without prior approval of the ACUC. The Animal Welfare Act and Public Health Service Guidelines require the ACUC to suspend activities not in accordance with approved procedures and report such activities to the responsible University Official (Vice Chancellor for Health Sciences or Vice Chancellor for Academic Affairs) and appropriate federal Agencies. **Please ensure that all personnel associated with this protocol have access to this approved copy of the AUP and are familiar with its contents.**

Sincerely yours,

Susan McRae, Ph.D.
Chair, Animal Care and Use Committee

SM/jd

Enclosure

APPENDIX II

Form: GPC-7 (11/00)

APPOINTMENT OF STUDENT'S GRADUATE ADVISORY COMMITTEE

DATE: 11-10-2015

TO: The Graduate Program Committee and
Chair of the Department of Microbiology and Immunology

FROM: Mark Marnell
Advisor & Chair, Graduate Advisory Committee

Student Name: Cody D. Moorman	
Date entered Graduate Program: 08/14	Banner ID: B00473849

Instructions: This form is to be prepared by the student after contacting faculty members. After completion and signatures, the ADVISOR submits this recommendation. Minimum of 5 graduate faculty members, 3 of whom must be fiscal graduate faculty members in Microbiology and Immunology, and at least one committee member must be a graduate faculty member in another Department.

GRADUATE ADVISORY COMMITTEE:

The following graduate faculty members have been contacted and indicate willingness to serve, if approved:

Names of Committee Members	Department & Phone Number	Initials
MARY JANE THOMASSEN	Internal Medicine	MJT
Rachel L. Roper	Microbiology	RLR
Isabelle LEMAIRE	Microbiology.	IL
Ryan M. Ruprecht	Microbiology	RMR

Approved by Advisor: Mark Marnell Date: 11-10-2015

Approved by Graduate Program Committee: [signature] Date: 11/11/15

Approved by Department Chair: Everett C Perrin Date: 11/11/15

Form: GPC-9 (11/00)

Results of the Doctoral Candidacy Examination
Comprehensive Preliminary Examination

Department of Microbiology and Immunology

DATE: 8/24/16

TO: Chair, Graduate Program Committee and
Chair, Department of Microbiology and Immunology

FROM: Dr. Mark Mannie
Advisor & Chair, Graduate Advisory Committee

Part 2 of the Doctoral Candidacy Examination, the Comprehensive Preliminary Examination, was held for:

Student Name: Cody Moorman	
During the week of: 8/22/16	Banner ID: B00473899

The members of the Graduate Advisory Committee agree that the student has successfully completed Part 2 of the Doctoral Candidacy Examination. Therefore, the Graduate Advisory Committee recommends that this student be admitted to candidacy for the doctorate in Microbiology and Immunology.

Chair, G.A.C.

Form: GPC-9 (11/00)

Results of the Doctoral Candidacy Examination
Comprehensive Preliminary Examination

Department of Microbiology and Immunology

DATE: 11/16/17

TO: Chair, Graduate Program Committee and
Chair, Department of Microbiology and Immunology

FROM: DR. MARK MANNIE
Advisor & Chair, Graduate Advisory Committee

Part 2 of the Doctoral Candidacy Examination, the Comprehensive Preliminary Examination, was held for:

Student Name: CODY MOORMAN	
During the week of: 11/13-17/17	Banner ID: B00473849

The members of the Graduate Advisory Committee agree that the student has successfully completed Part 2 of the Doctoral Candidacy Examination. Therefore, the Graduate Advisory Committee recommends that this student be admitted to candidacy for the doctorate in Microbiology and Immunology.

11-16-2017
Chair, G.A.C.

11/16/17

11/16/17

11/16/17

11/16/17